MITRE

Coupling Analyses of the High Altitude Electromagnetic Pulse (HEMP) to a SATCOM system

A Major Qualifying Project submitted to the faculty of

Worcester Polytechnic Institute

in partial fulfillment of the requirements for the

Degree of Bachelor of Science

October 16, 2014

Author:
Alexander G. Bennett

Supervisor:
Dr. Sergey Makarov

1 Abstract

This paper presents analytical results of the High Altitude Electromagnetic Pulse (HEMP) E1 and E2 coupling to an antenna system. HEMP is the effect caused by the detonation of a nuclear bomb in the upper atmosphere. The antenna system was modeled with the flexibility to support parametric trades relative to antenna height, cable length, and structure size. The coupling analysis was conducted using two software the Numerical Electromagnetic Code (NEC) and a transmission line model developed in MATLAB.

2 Acknowledgements

I would like to extend my thanks to all those that supported me throughout my Major Qualifying Project.

I would like to thank all of the employees at the MITRE corporation that were actively involved in my project.

Thank you to my adviser Professor Sergey Makarov for his support and motivation.

Thank you to Robert Figucia, the MITRE project leader, for the flexibility and support I needed to progress forward on this project.

Thank you to Janet Werth, for keeping things in perspective and helping me focus on completing the task at hand.

Thank you to Lucien Tieg, for assisting me in all things related to software.

Thank you to J.P. Wendler, for taking an active interest not only in helping me with this project but in myself and my educational experience.

Thank you to DeAnn Iwan, for being there to support and guide me through all things HEMP related.

Thank you to Tim Nash, for taking me on tour of the facilities at MITRE and for being a great office partner.

Thank you to all others who took an avid interest in me and my project.

3 Forward

As the sole author of this report I have taken the time to insure that the reader is well informed on the topic of HEMP prior to making it to the methodology, results, and analysis portion of this text. This being a technical report, most of the information that is found within is specialized knowledge that the vast majority of people will not use in their day to day lives. In order to add value to this paper beyond the subject of HEMP I have added an observation and conclusion section that contains knowledge that I believe can only be gained from the experience. Most of this knowledge is a "rules of thumb" that can be applied to the day to day operations of life as an engineer, project manager, business executive and leader. I feel that in adding this section I have added a human element to what would otherwise be a dry read for those not interested in the topic of HEMP. I also believe that in adding this section this report goes beyond the defined limits of what a traditional Major Qualifying Project paper must be. The intended audience of this report is rather broad, thus taking the liberty of making this report less specific towards the end will hopefully cater to a wider audience. The vast majority of the information in this report is meant to be read by my adviser, academics, the engineers at MITRE who worked on this project with me, and those interested in the topic of HEMP. I do expect that a few interested students may stumble upon this paper and possibly even follow in my footsteps. Thus to all of you that are taking the time to read this, enjoy the fruits of my labor, and God speed.

Contents

List of Figures

List of Tables

List of Equations

4 Introduction

A nuclear burst detonated in space would create a high-altitude electromagnetic pulse (HEMP) that could cause the functional collapse of control and communication systems. The study of this paper is how the early-time (E1) and intermediate-time (E2) pulses effect a key communications component, an Antenna system. Antenna systems represent a key infrastructural concern when considering the HEMP threat, as they play a vital role in communications and cannot be placed inside a HEMP shielded enclosure. The antenna system that is modeled in this paper is designed to MIL STD 188-125-2. The analysis provided in this text is in line with MIL STD 188-125-2.

5 Background

According to [1] it was anticipated that a nuclear burst would generate electromagnetic signals that could cause problems for electronic equipment. These anticipations were met during the Star Fish prime high altitude nuclear detonation. Starfish Prime was a high-altitude nuclear test conducted by the United States on July 9, 1962. The test was successully detonated at an altitude of 400 kilometers (250 miles). The actual weapon yield came very close to the design yield, which various sources have set at different values in the range of 1.4 to 1.45 megatons. Starfish Prime caused an electromagnetic pulse (EMP) which was far larger than expected, the pulse created by the Starfish Prime was accused of causing electrical damage in Hawaii. Around 1,445 kilometres away from the detonation point, 300 streetlights, burglar alarms, and a telephone company were damaged from the Starfish Prime pulse. The Starfish Prime was one of the first High Altitude Electromagnetic Pulses tested by the U.S. which led to the study of this field. After the U.S. Senate ratified the Partial Nuclear Test Ban Treaty, effectively ending above-ground nuclear tests conducted by the U.S., the U.S.S.R, and the U.K, E1 HEMP testing went underground. It was during these underground tests that adequate theories for E1 were developed. Although E1 HEMP can be considered very much the military threat some of the early pioneers in E1 HEMP research and specification were engineers at Bell Laboratories. This research was conducted prior to the 1980's and was not pushed forward considering the competitive commercial environment of the communications industry. As time passed interest in HEMP lessened in the U.S.. It wasn't until recently that this interest has increased world wide. Efforts by the EMP Commission, a commission that was established by congress during the fiscal year (FY) 2001 to assess the threat from HEMP, has been the largest contributing cause to the increased interest in HEMP research.

The EMP Commission concluded that a large-scale EMP attack could possibly cause widespread damage to unprotected civilian annd military electronic equipment for an extended period [3]. The immediate threat of an EMP attack is difficult to assess, some have observed that it is growing with worldwide access to newer technologies and proliferation of nuclear weapons. Under the threat of nuclear warfare a country was gauranteed a certain amount of security by what is known as mutually assured destruction. Mutually assured destruction has acted as a deterrent against hte exchange of multiple high-yield nuclear warheads. During a HEMP attack, a single, specially-designed low-yield nuclear explosion high above the United States, or over a battlefield, can produce a large-scale EMP effect that could result in the widespread loss of electronics, but no direct fatalities, and may not necessarily evoke a large nuclear retaliatory strike by the U.S. military [3]. This, along with the possible vulnerability of U.S. commercial electronics and U.S. military battlefield equipment to the effects of an EMP, may create a new incentive for other countries to develop or acquire nuclear capability [3].

Considering the scale of this EMP there are those that believe nothing can be done to protect against it. Some even believe that every electronic device in the U.S. will fail, and that under these circumstances the U.S. will be placed in a sort of induced "Dark Ages". These outcomes are doubtful, only a small fraction of electronic equipment would be affected by the HEMP. The greatest concern during a HEMP event is what will happen to power and communication systems.

5.1 HEMP Environment

When using the term environment it generally refers to the basic signal generated by a nuclear explosion [1]. When defining the E1 HEMP environment the only thing that is being defined is the incident EM signal. According to [11] E1 HEMP is produced by an exoatmospheric nuclear explosion. The atmospheric density gradually decreases with altitude, and so often some approximate altitude is given for the height of the nuclear burst, such as 30 km. HEMP does not really have a firm height-of-burst limit, and there is still E1 HEMP for lower altitude bursts, although with lower field levels [1]. HEMP is typically the EMP of most interest because it can cover such a large area.There are three parts to the standard HEMP waveform, the early-time, the intermediate time, and the late time HEMP.

Figure 1: E1, E2, and E3 HEMP

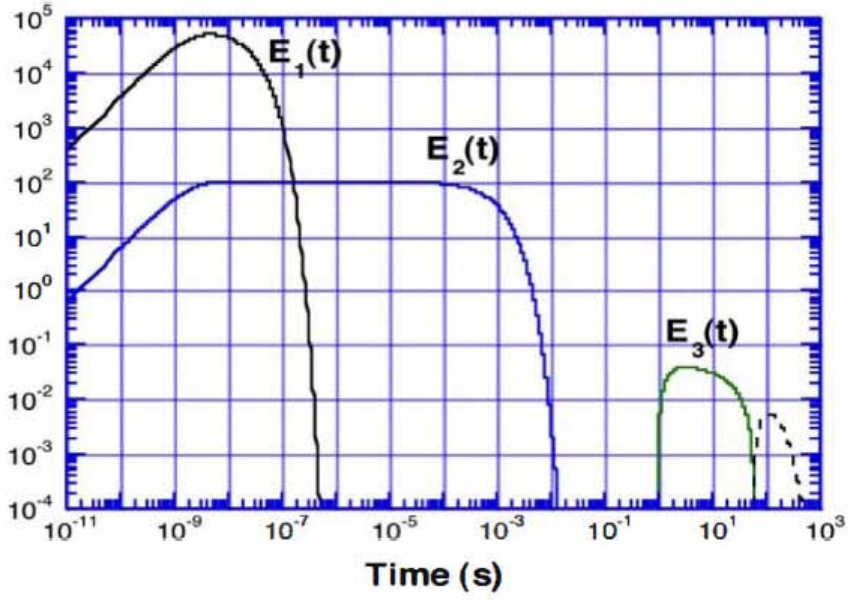

Early-time HEMP

E1 HEMP is a fast narrow pulse, typically going up to high electromagnetic field levels not commonly found in natural events [1]. The early time HEMP as described in [11] is caused by the high-energy gamma radiation that travels radially away from the burst center of a nuclear detonation. When this nuclear detonation occurrs at high altitudes where the mean free path of the gamma photons is large, these photons will travel great distances before they interact with another particle. The gamma rays that are directed toward the earth interact with dense atmosphere and air molecules to produce Compton electrons and positive ions. The Compton electrons begin by traveling radially away from the burst center, but are then acted upon by the Earth's magnetic field, which causes them to turn

about the magnetic field lines.
The acceleration of the charged particles caused by their rotation about the earth's magnetic field creates radiated electromagnetic fields. Thus the early-time HEMP is produced by the acceleration of charged particles in the Earth's magnetic field. At the ground (Earth's surface), and up into the atmosphere where humans might be present (at least up to about 50,000 ft) there is no weapon radiation - no radioactive particles, no gammas, no x rays, no neutrons, no betas; just an EM signal [1].

Figure 2: E1 HEMP creation [5]

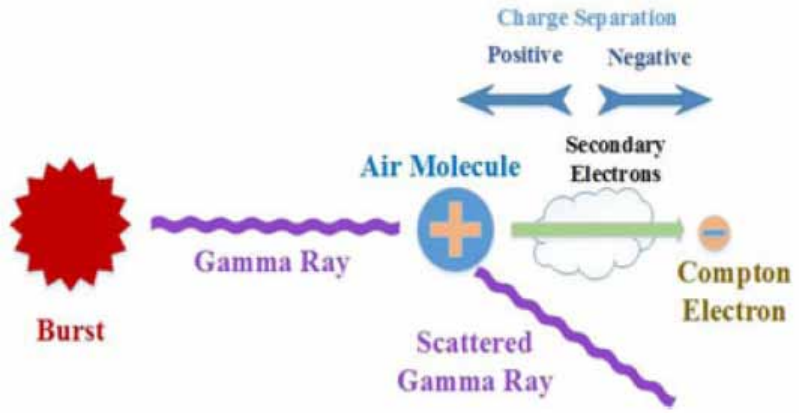

Besides being a very strong signal, E1 HEMP coverage is also very widespread. Figure 3 shows an example of the coverage of the signal with a burst height of 75 km. Within this burst the peak electromagnetic field is slightly south of the "Ground Zero". HEMP is governed by the Earth's magnetic field, and so the peak and null points are actually geomagnetically south and north from Ground Zero in the Northern Hemisphere.

Figure 3-a illustrates what the signal coverage of the burst would be at a height of 75 km. This begs the question as to what the signal coverage would be with different height of bursts (HOB). Figure 3-b gives an idea of what the signal coverage of the E1 HEMP would be with HOBs of 30, 120 and 300 miles.

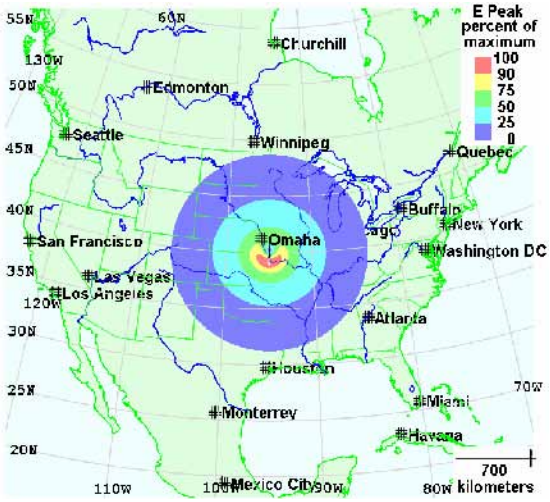

(a) E1 HEMP Signal Coverage 75 km [1]

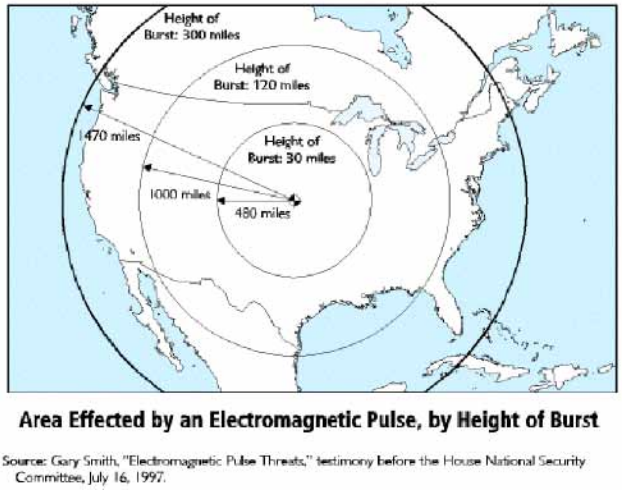

(b) E1 HEMP Signal Coverage Multiple HOB

Figure 3: Coverage of the E1 HEMP signal

There are several parameters that influence the creation of E1 HEMP. Some of these parameters are associated with the weapon being detonated, and the others are related to the geometeric relationships. The parameters that contribute to the calculation of E1 HEMP are available in Figure 4 below.

Figure 4: E1 HEMP Parameters [1]

E1 HEMP Calculation Inputs		
Parameter Categories		Parameters
Weapon	Gammas	Time evolution of gamma emission spectrum
	High energy x rays	Time evolution of high-energy x-ray emission spectrum
Geometry	Burst location	Latitude, longitude, altitude
	Observer location	Latitude, longitude (altitude if aircraft)

Given the number of parameters that effect the calculation of the E1 HEMP pulse when E1 HEMP is traditionally defined in an environment it is given solely as the incident E field. Other localized parameters that could effect the incident field are ignored. Such as reflection effects from being near the side of a very large metal building. As well as the absorption effects that occur on long metal conductors, such as power lines, fences, and railroad rails, all of which can collect electromagnetic energy, and enhance the HEMP for observers nearby. Some effects can be calculated for if the environment is known.

The extra effects that can be calculated for are typically the reflections of the HEMP pulse off the Earths surface. The reflections can be calculated if the ground conductivity and soil dielectric are known. At an observation point the incident pulse will be seen, and then that pulse will go down to the surface and then back up, so that the observer will also see a reflected pulse [1]. Because of the signs of the reflections for each component, the reflected vertical component will add to the incident

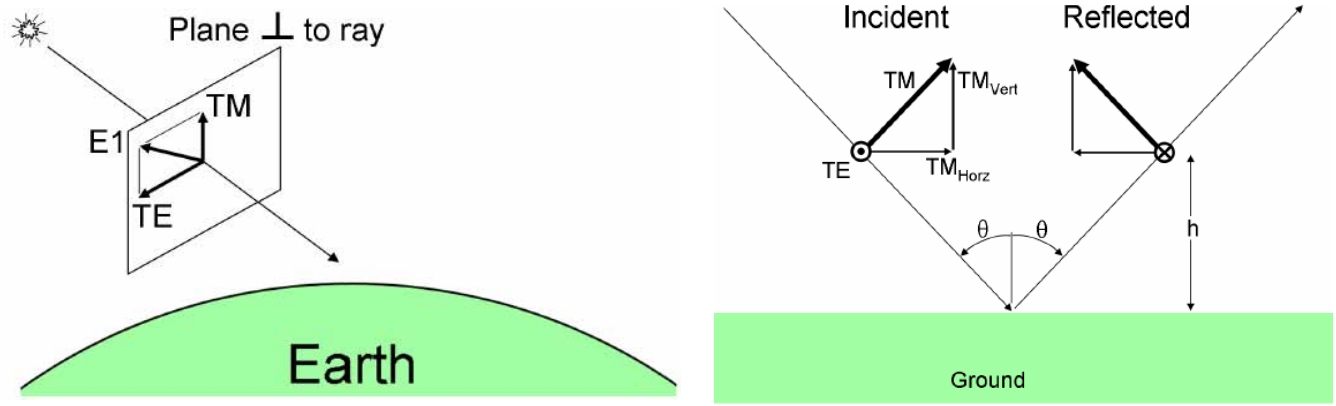

(a) Decomposition of the HEMP pulse

(b) Incident and Reflected Waves

Figure 5: Decomposition of the E1 Pulse with and how this decomposition combines with the incident and reflected waves.

pulse, while the other components (horizontal) will tend to cancel the incident pulse [1].
The time delay for the reflection is:

$$\delta = \frac{2h}{c} * cos(\theta) \tag{1}$$

where c is the speed of light, h is the observer height above the ground, and θ is the incident ray angle from vertical [1].
The shorter the offset time the more the total field seen is that of doubling the incident vertical field and canceling the horizontal field. This can be seen graphically in Figure 5.

Figure shows the decomposition of the E1 HEMP pulse into two electric field terms. E1 can be decomposed into the horizontal polarization of the electric field (Transverse Electric), and the component that is upward in the plane perpendicular to the burst-observer ray (Transverse Magnetic). Figure 5-b considers the earth to be a perfect conductor. The real Earth is not a perfect conductor. The calculations for imperfect ground are straight forward, but more complex. The reflection coefficients for the three terms all become functions of frequency, and the E1 HEMP's frequency content is very wide. Typically as frequency increases, the conductivity increases, and the permittivity decreases [1]. To account for this change in soil conductivity there has to be data available for the frequency dependence of soil, and this data would vary with soil type. When given an E1 HEMP standard a generic environment is used that does not account for all these variables.
The generic environment is a mathematical description of the HEMP pulse that can be taken from [12].

Double Exponential Model (DEXP)

The double exponential model of the HEMP pulse is characterized in the time domain as:

$$E(t) = E_o[e^{-\alpha(t-t_o)} - e^{\beta(t-t_o)}]u(t-t_o)V/m \tag{2}$$

The parameters in this equation are defined as follows:
$E_o = field\ intensity\ constant\ V/m$

$\alpha = decay\ constant\ rad/s$
$\beta = risetime\ constant\ rad/s$
$u(t - t_o) = unit\ step\ function$
$t_o = timeshift\ s$

The frequency domain expression for the DEXP model is:

$$E(\omega) = E_o(\frac{1}{j\omega + \alpha} - \frac{1}{j\omega + \beta}) \tag{3}$$

$\omega = 2\pi f = radian\ frequency\ rad/s$
$j = \sqrt{-1}$
These two expressions define the DEXP model. The DEXP is the simplest analytic tool used to approximate important characteristics of HEMP waveforms and simulators, but it does have its limitations. Thus the quotient exponential QEXP form was derived. [15]

Quotient Exponential (QEXP)

The quotient exponential pulse (QEXP) is not used in the IEC standard but in many others. It can be defined as:

$$E(t) = \frac{E_o}{[e^{\beta(t-t_o)} + e^{-\alpha(t-t_o)}]} \tag{4}$$

the frequency domain form is:

$$E(\omega) = \frac{E_o\pi}{(\alpha + \beta)} csc[\frac{\pi}{(\alpha + \beta)}(j\omega + \beta)]e^{-j\omega t_o}\frac{V}{m - Hz} \tag{5}$$

The quotient exponential and the double exponential model each have their advantages and disadvantages. The double exponential model is discontinuous at t = 0, which is the only drawback of this model [15]. The QEXP has the advantage that it has a continuous time derivative of all orders for all times. The disadvantage of this model is that it extends to $t = -\infty$ and has an infinite number of poles in the frequency domain [15].

Figure 6: E1 Pulse Time Domain using the DEXP model

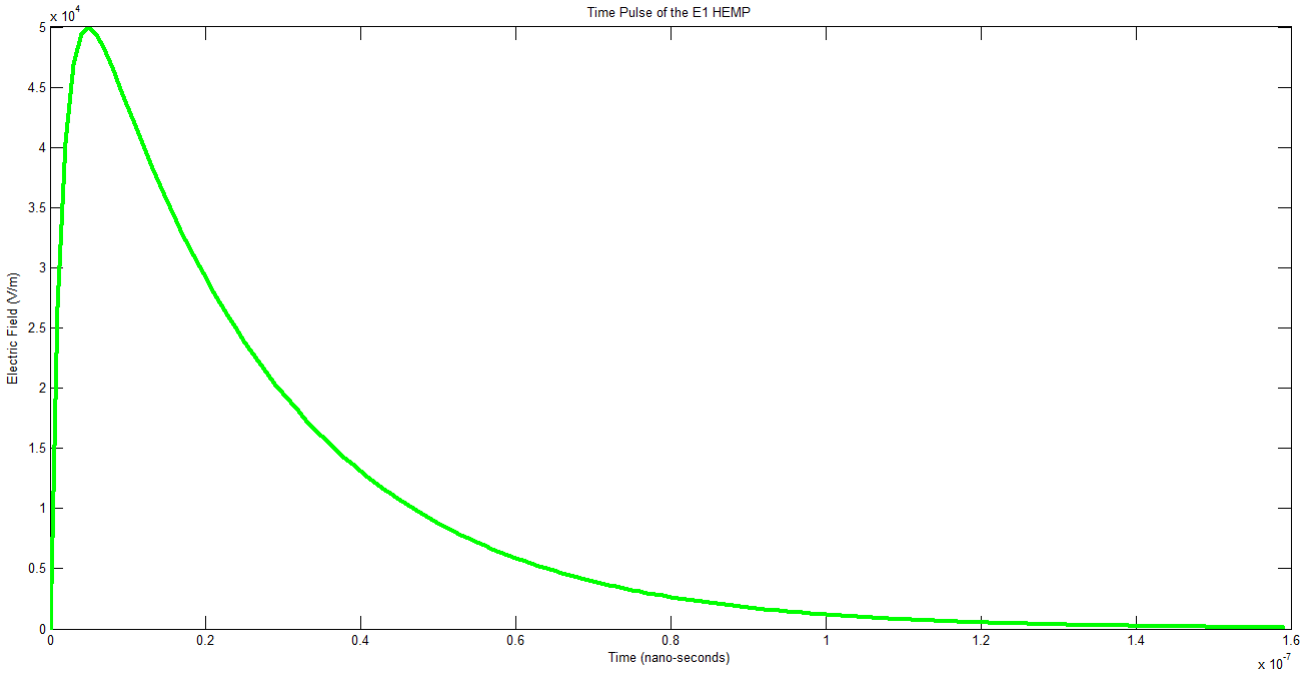

Figure 7: E1 Pulse Frequency Spectrum using the DEXP model

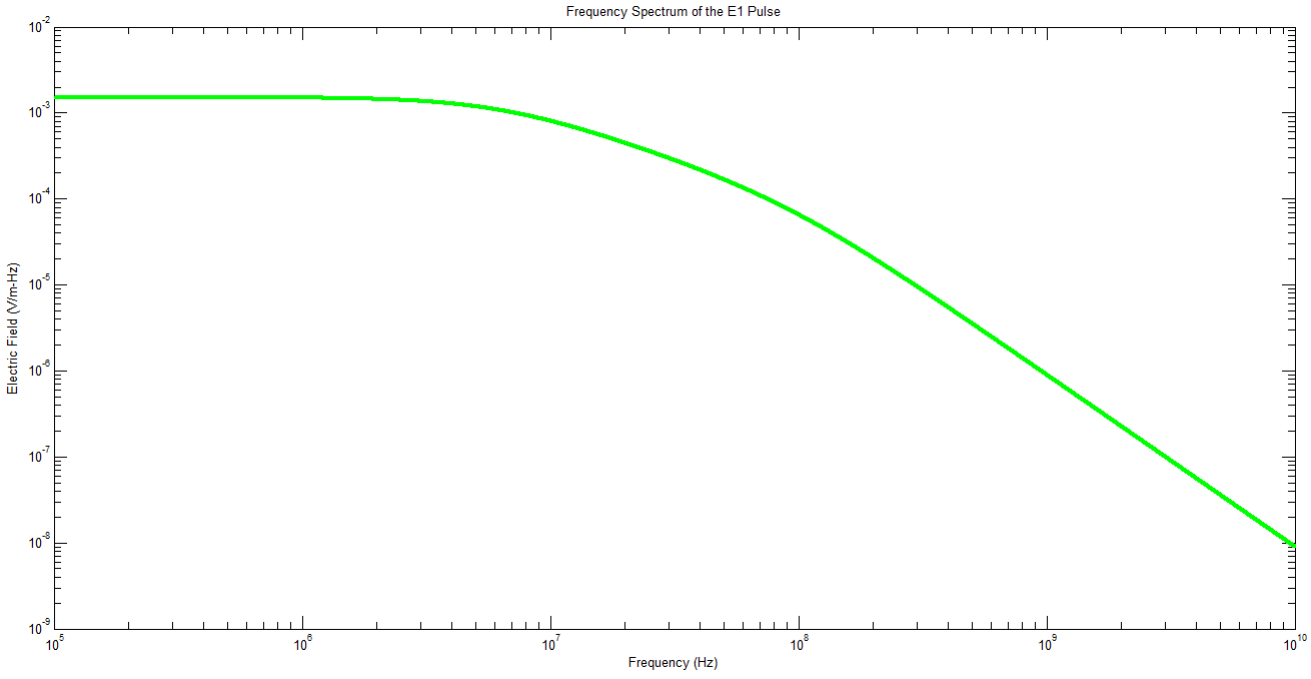

Some of the characteristics of the E1 pulse can be summarized from the standard developed from [12].

Figure 8: Summary of the IEC E1 characteristics [1]

IEC E1 HEMP Waveform Properties	
Characteristic	Value
Waveform peak	$E_{peak} = 50{,}000\,V/m$
Spectrum peak	$E_{low\,freq} = 0.00152\,V/m/Hz$
Waveform peak power	$P_{peak} = 6.64\times10^{6}\ W/m^2$
Spectrum peak power	$P_{low\,freq} = 6.11\times10^{-9}\ W/m^2/Hz$
Total energy	$W_{total} = 0.115\ J/m^2$
Time of peak	$t_{peak} = 4.84$ ns
Rise time, 10% to 90% of peak	$t_{10-90} = 2.47$ ns
Pulse width, full width at half maximum	FWHM = 23.0 ns
Pulse width, total energy over peak power	$W_{total} / P_{peak} = 17.3$ ns
Spectrum width, total energy over peak spectrum power	$W_{total} / P_{low\,freq} = 18.8$ MHz

For a more intuitive understanding consider a comparision provided between an FM radio signal and the E1 pulse [1]. An FM radio transmission at 100 MHz has a transmitted power of 10,000 watts (RMS), and we are recieving the signal at a distance of 1 mile. As an estimate assume a transmitting antenna gain of $\sqrt{2}$ the peak power at the 1 mile range would be 1.23 mW/m^2, and the electric field peak is 0.68 V/m. Thus the FM signal is smaller than the E1 HEMP electric field by a factor of 73,500 - or a factor of $5.4x10^9$ in power. E1 HEMP seems to provide an incredible amount of power, given that it is the result of a nuclear detonation this makes sense but there are certain aspects of E1 that make it important.
E1 HEMP is one of the greatest threats from a HEMP. The reasons for this are as follows [1]:
1. Its very high power levels are not usually seen, except in limited circumstances, such as very near lightning strikes or very high power RF sources.
2. Its very large area coverage, exposed simultaneously.
3. Modern society's reliance on microscopic, high frequency, electronic devices.
4. E1 HEMP can trigger the destructive release of other energy stores.

The actual time delay between the detonation of a nuclear warhead and when the electromagnetic pulse reaches the Earth's surface is not exactly instantaneous. Depending on the location of the observer in relation to ground zero the time that the electromagnetic pulse will reach the observer will differ. For a 100 km burst (62.1 miles) there are various time delays [1]:
From the burst straight down to ground zero: 0.333 ms.
From the burst to the farthest exposed point (tangent): 3.78 ms
From ground zero out to the tangent (1122 km, or 697 miles): 3.74 ms.
With the vast energy provided by the E1 HEMP pulse even a small antenna 10 cm (4 inches) long

can mean a voltage of about 5000 volts, and it could be much higher for longer lines. With the high voltages and frequencies associated with E1 HEMP there is no doubt that it can have system disturbing effects.
Typical system effects can be separated into two types. Temporary upset and permanent damage. Damage is as the word implies the system can no longer function correctly due to the coupling of the E1 HEMP to the system. Temporary upset occurs when the over voltage causes the system to temporarily malfunction or stop working. This can occur in control systems where some data may be corrupted due to an over voltage transient. Temporary upsets may cause nothing greater than a system reboot but in critical infrastructure a system reboot can be dangerous.
Specific hardware that can be easily effected by the E1 HEMP are, low voltage distribution transformers, insulators on distribution lines, control and sensor systems, central control systems (communications and control units), and power generators [1]. Each of these systems has been found to be under some sort of threat from HEMP E1.

Intermediate-time HEMP

As defined in [11] the intermediate time HEMP immediately follows the initial fast transient. The scattered gamma rays and inelastic gammas from weapon neutrons create additional ionization resulting in the second part of the HEMP signal (intermediate time) [12]. This HEMP waveform has approximately the same EMP effect of a lightning stike. It lasts from about 1 μs to 0.1 s. Due to its similarity to lightning strikes the E2 pulse is considered the easiest to protect against. The biggest concern with the E2 pulse is that it follows directly after the E1 pulse, which may have damaged the components used to protect against lightning strikes. The temporal and spectral graphs of the E2 pulse are depicted below. As can be seen the E2 pulse does not have electric field magnitudes equivalent to the E1 pulse but it last for a much longer duration. Which means it can couple to cables for much greater lengths of time. The fields at the ground from the neutron gamma signal of the intermediate time pulse are greatest for low altitude bursts between 20 and 50 km. The ground reflections are particularly important for considering the electromagnetic effects of the E2 pulse for coupling to cables only the vertical electric field has a substantial impact [2].

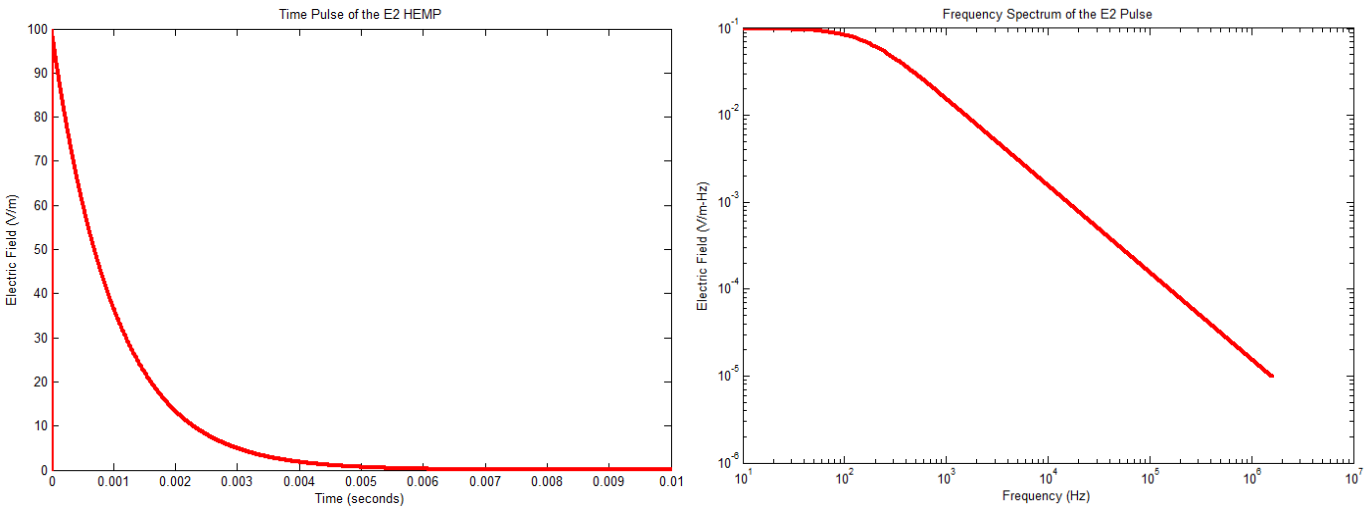

(a) Time Domain of the E2 pulse

(b) Frequency Spectrum of the E2 pulse

Figure 9: Temporal and Spectral graphs of the E2 pulse

Late-time HEMP

The late-time HEMP is designated the magnetohydrodynamic EMP (MHD-EMP) and is generated by the same nuclear burst as the E2 and E1 HEMP. It is characterized by a low amplitude electric field (tens of millivolts per meter), a slow rise time (seconds), and a long pulse duration (hundreds of seconds) [12]. The late-time HEMP has two phases. The first is a 1-10 second time period that is known as the "Blast Wave" [2]. The second which lasts between 10-300 seconds is known as the "Heave". The blast wave is the expansion of the nuclear fireball, that expells that geomagnetic field and creates a magnetic bubble. During later times the debris in the bubble flows along the geomagnetic field lines then heats and ionizes the upper atmosphere [2], causing the upper atmosphere to expand buoyantly and rise. The rising conducting patch crosses the geomagnetic field lines, causing currents to flow in the patch and produce magnetic fields on the surface of the earth beneath the patch [2]. The creation of the magnetic field along the earths surface is the "Heave".

During an exoatmospheric nuclear event, about 75% of the energy from the detonation is emitted as x-rays. The majority of the 25% remaining is in kinetic energy of the weapon debris, which after the detonation, has become highly ionized. As the debris expands outward it forms a "magnetic bubble". The expansion of the bubble is determined by the velocity of the debris, which usually is greater than 1000 km/s, the later expansion depends on the altitude of the burst [1]. At altitudes less than 300 km, the dominant effect slowing the expansion is the density of the atmosphere, and as the bubble expands it becomes asymmetric as it becomes easier to expand upward into more rarefied air than downward into denser air. At higher altitudes, the expansion is slowed by the anisotropic magnetic pressure, and the kinetic energy of the debris is converted into magnetic energy of distorted field lines. For the early time approximately sperical expansion of the magnetic bubble, the perturbed magnetic fields at the surface of the ground would be nearly those of a magnetic dipole which can be given by:

$$M(t) = -\frac{B_o R(t)^3}{2} \tag{6}$$

R(t) is the time dependent bubble radius and B_o is the magnitude of the geomagnetic field [1]. Typically, the magnetic bubble reaches its maximum size within less than a second after the detonation, and then takes a few more seconds to collapse. The blast wave of the E3 pulse can be visualized in Figure 10 [2].

The next phase of the E3 pulse is what is called the heave. For bursts higher than 130 km altitude the bomb debris and shock heated air ions stream downward along geomagnetic field lines until they deposit their energy at altitudes near 130 km [2]. The two processes contribute to both the heating and additional ionization of the ionosphere. After the expansion of the heated air, it begins to buoyantly rise. As this conducting layer rises across the geomagnetic field, a current is induced by the dynamo effect. The dynamo current flowing to the west is accompanied by northern and southern return currents in regions where the heating and buoyant rise is smaller, so that the overall current looks like a figure eight [2]. This process induces a current in the ground in the opposite direction, due to the finite conductivity of the ground the current in the ground becomes accompanied by an electric field in the same direction. This is illustrated in Figure 11.

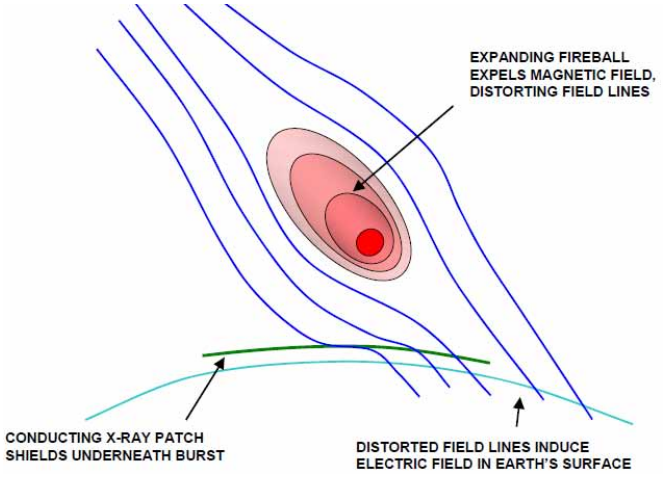

Figure 10: E3 Blast Wave

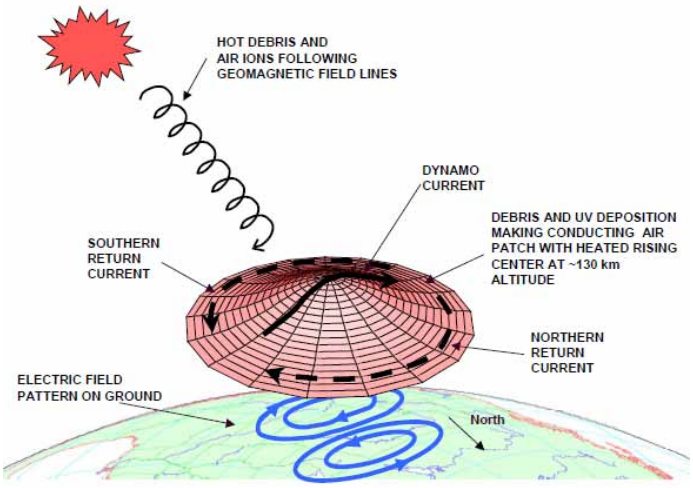

Figure 11: E3 Heave

There are several points that are important when considering the formation of the E3 pulse. The first is that the debris and UV processes depends on the altitude of the burst. For very high-altitude bursts, where the debris expansion is largely magnetically contained, a portion of the downward directed debris expansion impinges upon and is contained by the earth atmosphere and ionosphere [2]. As the height of the burst is lowered the amount of shock heated air ions and the attendant energy deposition in the neutral atmosphere is decreased. For bursts below 200 km, UV processes increasingly contribute to heating of the neutral atmosphere. The peak heating region for UV processes is centered below the burst. Second, energy deposition occurs during the first few seconds following the burst. As the heated energy deposition atmosphere begins to rise it traverses the air above it and pushes the E-region of the ionosphere along in its upward motion. Within 10-20 seconds this region can reach supersonic velocities. High conductivity regions in the E region of the ionosphere act as a perfect conductor out to several hundred kilometers horizontally. As a result, the horizontal component of the geomagnetic field is trapped between this "perfect" conducting atomic ionization layer and the earth, such that as the heave region rises the spacing of the geomagnetic field lines beneath the heaving layer is stretched out and the horizontal component decreases. This process continues until the ionization of the heave region decreases to a value where it fails to act like a perfect conductor. As the magnetic flux begins to slip through this region, the magnetic field between the layer and the earth relaxes to its ambient state [2].

In summary, the first process is an ionospheric blast that deforms the geomagnetic field lines and produces an early phase of the MHD-EMP. This reaches the Earth's surface in 2 to 10 seconds and can be seen worldwide. The second effect is what is known as the "atmospheric heave", in which hot debris and air ions are moved across geomagnetic field lines to cause large circulating currents in the

ionosphere [11]. These ionospheric currents induce image currents in the ground over a period of 10 to 100 seconds. The field strengths although being small in amplitude, approximately tens of volts per kilometer, occur over long times and thus can cause problems for long power and communication lines [11].

5.1.1 HEMP Standards

There are several HEMP environment standards, some are classified such as DoD-STD-2169 others are public knowledge such as IEC STD 61000-2-9. The first HEMP environment standard to exist was one created by Bell Labs in the 1960s. Since then revisions have been made to this environment and the most common one in use today is the IEC 61000-2-9, which is the HEMP environment that will be used in this report. Unclassified HEMP standards are characterized by idealized double exponential (DEXP) and quotient exponential (QEXP) waveforms. The HEMP standards are derived by enveloping (in time and frequency domains) many possible waveforms. Then, a mathematical model is created that best expresses both the temporal as well as the spectral characteristics of the envelope [15].

The environments that define these parameters are listed in Table 1. Within the table is a history of HEMP environments from the 1960s onwards. With each environment is associated a specific model.

Table 1: Parameters of Unclassified HEMP Standards

Parameter	Bell Labs (1960s) DEXP	IEC-77C (1993) DEXP	Leuthauser (1994) QEXP	VG95371-10 (1995) DEXP	IEC 61000-2-9 (1996) DEXP
Reference	[6]	[7]	[8]	[9]	[12]
$t_{10\%-90\%}$	4.6 ns	2.5 ns	1.9 ns	0.9 ns	2.5 ns
Peak Field E_o	50 kV/m	50 kV/m	60 kV/m	65 kV/m	50 kV/m
FWHM	184 ns	23 ns	23.8 ns	24.1 ns	23 ns
constant	1.05	1.3	1.08	1.085	1.3
α (1/sec)	$4x10^6$	$4x10^7$	$2.20x10^9$	$3.22x10^7$	$4x10^7$
β (1/sec)	$4.76x10^8$	$6x10^8$	$3.24x10^7$	$2.07x10^9$	$6x10^8$
Energy Density (J/m^2)	0.891	0.114	0.167	0.196	0.114

5.1.2 Ground HEMP Interface

When the HEMP waveform interacts with the ground, two ground parameters determine the nature of the interaction. The conductivity of the soil, and the dielectric constant of the soil. Table 2 is a list of nominal values for the soil conductivity and dielectric constant from a particular terrain.

Soil conductivity is dependendent on the soil constituents and moisture content; soils containing copious amounts of soluble ions have larger conductivities than those whose soluble ions have been leached out after years of heavy rainfall and runoff. The values in Table 2 are nominal values of the soil conductivity; conductivities within a given type may vary over a range of at least an order of magnitude because of differences in constituents. [13]

The dielectric constant of soil and rock also depends on their constituents. The range of values of the dielectric constant of soil is much smaller than that of soil conductivity because the primary

Table 2: Nominal Values of Dielectric Constant and Conductivity for Surface Soil and Water [13]

Terrain	Dielectric Constant, ϵ_r	Conductivity, σ (mhos/m)
Dry, Sandy Coastal Land	10	$2x10^{-3}$
Marshy, Forested Flat Land	12	$8x10^{-3}$
Rich agricultural land	15	$1x10^{-2}$
Pastoral land, Medium hills	13	$5x10^{-3}$
Rocky land, Steep hills	10	$2x10^{-3}$
Mountainous regions	5	$1x10^{-3}$
Fresh Water	80	$5x10^{-3}$
Sea Water	80	4

constituents affecting the dielectric constant are pulverized stone and water. The value of the dielectric constant is relatively independent of frequency, although some change is observed with large changes in frequency. [13]
Table 3 illustrates the change of the dielectric constant with frequency.

Table 3: Dependence of dielectric constant on frequency. [13]

Material	Composition	Temperature (° C)	ϵ_r			
			10^3 Hz	10^6 Hz	10^8 Hz	10^9 Hz
Soil	Sandy dry	25	2.91	2.59	2.55	2.55
Soil	Loamy dry	25	2.83	2.53	2.48	2.44
Ice	From pure distilled water	-12		4.15	3.45	3.20
Snow	Freshly Fallen	-20	3.33	1.20	1.20	1.20
Snow	Hard-packed followed by rain	-6		1.55		1.5
Water	Distilled	25		78.2	78	76.7

The dielectric constant, like the soil conductivity, is reduced when the soil becomes frozen. [13]
The Earth's conductivity and permittivity are important for two reasons. The total driver of the coupling is the incident E1 HEMP pulse plus its reflection off the ground. Second, the coupled wire signals are manifested by voltage and current pulses on the line, but really involve electromagnetic energy around the wire, including the ground. For this reason the wire height and ground parameters are important [1].

Interaction of Soil and Plane Wave

At the surface of the earth, part of the incident wave is reflected back into the air and part is transmitted into the soil. Conductors above the surface of the earth are driven by the total electric field (incident plus reflected) plane waves. The reflected waveforms are imbedded in the equation for the total electric field. This implies that the only equations that need to be considered are the horizontal and vertical waveform equations. [13] The expressions for vertical polarization of the incident field, with suppressed time-dependence, are

$$E_{zv}(h,z) = E_{iv}e^{-jkzcos(\Psi)cos(\Phi)}(1 - R_v e^{-jk2hsin(\Psi)})sin(\Psi)cos(\Phi) \tag{7}$$

$$E_x(h,z) = E_{iv}e^{-jkzcos(\Psi)cos(\Phi)}(1 + R_v e^{-jk2hsin(\Psi)})cos(\Phi) \tag{8}$$

where R_v is the Fresnel reflection coefficient for a vertically polarized wave, defined by

$$R_v = \frac{\epsilon_r(1 + \frac{\sigma}{j\omega\epsilon})sin\Psi - [\epsilon_r(1 + \frac{\sigma}{j\omega\epsilon}) - cos^2\Psi]^{\frac{1}{2}}}{\epsilon_r(1 + \frac{\sigma}{j\omega\epsilon})sin\Psi + [\epsilon_r(1 + \frac{\sigma}{j\omega\epsilon}) - cos^2\Psi]^{\frac{1}{2}}} \tag{9}$$

. Fresnel equations describe the behaviour of light when moving between media of differing refractive indices.
For horizontal polarization of the incident field, the fields at a height h above the ground are

$$E_x(h,z) = 0 \tag{10}$$

Where E_x is the vertical polarization field.
E_{zh} is the horizontal polarization field, at a height h above the surface.

$$E_{zh}(h,z) = E_h sin\Phi(1 + R_h e^{-j2khsin\Psi})e^{-jkzcos\Phi cos\Psi} \tag{11}$$

R_h is the reflection coefficient for the horizontally polarized wave given by:

$$R_h = \frac{sin\Psi - [\epsilon_r(1 + \frac{\sigma}{j\omega\epsilon}) - cos^2\Psi]^{\frac{1}{2}}}{sin\Psi + [\epsilon_r(1 + \frac{\sigma}{j\omega\epsilon}) - cos^2\Psi]^{\frac{1}{2}}} \tag{12}$$

In these expressions σ, ϵ_r and $\epsilon = \epsilon_o\epsilon_r$ are the conductivity, dielectric constant, and permittivity of the soil. The variable $k = \omega\sqrt{\mu_o\epsilon_o}$ is the phase factor (or wave number) for the air. The magnitudes for the reflection coefficients R_v and R_h are between 0 and 1.0. For a perfectly conducting ground ($\sigma \longrightarrow \infty$), $R_h = -1$ and $R_v = 1$. [13]
For an arbitrary polarization of the incident wave the electric field can be resolved into its vertically polarized and horizontally polarized components:

$$E_i = \vec{v}E_{iv} + \vec{h}E_{ih} \tag{13}$$

where

$$E_{iv} = E_i cos(\theta) \tag{14}$$

$$E_{ih} = E_i sin(\theta) \tag{15}$$

$\vec{v}$ and $\vec{h}$ are unit vectors in the plane of incidence and normal to the plane of incidence.

5.2 The Antenna System

Figure 12: HEMP and Antenna System Model

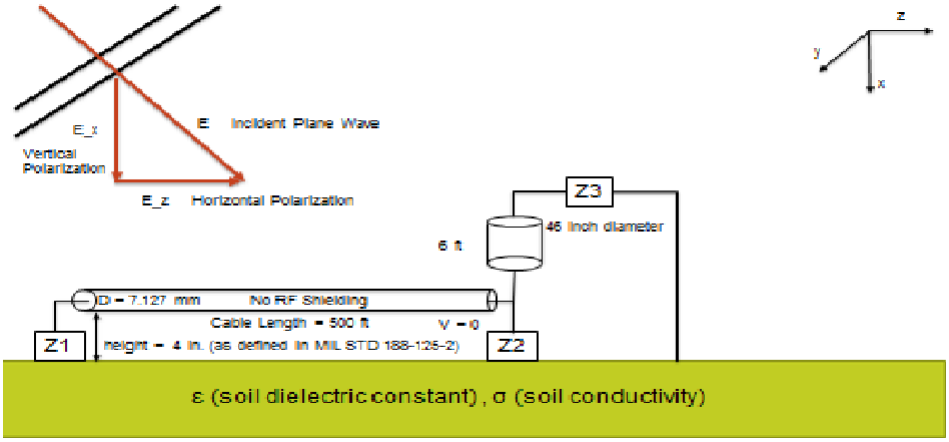

The antenna has a circular reflector with a diameter of 46 inches, or 0.5892m. It is sits on a pedestal that is between 4 ft to 6 ft (1.2191 m to 1.8288 m) off the ground. On the antenna pedestal is an electronics box that protects the antenna electronics from HEMP effects. The antenna electronics are connected to a grounding system. The grounding system is a level of protection that is used to make sure voltages built up on the 500 ft (152.4 m) cable doesn't effect the electronics on the antenna. The grounding system is composed of overvoltage protection elements, such as surge protectors, MOV's, or spark gaps. The power cable is connected to other equipment that is either HEMP shielded or does not have to be.

The dielectric constant and conductivity of the ground effect the reflections of the electromagnetic field on the Earth ground interface. All parameters of the geometric relationship between the system and its environment (height above ground, area, etc. etc.) are in accordance with MIL STD 188-125-2. The standard [10] states that all cables shall only be a height of 4 in (10 cm) from the ground surface. If a cable is to be higher than 10 cm from the ground than the total area between the cable and ground must be less than 30 m^2. Figure 13 below from [10] displays all required specifications.

Figure 13: MIL STD 188-125-2 Specifications

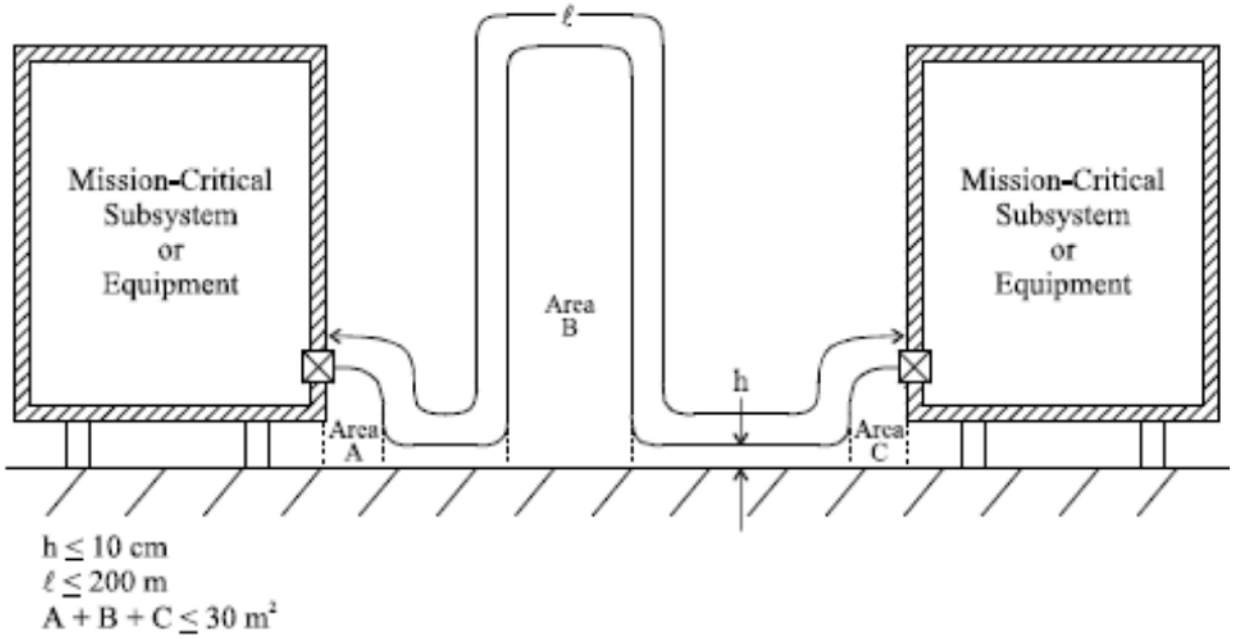

a. Intrasite cable.

5.2.1 Antenna Cable

The importance of the length, height and diameter of the cable delivering power to the antenna electronics is related to how well the electromagnetic field couples to the cable. How the electromagnetic pulse couples to the cable is described pictorially in Figure 14.
There are several aspects to the problem of the electromagnetic pulse coupling to the antenna cable. Only the part of the electric field that is parallel to the cable couples to the cable. This type of coupling varies as the cosine of the angle between the line and the E1 electric field. It isn't only the incident field that couples to the cable but the total electric field. As in both the reflected and the incident plane waves couple to the cable. The horizontal component of the electric field tends to decrease with the coupling of the reflected pulse, and the vertical electric field tends to increase. The reflected pulse shape and amplitude depend on ground parameters and is frequency dependent. There is even more variation if the frequency dependence of the ground parameters is taken into account. Next the signal that is generated on the wire propogates toward both ends. These signals are like the transverse electromagnetic signals on transmission lines [1]. This is not a perfect TEM signal because some of the electromagnetic field is in the ground, which slows down the propagating signal. The closer the cable is to ground the more the signal speed is decreased and the greater attenuation of the signal. The wire orientation will change the way that the cable couples to the electromagnetic field. If the cable is oriented 90 degrees relative to the pulse, E1 HEMP excites the full cable all at once. Then the pulse would drain off the line at both ends. If the cable is oriented towards the burst (near the tangent and the wire radial) then the pulse will not couple to the cable at all (for perfect parallel to the wire conditions). Slightly off perfect orientation of the cable will cause build up of currents at the end of the cables. As the signal speed on the wire will be less than the speed of the pulse (which is, c, the speed of light) there is no way to get perfect phasing between the two signals. In terms of transmission line theory, the slower signal speed along the cable can be considered to be

from increased inductance.

Figure 14: Coupling to the Antenna Cable [1]

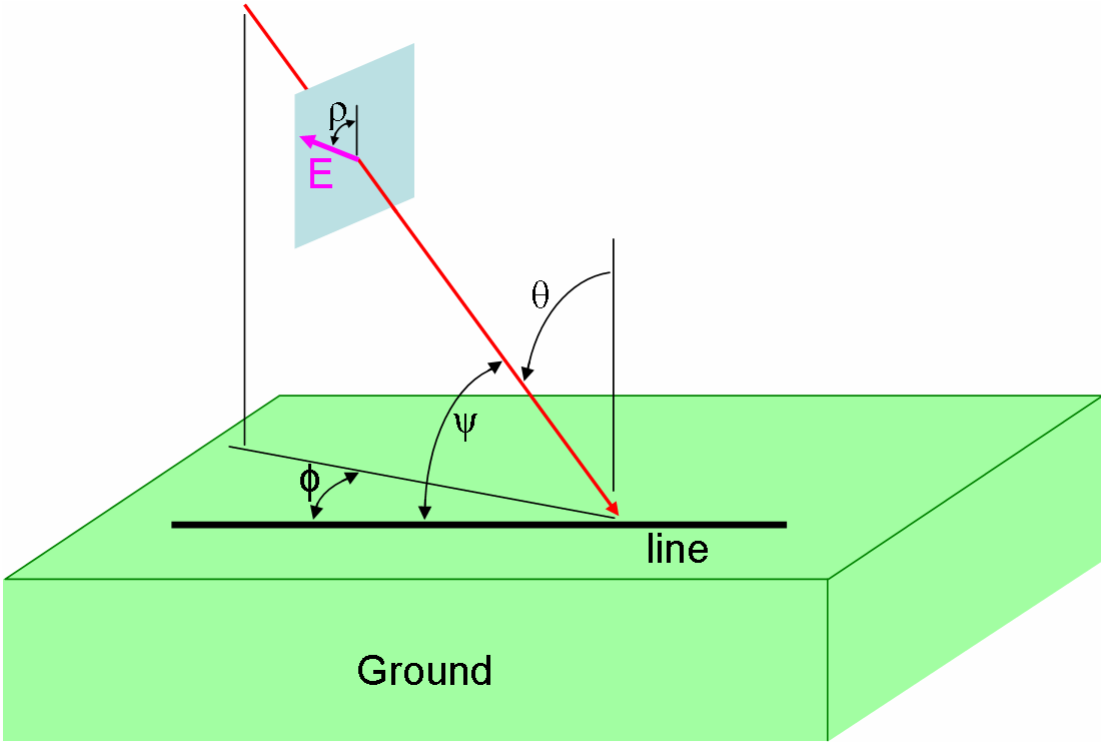

$$v = \frac{1}{\sqrt{L * C}} \tag{16}$$

Where L is the inductance per-unit length and C is the admittance per-unit-length. For a perfectly conducting ground this velocity v would be equivalent to the speed of the pulse ,c, which is the speed of light. In going from perfect to imperfect ground, we get an increase in the inductance, and proportionally less decrease in the capacitance which causes a reduction of the speed of the signal along the cable. There are also losses associated with the coupling of the electromagnetic wave to the cable. These come from both the wire resistance and the ground losses. Typically for long cables there comes a point in increasing the wire length where there is little effect from having a longer length, any signal that is generated farther out is attenuated too much when it gets to the wire end [1]. At the wire ends of a finite cable, some of the energy of the signal gets absorbed by the loads, and some can be reflected back into a signal going back down the line. The line and load impedances determine the split of energy between the load and reflection. If the line is short the reflected energy would eventually be incident on the other end of the line [1]. The load circuit also includes the grounding resistance. Thus the transmission line has a return path in currents in the ground and the ground rod resistance is part of the circuit. Along with the horizontal part of the wire there is also the vertical cables that must be considered. The coupling to the vertical cables is similar to the coupling to the horizontal cables but it is driven by the vertical part of the E1 HEMP field.


Figure 15: A Cassegrain antenna (left) Gregorian antenna (right)

5.2.2 Types of Antennas

The type of antenna used for this particular SATCOM system is a parabolic antenna. Parabolic antennas come in many styles but they are all considered reflector antennas. Reflector antennas utilise the fact that electromagnetic waves can be reflected to a focal point using a metal plate. These antennas usually take one of two forms, the corner reflector, or the parabolic reflector and are generally characterised by having a very high gain. The reflector itself is not the antenna and therefore some form of conventional antenna is placed at the focal point of the reflector for example a monopole. Typical parabolic reflectors have a very high gain (30-40 dB is common) and a low cross polarization. Parabolic antennas can be seperated into the types of feeds they use. Antenna feed refers to the components of an antenna which feed the radio waves to the rest of the antenna structure, or in receiving antennas collect the incoming radio waves, convert them to electric currents and then transmit them to the receiver. Antennas typically consist of a feed and additional reflecting or directive structures whose function is to form the radio waves from the feed into a beam or other desired radiation pattern. The feed consists of a dipole driven element, which converts the radio waves to an electric current, and a coaxial cable or twin lead transmission line conducts the received signal from the antenna into the receiver. The Gregorian style antenna is a type of antenna used at Earth Station, it has a similar design to a Cassegrain antenna only the Gregorian antenna's secondary reflector is concave vs. convex for the Cassegrain antenna. Thus a Gregorian antenna has a double reflector antenna with the second reflector located at a distance greater than the main reflector. The disadvantage of the Gregorian antenna to the Cassegrain style is that it is less compact.
The Cassegrain antenna is a subcategory of reflector antennas. The Cassegrain antenna consists of two reflectors (primary and secondary) and a feeder. The main characteristics of Cassegrain antennas is their high directivity. The bigger diameter of antenna reflector that is used, the better the gain that is achieved. Typical applications for the Cassegrain antenna are radar, space communication, radio astronomy, and wireless communication.
In telecommunications and radar, a Cassegrain antenna is a parabolic antenna in which the feed radiator is mounted at or behind the surface of the concave main parabolic reflector dish and is aimed at a smaller convex secondary reflector suspended in front of the primary reflector. The beam of radio waves from the feed illuminates the secondary reflector, which reflects it back to the main reflector dish, which then reflects it forward again to form the desired beam.
The advantages of the Cassegrain antenna are as follows. The feed antennas and associated waveguides and "front end" electronics can be located on or behind the dish, rather than suspended in front where they block part of the outgoing beam. The feed antenna is directed forward, rather than backward toward the dish as in a front-end antenna, the spillover side lobes caused by portions of the beam that miss the secondary reflector are directed upwards toward the sky rather than downwards toward the earth. The presence of a second reflector in the signal path allows additional opportunities for

tailoring the radiation pattern for maximum performance.
The disadvantage of using a Cassegrain is that the feed horn must have a narrower beamwidth (higher gain) to focus its radiation on the smaller secondary reflector, instead of the wider primary reflector as in front-fed dishes. The angular width of the secondary reflector subtends at the feed horn is typically 10 - 15 degrees, as opposed to 120 - 180 that the main reflector subtends in a front-fed dish. Therefore the feed horn must be longer for a given wavelength. The feed horn is used to direct radio waves into a beam. Usually used for UHF and microwave frequency, which is above 300 MHz.
The gain and directivity are quantities which define the ability to concentrate energy in a particular direction and are directly related to the antenna radiation pattern. The fields across the aperture of the parabolic reflector is responsible for the antenna's radiation. Directivity or gain is the ratio of the power radiated by an antenna in its direction of maximum radiation to the power radiated by a reference antenna in the same direction. The gain for a parabolic antenna is:

$$G = \frac{6D^2}{\lambda^2} \tag{17}$$

5.2.3 Antenna Electronic System

The antenna electronics include several "black boxes" of electronics. These boxes are typically over-voltage protected using circuits designed for this purpose. These circuits can include anything from MOVs (Metal Oxide Varistors) to avalanche diodes, depending on the expected overvoltage. These electronics are typically also encased in some sort of HEMP shielded box. The box itself is usually located on the antenna pedestal, and has short shielded cables connecting this box to the rest of the antenna. The length of the cables can vary but most are within two to four feet long. This cable could act as an antenna and potentially induce a current inside the black box that would destroy or disrupt the electronics used for communication.

5.3 Coupling of Above Ground Cables

As was noted in the previous section, the voltage and current induced on a conductor by a plane wave incident on the surface can be approximated by treating the conductor as a transmission line with a distributed source, which is the resultant field $E_z(h, z)$. "The resultant field is divided into two parts: that which exists if the reflecting surface is a perfect reflector and a correction for the fact that imperfect reflection occurs"[13]. For coupling analysis most metals can be considered perfect reflectors. For typical soils, the correction term may be larger than the part attributed to perfect reflection. Therefore, imperfect conductivity, or imperfect reflectivity, of the soil is almost always important, and is sometimes dominant, in the analysis of above-ground conductors.[13]

5.3.1 Transmission Line Model

When analyzing the coupling of electromagnetic waves to transmission lines and similar structures, the source voltage is considered a distributed source voltage. A distrbuted source voltage is, by definition, one that has an increment of source voltage in each increment of line length [13]. This transmission line is identical to classical transmission lines, and the impedance per unit length and the admittance per unit length are as follows:

Figure 16: Equivalent transmission line model

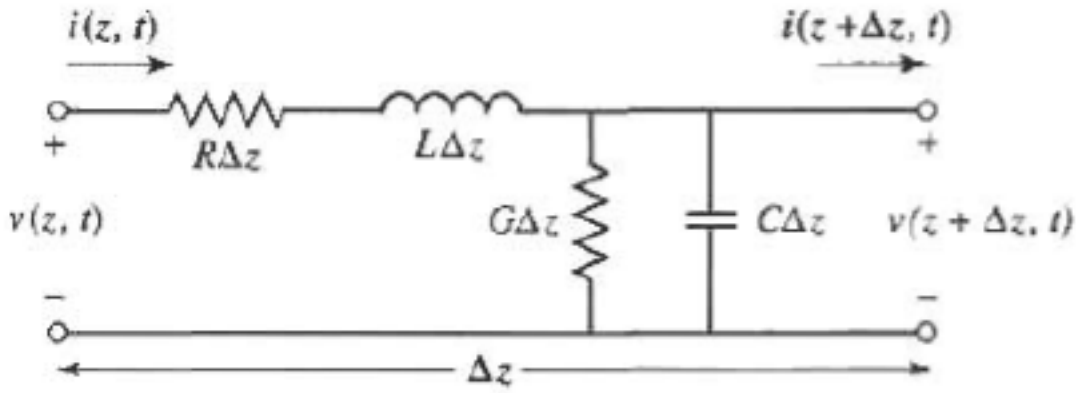

$$Z = R + j\omega L \tag{18}$$

$$Y = G + j\omega C \tag{19}$$

.

The differential equations for the voltage and current along the transmission line of Figure 16, for harmonically varying signals ($e^{j\omega t}$), are

$$\frac{dV}{dz} = E_z - IZ \tag{20}$$

$$\frac{dI}{dz} = -VY \tag{21}$$

By taking the integral and solving for I(z) and V(z), the solutions are:

$$I(z) = [K_1 + P(z)]e^{-\gamma z} + [K_2 + Q(z)]e^{\gamma z} \tag{22}$$

$$V(z) = Z_o([K_1 + P(z)]e^{-\gamma z} - [K_2 + Q(z)]e^{\gamma z}) \tag{23}$$

where

$$P(z) = \frac{1}{2Z_o}\int_{Z_1}^{Z} e^{\gamma v} E_z dv \tag{24}$$

$$Q(z) = \frac{1}{2Z_o}\int_{Z}^{Z_2} e^{-\gamma v} E_z dv \tag{25}$$

The solution to the integrals P(z) and Q(z) are different for horizontal and vertical polarizations. For the horizontal polarization the solution becomes:

$$P(z) = \frac{E_{ih} sin(\phi)(1 + R_h e^{-j2khsin(\psi)})}{2Z_o(\gamma - jkcos(\psi)cos(\phi))}(e^{z(\gamma - jkcos(\psi)cos(\phi))} - e^{z_1(\gamma - jkcos(\psi)cos(\phi))}) \tag{26}$$

$$Q(z) = \frac{E_{ih} sin(\phi)(1 + R_h e^{-j2khsin(\psi)})}{2Z_o(-\gamma - jkcos(\psi)cos(\phi))}(e^{-z2(\gamma - jkcos(\psi)cos(\phi))} - e^{-z(\gamma - jkcos(\psi)cos(\phi))}) \tag{27}$$

For vertical polarization of the incident field along the z-axis (horizontal axis):

$$P(z) = \frac{E_{iv}(1 - R_v e^{-jk2hsin(\psi)})sin(\psi)cos(\phi)}{2Z_o(\gamma - jkcos(\psi)cos(\phi))}(e^{z(\gamma - jkcos(\psi)cos(\phi))} - e^{z1(\gamma - jkcos(\psi)cos(\phi))}) \tag{28}$$

$$Q(z) = \frac{E_{iv}(1 - R_v e^{-jk2hsin(\psi)})sin(\psi)cos(\phi)}{2Z_o(-\gamma - jkcos(\psi)cos(\phi))}(e^{-z2(\gamma + jkcos(\psi)cos(\phi))} - e^{-z(\gamma + jkcos(\psi)cos(\phi))}) \tag{29}$$

The constants K_1 and K_2 are determined from the terminating impedances Z_1 and Z_2, and Z_o is the characteristic impedance given by $Z_o = \sqrt{\frac{Z}{Y}}$, as in conventional transmission lines [13]. Where

$$K_1 = \rho_1 e^{\gamma z_1} \frac{\rho_2 P(z_2) e^{-\gamma z_2} - Q(z_1) e^{\gamma z_2}}{e^{\gamma(z_2 - z_1)} - \rho_1 \rho_2 e^{-\gamma(z_2 - z_1)}} \tag{30}$$

$$K_2 = \rho_2 e^{\gamma z_2} \frac{\rho_1 Q(z_1) e^{-\gamma z_1} - P(z_2 e^{\gamma z_1}}{e^{\gamma(z_2 - z_1)} - \rho_1 \rho_2 e^{-\gamma(z_2 - z_1)}} \tag{31}$$

the reflection coefficients ρ_1 ρ_2 at the ends of the line are given by [13]

$$\rho_1 = \frac{Z_1 - Z_o}{Z_1 + Z_o}, \rho_2 = \frac{Z_2 - Z_o}{Z_2 + Z_o} \tag{32}$$

These calculations are based on the assumption that the low-frequency characteristic impedance of the aerial line can be used at frequencies where the line height is a few wavelengths. [13]

The series impedance per unit length is composed of three components. The inductive reactance (which is associated with the magnetic field between cable and ground), the internal impedance of the ground plane, and the internal impedance of the cable. [13]

The series per-unit-length inductive reactance, Z_l' is given by

$$Z_l' = j\omega \frac{\mu_o}{2\pi} arcosh(\frac{h}{a}) \simeq j\omega \frac{\mu_o}{2\pi} ln(\frac{2h}{a})(a \ll h) \tag{33}$$

The admittance per unit length is usually dominated by the capacitive reactance [13]. Where Y_l' is:

$$Y_l' = j\omega \frac{2\pi\epsilon_o}{arcosh(\frac{h}{a})} \simeq j\omega \frac{2\pi\epsilon_o}{ln(\frac{2h}{a})} (a \ll h) \tag{34}$$

Added with these typical transmission line elements, the series per-unit-length impedance elements Z_w' and Z_g' which account for the internal wire impedance and the earth return impedance also affect coupling. [4]. The internal wire impedance is [4]:

$$Z_w' = \frac{\gamma_w}{2\pi a \sigma_w} \frac{I_o(\gamma_w a)}{I_1(\gamma_w a)} \tag{35}$$

$I_o()$ and $I_1()$ are modified Bessel functions, and γ_w is the complex propagation constant in the wire material:

$$\gamma_w = \sqrt{j\omega\mu_o(\sigma_w + j\omega\epsilon_w\epsilon_o)} \tag{36}$$

An approximation of the internal impedance per unit length of the finitely conducting ground plane is given by [13]:

$$Z_g \approx \frac{\omega\mu}{8} + j\omega \frac{\mu}{2\pi} log \frac{\delta}{\sqrt{2}\gamma_o h} \tag{37}$$

where:

$$\gamma_s = \sqrt{j\omega\mu(\sigma + j\omega\epsilon)}, \delta = \frac{1}{\sqrt{\pi f \mu \sigma}}, \gamma_o = 1.7811 \tag{38}$$

Another approximate and accurate expression for this term is provided by Sunde [4] [14] as

$$Z_g' \approx \frac{j\omega\mu}{2\pi} ln[\frac{1 + \gamma_g h}{\gamma_g h}] \tag{39}$$

Using the above parameters it is possile to define the total per-unit-length impedance and admittance parameters for the transmission line [4] as

$$Z'(\omega) = Z_l' + Z_w' + Z_g' \tag{40}$$

For most practical problems involving power lines, aerial communications cables etc., over soil, the internal impedance of the cable can be neglected. If the ground plane is metal and the height is only slightly larger than the radius, the internal impedance of the ground plane may be comparable to that of the cable. [13]

5.3.2 Effects of Changing the Ground Plane

When soil is used as the ground, or return path, the characteristic impedance and propagation factor of a wire with radius a and height h above the ground plane[13] is:

$$Z_o \approx \sqrt{\frac{L}{C}} (1 + \frac{1}{2log\frac{2h}{a}} [log(\frac{1 + \sqrt{j\omega\tau_h}}{\sqrt{j\omega\tau_h}} + \frac{1}{\sqrt{j\omega\tau_a}})]) \tag{41}$$

and the propagation factor is:

$$\gamma \approx j\omega\sqrt{LC}(1 + \frac{1}{2log\frac{2h/}{a}}[log\frac{1+\sqrt{j\omega\tau_h}}{\sqrt{j\omega\tau_h}} + \frac{1}{\sqrt{j\omega\tau_a}}]) \tag{42}$$

where:
$\sqrt{\frac{L}{C}} = 60\ log\frac{2h}{a}$
$\sqrt{LC} = \frac{1}{c}$
$\tau_h = \mu_o\sigma h^2$
$\sigma = soil\ conductivity$
$\mu_o = 4\pi x10^{-7}H/m$
$\sigma_c = cable\ shield\ conductivity$
$\mu_c = cable\ shield\ permeability$
$c = 3x10^8 m/s(speed\ of\ light)$

When the metal cable is over soil it is typically the case that the $\frac{1}{\sqrt{j\omega\tau_a}}$ term is negligible compared to the log term in the brackets [13]. When $\sqrt{\omega\tau_h} \gg 1$, the term in the brackets becomes very small and:

$$Z_o \approx 60log\frac{2h}{a}\gamma \approx \frac{j\omega}{c} = jk \tag{43}$$

When the cable is over a metal ground plane the characteristic impedance and propagation factor for a cable of radius a at a height h [13] are:

$$Z_o = 60cosh^{-}1(\frac{h}{a}) \approx 60log(\frac{2h}{a})(h \gg a) \tag{44}$$

the propagation factor is:

$$\gamma = \alpha + jk \tag{45}$$

where:
$k = w/c$
$\alpha = \frac{1}{2Z_o}[\frac{1}{2\pi a}\sqrt{\frac{\pi f\mu_c}{\sigma_c}} + \frac{1}{4\pi h}\sqrt{\frac{\pi f\mu}{\sigma}}]$
$\mu_c = Permeability\ of\ cable\ shield$
$\sigma_c = Conductivity\ of\ cable\ shield$
$\mu = Permeability\ of\ ground\ plane$
$\sigma = Conductivity\ of\ ground\ plane.$

5.4 Simulation Tools

There are many different types of software that can be used to simulate the HEMP environment and how the pulse induces currents along the antenna and 500 ft cable. Two of these different softwares were used within the scope of this analyses. The first was the Numerical Electromagnetics Code, the second was done in Matlab using the transmission line model developed in [13].

5.4.1 Numerical Electromagnetic Code

The Numerical Electromagnetics Code or NEC is a popular antenna modeling software package for wire and surface antennas. For the scope of this analyses it is being used to analyze the induced currents along the cable and antenna by an incident plane wave. The first iteration of NEC was developed in the 1970's and originally written in Fortran. Since its development there have been several more iterations of NEC; in this report NEC version 4.2 was used. NEC 4.2 remains proprietary with the Lawrence Livermore National Laboratory and the University of California and it requires a license. Although NEC 4.2 is not publicly available this analysis can also be done in MININEC which is publicly available. The only difference is that NEC 4.2 offers double precision that allows for the simulation of larger models.

The NEC is based on the method of moments solution of the electric field integral equation for thin wires and the magnetic field integral equation for closed, conducting surfaces. The algorithm has no theoretical size limit and can be applied to very large arrays or for detailed modeling of very small antenna systems, but the implementation has many practical limits. NEC models can include wires buried in a homogeneous ground, insulated wires and impedance loads.

The method of moments is a method of estimation of population parameters. It starts with deriving equations that relate the population moments (i.e., the expected values of powers of the random variable under consideration) to the parameters of interest. Then a sample is drawn and the population moments are estimated from the sample. The equations are then solved for the parameters of interest, using the sample moments in place of the (unknown) population moments. This results in estimates of those parameters.

NEC is built around the numerical solution of integral equations for the currents induced on the structure by sources or incident fields. This approach avoids many of the simplifying assumptions required by other solution methods and provides a highly accurate and versatile tool for electromagnetic analysis. The integral equation approach is best suited to structures with dimensions up to several wavelengths. Although there is really no theoretical size limit to the model, the numerical solution requires a matrix equation of increasing order as the structure size is increased relative to wavelength. Thus modeling larger structures requires more computer time and file storage that is practical on some machines [21].

Within NEC a wire segment is defined by the coordinates of its two end points and its radius. Modeling a wire structure with segments involves both geometrical and electrical factors. The main electrical consideration is the segment length δ relative to the wavelength λ. In most cases δ should be less than about 0.1 λ at the desired frequency. Within the context of the models used in this report 0.05 λ was used as the segment length. The wire radius, a, relative to λ is limited by the approximations of the electric field integral equation. Two approximations are available in NEC: the thin-wire kernel and the extended kernel, the current on the surface of a segment is reduced to a filament of current on the segment axis. In the extended thin-wire kernel, a current uniformly distributed around the segment surface is assumed [21].

In either of these approximations, only currents in the axial direction on a segment are considered, and

there is no allowance for variation of the current around the wire circumference. The acceptability of these approximations depends on both the value of $\frac{a}{\lambda}$ and the tendency of the excitation to produce circumferential current or current variation [21].
NEC includes a patch option for modeling surfaces using the magnetic-field integral equation. This formulation is restricted to closed surfaces with nonvanishing enclosed volume. For example, it is not theoretically applicable to a conducting plate of zero thickness and, actually, the numerical algorithm is not practical for thin bodies (such as solar panels).
There are other rules for the segment model.
Segments (or patches) may not overlap since the division of current between two overlapping segments may result in a singular matrix equation.
A large radius change between connected segments may decrease accuracy particulary with small $\frac{\delta}{a}$.
The problem may be reduced by making the radius change in steps over several segments.
A segment is required at each point where a network connection or voltage source will be located.
The two segments on each side of a charge density discontinuity voltage source shoud be parallel and have the same length and radius.
The number of wires joined at a single junctionn cannot exceed 30 because of a dimension limitation in the code.
When wires are parallel and very close together, the segments should be aligned to avoid incorrect current perturbation from offset match point and segment junctions [21].
NEC is programmed using "Data Cards", these data card decks for a single NEC run must begin with one or more comment cards which contain a brief description and structure parameters for the run. The cards after the comment cards must be a geometry card. Thus a CE card must always occur in a data deck and may be preceded by as many CM cards as are needed to describe the run. The next set of cards are the geometry input cards.
There are several of these cards, below is a table of the cards and their meaning.

For the purpose of this analysis and the models developed the most important geometry cards to understand would be the wire specification card GW and the geometry end card GE.
The wire specification cards purpose is to generate a string of segments to represent a straight wire. The card is defined by different parameters, these parametes are listed in the table below.

Table 5: Parameters of the GW card [21]

Parameter	ID	Description
ITG	I1	Tag number assigned to all segments of the wire.
NS	I2	Number of segments into which the wire will be divided.
XW1	F1	X coordinate
YW1	F2	Y coordinate
ZW1	F3	Z coordinate
XW2	F4	X coordinate
YW2	F5	Y coordinate
ZW2	F6	Z coordinate
RAD	F7	Wire radius, or zero for tapered segment option.

The GW card was used to create the model of the 500 ft cable (152.4 meters) in NEC, along with the grounding rods that are connected at the ends of the horizontal cable. Within the NEC model there were other geometry cards that were used that were important. Such as the GE card. The

Table 4: Geometry Cards [21]

Description	ID	Summary
Wire Arc Specificationl	GA	Used to generate a circular arc of wire segments
End Geometry Input	GE	Terminates reading of geometry data cards and reset geometry data if a ground plane is used.
Read Numerical Green's Function	GF	Read a previously written Numerical Green's Function ("NGF") file
Helix/Spiral Specification	GH	Generates a helix or spiral of wire segments.
Coordinate Transformation	GM	Translate or rotate a structure with respect to the coordinates system or to generate new structures translated or rotated from the original.
Generate Cylindrical Structure	GR	Reproduces a structure by rotating about the Z-axis to form a complete cylindrical array, and to set flags so that symmetry is utilized in the solution.
Scale Structure Dimensions	GS	Scales all dimensions of a structure by a constant.
Wire Specification	GW	Generates a string of segments to represent a straight wire.
Reflection in Coordinate Planes	GX	Forms structures having planes of symmetry by reflecting part of the structure in the coordinate planes, and to set flags so that symmetry is utilized in the solution.
Surface Patch	SP	Input parameters of a single surface patch
Multiple Patch Surfacce	SM	Cover a rectangular region with surface patches.

cards that were used in the NEC model are available in Appendix C of this report.
Other than the geometry cards there are other cards available in NEC that are called program control cards. The program control cards follow the structure geometry cards. They set electrical parameters for the model, select options for the solution procedure, and request data computation. The cards are listed below by their mnemonic identifier with a brief description of their functions [21].

There is no fixed order for the cards. The desired parameters and options are set first followed by requests for calculation of currents, near fields and radiated fields. Within this model the cards that were used were the FR, GN, LD, EX, XQ, and EN cards that were used. The parameters of each of these cards is available in Appendix C of this report.

5.4.2 MATLAB

MATLAB is a high-level language and interactive environment for numerical computation, visualization, and programming. MATLAB allows matrix manipulations, plotting of functions and data, implementation of algorithms, creation of user interfaces, and interfacing with programs written in other languages, including C, C++, Java, and Fortran. The transmission line model was developed in MATLAB and was used to create a second model of the HEMP environment and to analyze the

Table 6: Program Control Cards [21]

Group Number	ID	Description
Group I	EK	Extended thin wire kernal flag
	FR	Frequency Specification
	GN	Ground parameter specification
	LD	Structure impedance loading
Group II	EX	Structure excitation card
	NT	Two-port network specification
	TL	Transmission line specification
Group III	CP	Coupling calculation
	EN	End of data flag
	GD	Additional ground parameter specifications
	NE	Near electric field request
	NH	Near magnetic field request
	NX	Next structure flag
	PQ	Wire charge density print control
	PT	Wire-current print control
	RP	Radiation pattern request
	XQ	Execute card

induced currents along the cable and antenna.

6 Methodology

In order to analyze the coupling of the E1 pulse to the antenna system an analysis of the E1 pulse and its environment was completed. After this analysis then the development of the horizontal cable model was completed in both NEC and using a transmission line analysis developed in MATLAB. A comparison of these two analysis was done in order to verify the outputs of both the NEC and transmission line models at specific frequencies. Once this comparison was complete a larger NEC model was developed to calculate the total current developed at specific segments of the cable from the HEMP pulse.

6.1 Analyzing the E1 Pulse

The HEMP environment was taken from the IEC 61000-2-9 standard [12]. This model presents an enveloped expression of the E1 HEMP pulse that can be used to analyze various features of the pulse. The first analysis that was done was to compare the energy at specific times of the pulse. If we take the time domain graph of the HEMP pulse.

Figure 17: E1 Period Analysis

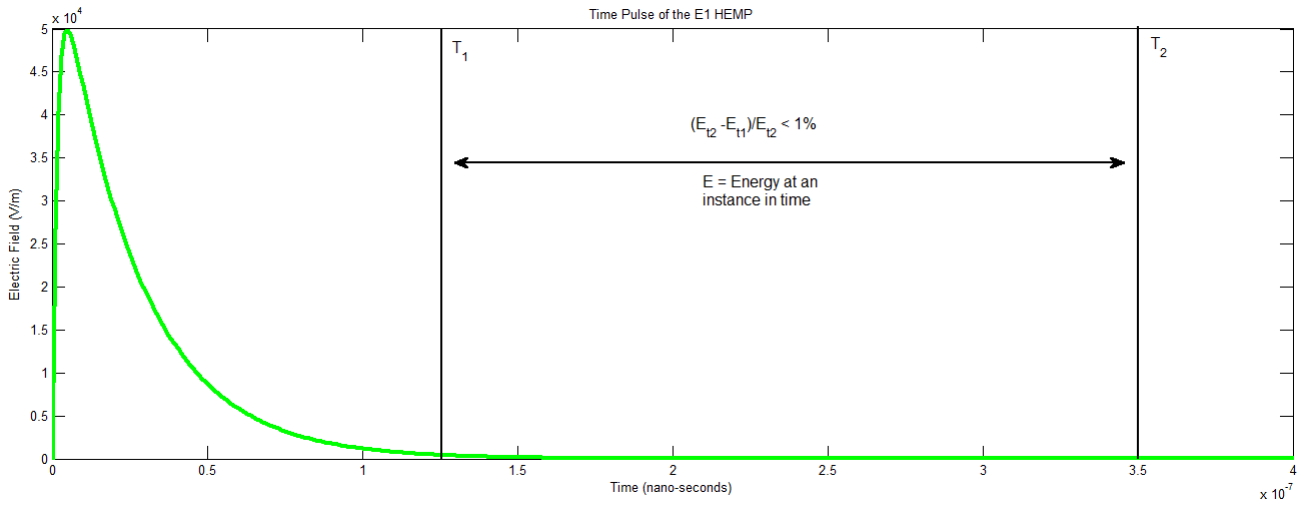

We can see that after a certain number of seconds the energy of this pulse decreases to zero. Deciding on what the maximum period of the pulse was, meant taking the integral of the pulse up to different times. Then comparing the energy lost when the pulse is integrated from time t=0 to t1 vs t=0 to t2. As long as this percentage was less then one percent then it could be assumed that time t1 was the correct length of the pulse in the time domain.
The next step in analyzing the pulse was by taking its frequency response and choosing the correct bandwidth. This was accomplished using the same method that was used to find the period of the pulse. By integrating to a frequency that would capture all of the E1 pulse and then integrating to an intermediate frequency F1, that could be used as the upper band limit of the HEMP pulse. If the percentage of energy lost was less than 1% then this frequency was used.

Figure 18: E1 Upper BandlimitAnalysis

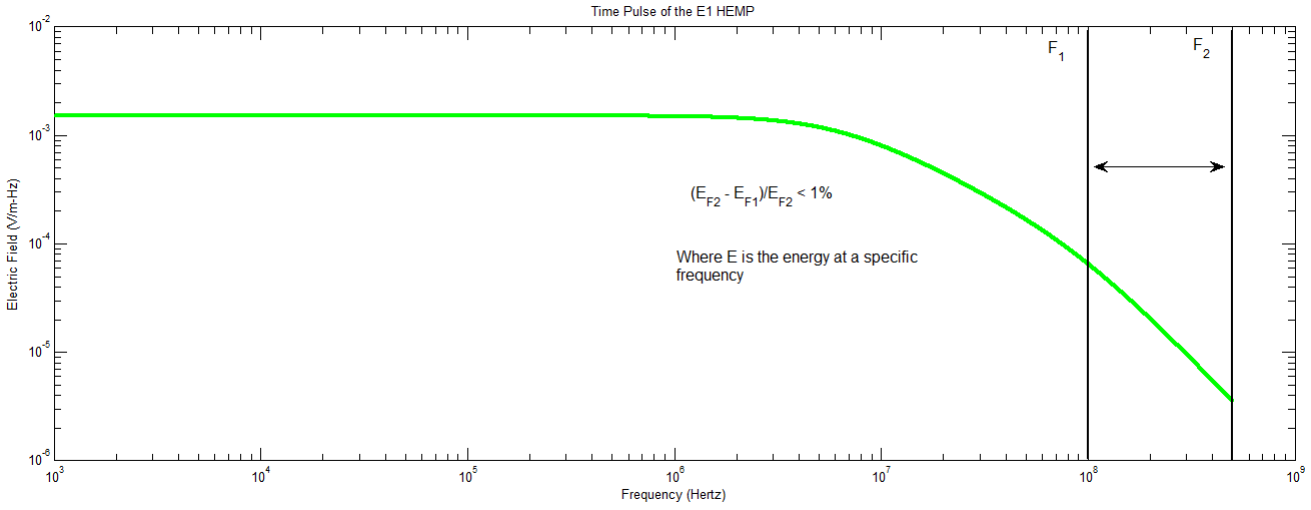

The period of the pulse and the upper band limit were then used to decide how many samples were required for the fourier transform. The reason the pulse had to be properly sampled for the fourier transform was to avoid aliasing after the inverse Fourier transform.Thus the proper sampling frequency and period had to be chosen in order to prevent aliasing while taking the fast fourier

transform and inverse fast fourier transform. This is important because the output of the NEC runs are given per frequency, so in order to reconstruct the data in the time domain, the inverse fourier transform of the pulse needs to be taken. The number of samples is also important because that tells us how many frequencies need to be run in NEC in order to properly recreate the effects of the pulse in the time domain within our model. NEC although being an extremely useful computational tool, can take a while to simulate a model depending on the size of the model. Limiting the amount of frequencies helps decrease the time required to run. These decisions were all made based off of the single analysis of the E1 HEMP pulse.
Prior to this analysis a model had to be developed in NEC that could be verified against some other model in order to guarantee that the information that was being produced by NEC was correct. As the cost of actually simulating a HEMP event was too great for the scope of this analysis, the best that could be done was to produce multiple models and verify that each one gave similar results to a given degree of accuracy.

6.2 Modeling the 500ft Antenna Power Line in NEC

There were two models developed of the 500 foot antenna power line. The first model was completed in NEC.

The code for this NEC model is available below. It represented one of the first models developed to describe the 500 ft power cable. The number of segments a was decided by taking $\frac{\lambda}{20}$ where λ is the wavelength of a 750 MHz signal ($\lambda = 0.4$ and $\Delta = 0.02$).
CE Model 1: 500 ft Power wire in Dry, Sandy Coastal Land, with HEMP pulse at 750 MHz

Table 7: Model 1 of the 500 ft cable[21]

CE	Model 1: 500 ft Power wire in Dry, Sandy Coastal Land, with HEMP pulse at 750 MHz
GW	1, 457, 0, 0, -3.048, 0, 0, 0, 0.00636
GW	2, 16, 0, 0, 0, 0, 0, 0.1016, 0.00636
GW	3, 7620, 0, 0, 0.1016, 152.4, 0, 0.1016, 0.00636
GW	4, 16, 152.4, 0, 0.1016, 152.4, 0, 0, 0.00636
GW	5, 457, 152.4, 0, 0, 152.4, 0, -3.048, 0.00636
GE	-1, 1
FR	0, 12, 0, 0, 62.5, 62.5
GN	2, 0, 0, 0, 13, .2
EX	1, 1, 1, 0, 45., 0., 0., .25, 1., 0., 50000
LD	4, 0, 473, 474, 10
LD	4, 0, 8093, 8094, 10
XQ	

Within this code it starts off with the comment card CE that describes the Model. The next cards are the geometery cards. The first GW card creates a wire, analyzing each specific piece of this card provides information on the ground rod. The first piece of information gives the tag number which is 1. The second element is the number of segments, 457. The next three elements identify the starting coordinates of the cable, which is X = 0, Y = 0, and Z = -3.048 meters. The reason the Z value is

negative is because it goes below the surface. The following three elements designate the end point of the wire, which is, X = 0, Y = 0, and Z = 0. Thus these elements say that the cable is terminating at ground. The reason for this is that NEC is unable to compute the effects of an incident wave when the cable goes through the ground-air interface. Thus the programmer must create a structure that ends and starts at this interface in order to bypass this. The final element in the first GW card is the radius of the cable. The radius of the wire was another design decision that was made in order to accomodate a specific amount of current flowing through the power cable. The actual power cable that will be feeding the antenna is composed of three cables, each capable of carrying 30 Amps of current , the wire gauge that is capable of this function is wire gauge number 7, whose maximum amperage for power transmission is 30 amps. The wire gauge that was chosen was wire gauge 6 to give some margin to work with, as wire gauge 6 can transmit a maximum of 36 Amps. The rest of the GW cards specificy the rest of the cable. As can be seen the 500 ft cable is broken into 7620 segments, which means that there will be 7620 different current calculations along the length of that cable for a given frequency.
The rest of the cards in Model 1 after the geometry end card, GE, define the environment and the pulse. The first card FR declares the frequency of the pulse from 62.5 MHz to 750 MHz in 12 steps. This can be seen by looking at the FR card, whose parameters are defined in Appendix C of this report. The next card the GN card defines the ground parameters. The ground parametes indicate that it is an imperfect ground with a dielectric constant of 13 and a ground conductivity of 0.2 Mho/m. The next card the EX card defines the excitation field, it is a plane wave with a magnitude of 50,000 V/m and has components in both the vertical and horizontal polarizations. The LD card defines the load impedances on the cable, these load impedances are contributed to the ground rods at the end of the cable, although the purpose of these grounding rods is to ground the currents along the cable they do not have perfect conductivities. Which gives them a small impedance of approximately 10 Ohms. The XQ card at the end tells the code to run. Once this model was run the outputs were compared to a second model developed using the transmission line equations in [13].

6.3 Creating the Transmission Line Model in Matlab

The transmission line model for the 500 ft cable was taken directly from [13]. The first steps in creating this model was to define important parameters that would change the amount of induced currents along cable for a specific frequency. These functions are the equations defined in [13]. These equations are available in the background section of this report. The following figure presents the flow chart of the functions used and how they all add up to give the current along the cable.

Figure 19: Flow Chart of Transmission Line Model

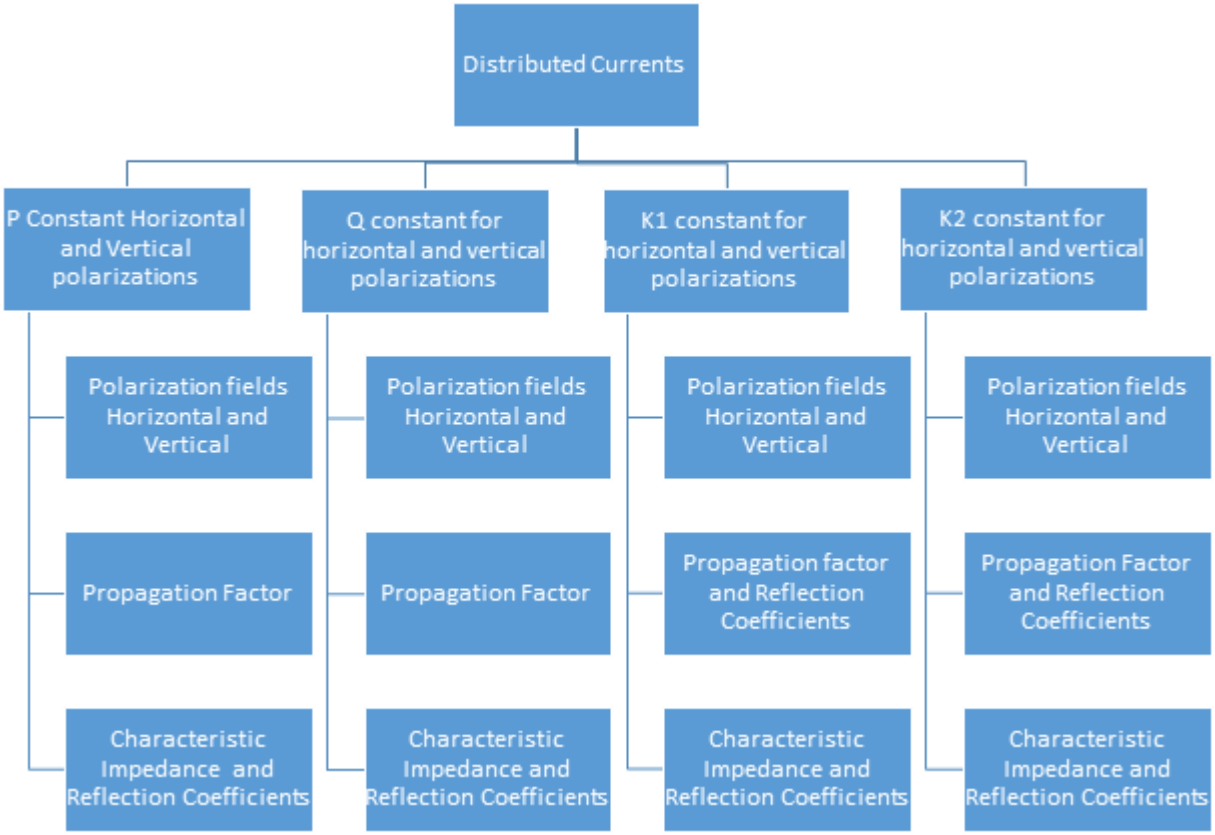

Table 8 gives the list of important parameters that were fed into the MATLAB functions. All of these functions are available in Appendix A of this report.

Table 8: Model 1 of the 500 ft cable[21]

Parameter	Parameter Description
E_o	This is the magnitude of the incident pulse In this particular case the magnitude of the incident plane wave is set to 50 kV/m.
Alpha	A constant determined by [12] that is used in the double exponential model of the E1 pulse.
Beta	A constant determined by [12] that is used in the double exponential model of the E1 pulse.
K	A constant determined by [12] that is used in the double exponential model of the E1 pulse.
Frequency	A specific frequency of the incoming E1 HEMP
ω	The angular frequency of the HEMP pulse
Ψ	The elevation angle of the incoming pulse
Φ	The azimuth angle of the incoming pulse
Height of the cable	The height of the cable off the ground helps to determine how the reflections of the E1 pusle off ground couple to the cable
σ	The conductivity of the ground measured in Mhos/m
ϵ_r	The dielectric constant of the ground.
C	The speed of light in free space (vacuum)
μ_o	The magnetic permeability of free space.
τ_h	This is a time constant that is determined by the multiplication of the magnetic permeability the conductivity of the ground and the height of the cable squared.
θ	The polarization angle.
Z_1	The terminal impedance at the beginning of the cable
Z_2	The terminal impedance at the end of the cable
z_1	The beginning of the cable
z_2	The end of the cable
z	A vector that gives segments of the cable
a	the radius of the cable measured in meters

Distributed currents is the main function that all the other functions feed into. It calculates the currents distributed along the length of the cable.

As the table shows the list of parameters is fairly substantial. It would be difficult to visualize from both the code in NEC and the transmission line model developed in MATLAB what is actually being modeled in physical reality. The figure below gives a good depiction of the cable and grounding rods that are being modeled by these two software.

Figure 20: Pictoral representation of the 500 foot cable model [1]

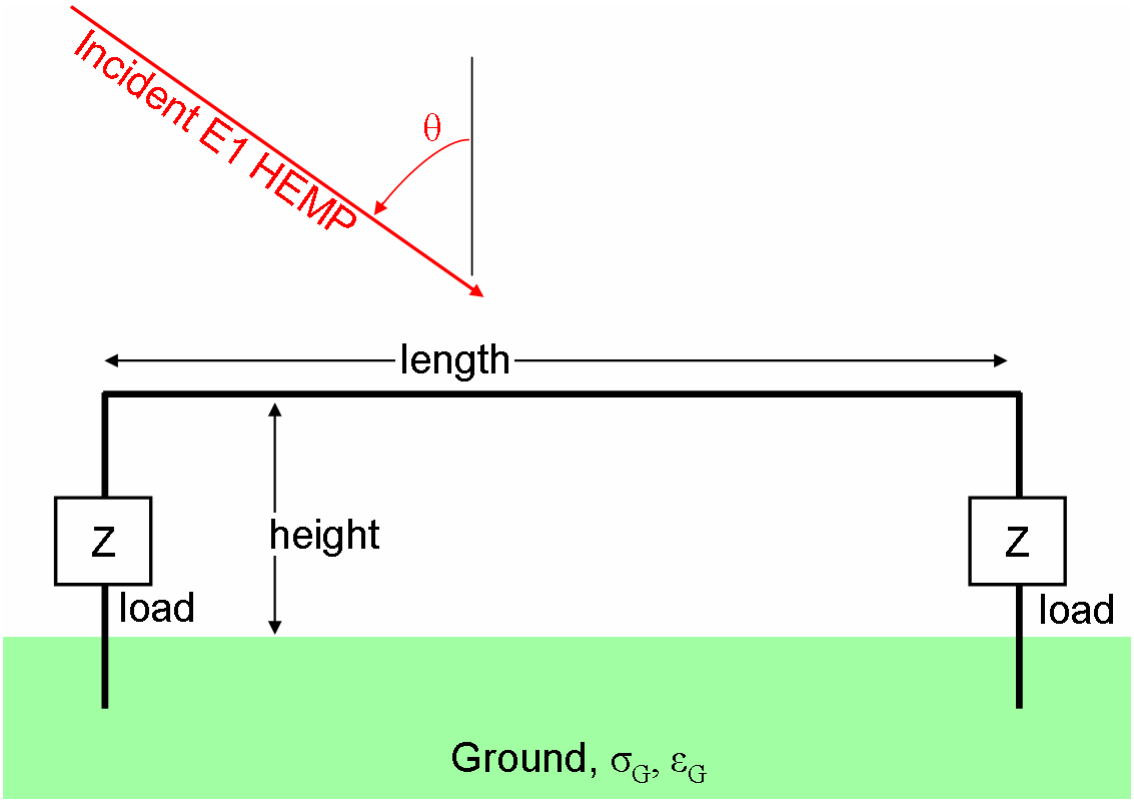

After verifying the NEC model against the matlab model the next step was to develop a larger model that could be used to find the current at different points along the cable within the time domain.

6.4 Finding the total current at different cable segments

Once the NEC model was verified the total current at different segmet lengths needed to be found in the time domain. In order to do this a larger NEC model was developed with an upper band limit of 500 MHz sampling at frequency increments of 6.25 MHz. This would give the NEC model enough samples to correctly recreate the pulse in the time domain. As was decided previously in the analysis of the E1 pulse. With the result of these outputs the NEC runs were also automated such that the ground parameters could be changed with changing frequency, as both the conductivity and the dielectric constant of the soil are frequency dependent. With the NEC runs automated the only thing to do was to wait for the outputs in order to run them through MATLAB code that would analyze them correctly. The script that was used in MATLAB in order to analyze the NEC runs is available in Appendix B of this report. The flow chart to this script is given in the figure below. The first step was to take the NEC results and then organize them into a folder. This was done simply enough, then after they were organized by category, for instance horizontal vs vertical polarization, then a MATLAB script was developed that would cycle through this folder and remove the current data from each NEC result. There was a total of 80 NEC outputs in the first iteration of this model which means that the MATLAB script would cycle through 80 different outputs and then organize the data from each of those outputs in a matrix. The information that is being taken by the MATLAB script was the real and imaginary components of the current for each segment. Once all of

this information was collected and stored in a m x n matrix, m being the number of frequencies and n being the total number of segments, then the actual analysis of this information could begin. The first step of this analysis was to scale the currents by their appropriate values per frequency. For every frequency enveloped in the pulse there is an associated electromagnetic field. This could be seen in the earlier figures displaying the frequency spectrum of the pulse. The process being used to analyze this model did not scale the electric field per frequency prior to running the model in NEC. Instead the process that was created scales the currents by their appropriate energy, which in this case is the fourier transform of the time domain pulse, which would give the frequency spectrum, then for each frequency run in NEC multiply that by its corresponding electric field then divide by the E_o used in the NEC model. This process properly scales the current for each frequency. After the currents had been scaled the next step was to account for negative frequencies in order to perform the inverse fourier transform. The output of NEC is the current induced along the segments of the cable per frequency. In order to get this in the time domain an inverse fourier transform must be applied. In order to do take the inverse fourier transform the negative frequencies of the fourier transform must be accounted for. In order to account for these negative frequencies the conjugate of the positive frequency results was taken. Then these negative frequency results were appended to the beginning of the matrix containing the positive frequencies. As a side note on negative frequencies and how and why they exist see the paragraph below.

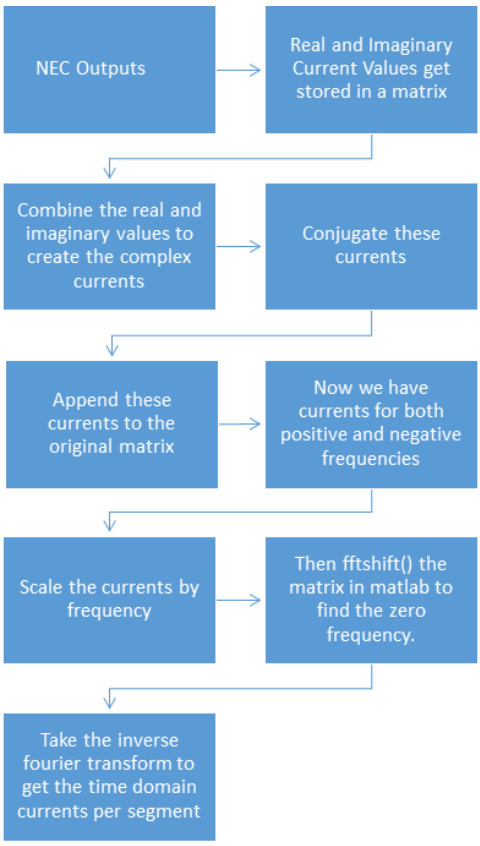

Figure 21: Process of finding the total current flow chart

The actual concept of negative and positive frequency is similar to the idea of rotating a wheel one way or another. A signed value of frequency can indicate both the rate and direction of rotation. Similar to the rotating vector the complex-valued function: $e^{j\omega t} = cos(\omega t) + j * sin(\omega t)$ exhibits different properties for positive and negative values of the parameter ω. The most well-known application of negative frequency is the calculation of the fourier transform. The negative frequencies themselves are an integral part of a Fourier transform. An explanation of this is that the product of two complex sinusoids is also a complex sinusoid whose frequency is the sum of the original frequencies. So when ω is positive, $e^{-j\omega t}$ causes all frequencies of x(t) to be reduced by amount ω.Whatever part of x(t) that was at frequency ω is changed to frequency zero, which is just a constant whose amplitude level is a measure of the strength of the original ω content. Whatever part of x(t) that was at frequency zero is changed to a sinusoid at frequency $-\omega$. Similarly, all other frequencies are changed to non-zero values. This mathematical meaning behind the concept of a negative frequency may not be intuitive to understand. The history behind negative frequencies may be an easier way of understading the conept. In 1800, Fourier showed that any periodic signal with period T satisfying the Dirichlet conditions can be expanded to the infinte set of complex exponents with frequencies +-k/T, where k = 0,1,2 ... Based on Fourier's proof it was shown that frequencies can be both positive and negative. The meaning of the negative frequency is purely mathematical similar to the imaginary part of a complex signal.

The next step after appending the negative frequencies, is to take the inverse fourier transform of this data. Once this is complete doing an analysis on the maximum current per segment is next.

6.5 Modeling the full Antenna System

After the cable was successfully modeled, and an analysis on where the maximum power was located along the cable, the next iteration of the NEC model would include the Antenna. With this model complete the same process that was used to find the total currents along the cable will be used to find the total currrent developed along the cable and the antenna, with some minor modifications to the MATLAB code to properly read the NEC output files.

7 Analysis and Results

The following results are for each section of the methodology. It begins with a detailed analysis of E1 HEMP and proceeds with the analysis of the currents along the 500 ft cable from both the NEC and transmission line models and ends with the final analysis of the entire antenna system.

7.1 Analysis of the E1 pulse

The analysis of the E1 pulse consisted of finding the pulse width that would allow for the least amount of power and energy loss. As was described in the methodology two times were chosen time 1 and time 2. Time 1 was 150 nano-seconds and time 2 was 500 nano-seconds. Taking the integral of the pulse up to these two times and then finding the percentage difference of energy between time 2 vs time 1, the difference of energy is equivalent to 0.27%. Thus for the sake of analyzing the HEMP E1 pulse the pulsewidth can be assumed to be 150 nano-seconds. Taking this pulse width the total power can be found by integrating the power of the HEMP pulse from 0 to 150 nano-seconds and then dividing by 150 nano-seconds. The power of the E1 pulse can be described as the following:

$$Power = \frac{{E_o}^2}{Z_o} \tag{46}$$

Where Z_o in this equation is the impedance of free space. The impedance of free space is a physical constant relating the magnitudes of the electric and magnetic fields of electromagnetic radiation travelling through free space. It has an approximate value of $120 * \pi$.
Integrating this average power over the pulse width and then dividing by the pulse width gives a value for total power in the E1 pulse of:

762703.9 W/m.
The calculated power of the HEMP pulse is less than the peak power given in the summary of HEMP pulses. The next steps of the E1 pulse analysis involve taking the fourier transform of the pulse and the inverting this transform back into the time domain.

Fourier Analysis of the E1 Pulse

Taking the E1 pulse with 160 time elements from 0 to 159 nano-seconds, gives one period of the pulse in the view of the fourier transform. Transforming the pulse from the time domain to the frequency

domain with the appropriate number of samples in MATLAB involved using the fft function.
The fft function is a built in function of matlab that computes the fast fourier transform. The fast fourier transform is an algorithm to compute the discrete fourier transform and its inverse. If the input to the fft function is a vector it returns the discrete Fourier transform of the vector. If the input X to the fft function is a matrix then the fft function returns the Fourier transform of each column of the matrix.
The time domain analysis of the pulse is a single vector with each element in representing an electric field magnitude at a specific time. When the fft was taken it returned the discrete Fourier transform of these values. Where now each element in the vector represents an electric field at a specific frequency of the pulse. The graph of the prior E1 pulse and its transform are available below.

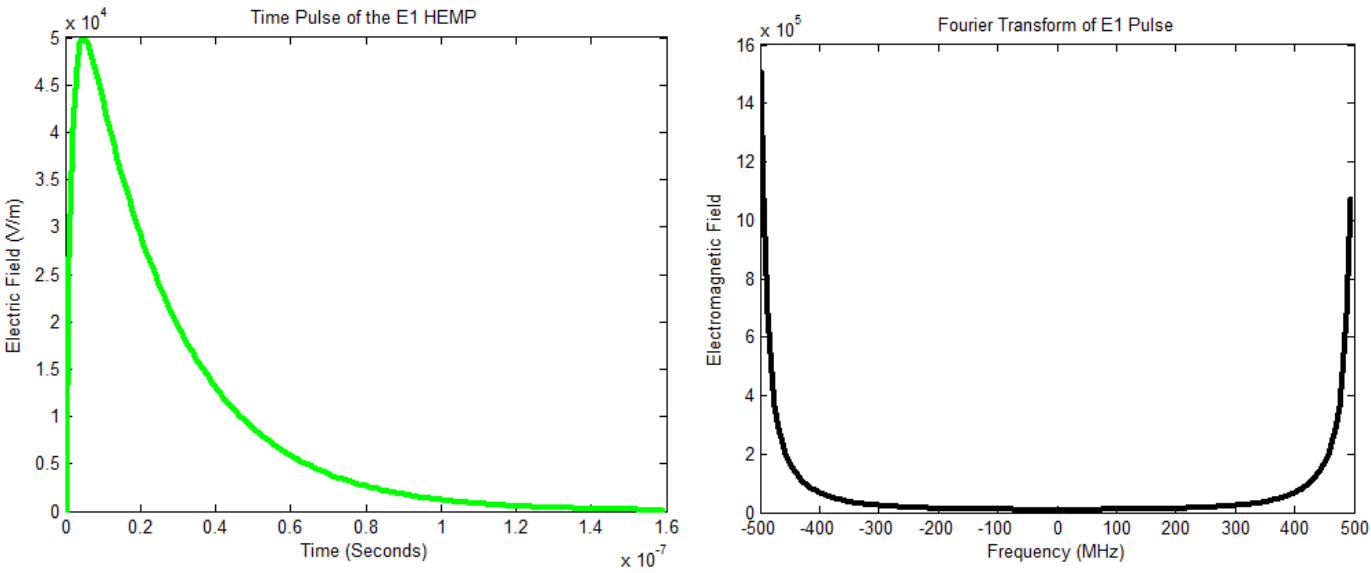

(a) Time Domain of the E1 pulse

(b) Fast Fourier Transform of the E1 PUlse

Figure 22: E1 Pulse and its discrete Fourier Transform

Once the discrete Fourier transform of the HEMP pulse was found the fast fourier transform shift function, fftshift, in matlab was used to find the zero frequency. What the fftshift function does is rearranges the outputs of the fft, fft2, and fftn by moving the zero-frequency component to the center of the array. It is useful for visualizing a Fourier transform with the zero-frequency component in the middle of the spectrum. The graph of the fftshift of the discrete Fourier transform is available below.

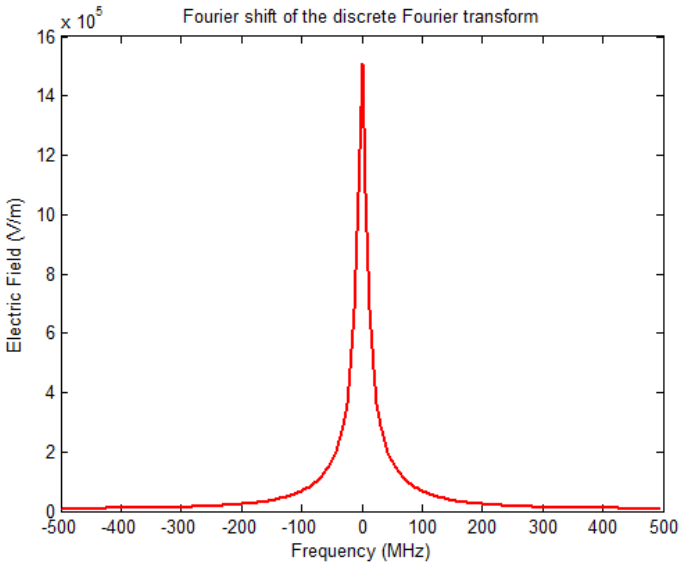

(a) Fourier shift of the discrete Fourier transform.

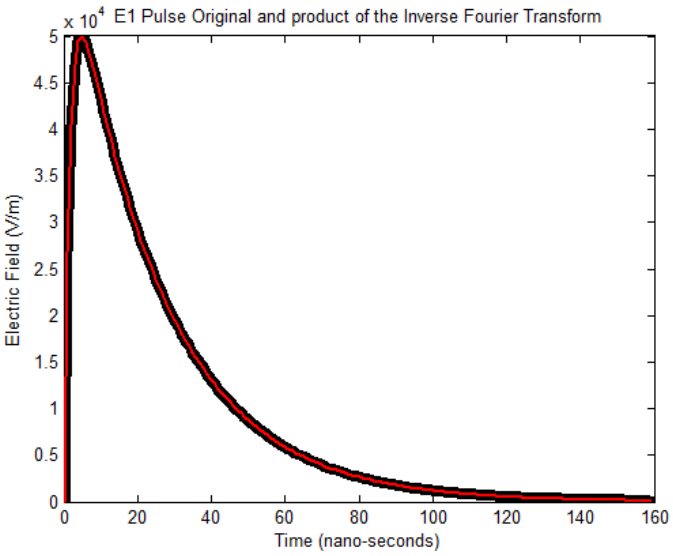

(b) The original E1 pulse and the E1 pulse after the inverse Fourier transform.

Figure 23: Fourier shift to find the zero frequency and the inverse Fourier transform

The shifted discrete Fourier transform will be used in later calculations to scale the currents of the NEC results to there appropriate values. The final step is to reconvert the shifted Fourier transform to the time domain. This is done using the ifft function in Matlab. The ifft returns the inverse discrete Fourier transform (DFT) of vector X, computed with a fast Fourier transform algorithm. Comparing the inverse fourier transform to the original pulse in the time domain, it can be seen that both the original and the E1 pulse are the exact same. Thus in the process of taking the Fourier transform and then inverting the transform back to the time domain no information was lost. Which implies that the correct sample size was used and that this procedure can be used to analyze the total currents along the cable from the output of NEC.

7.2 Results of the NEC model

Once the analysis of the E1 pulse was completed several models of the 500 ft cable were developed in NEC. The models that were developed are available in Appendix D of this report. The resulting calculation of the currents along the cable from Model 4 are available below.

Figure 24: Magnitude of Current for Frequency of 10 MHz. Model 4

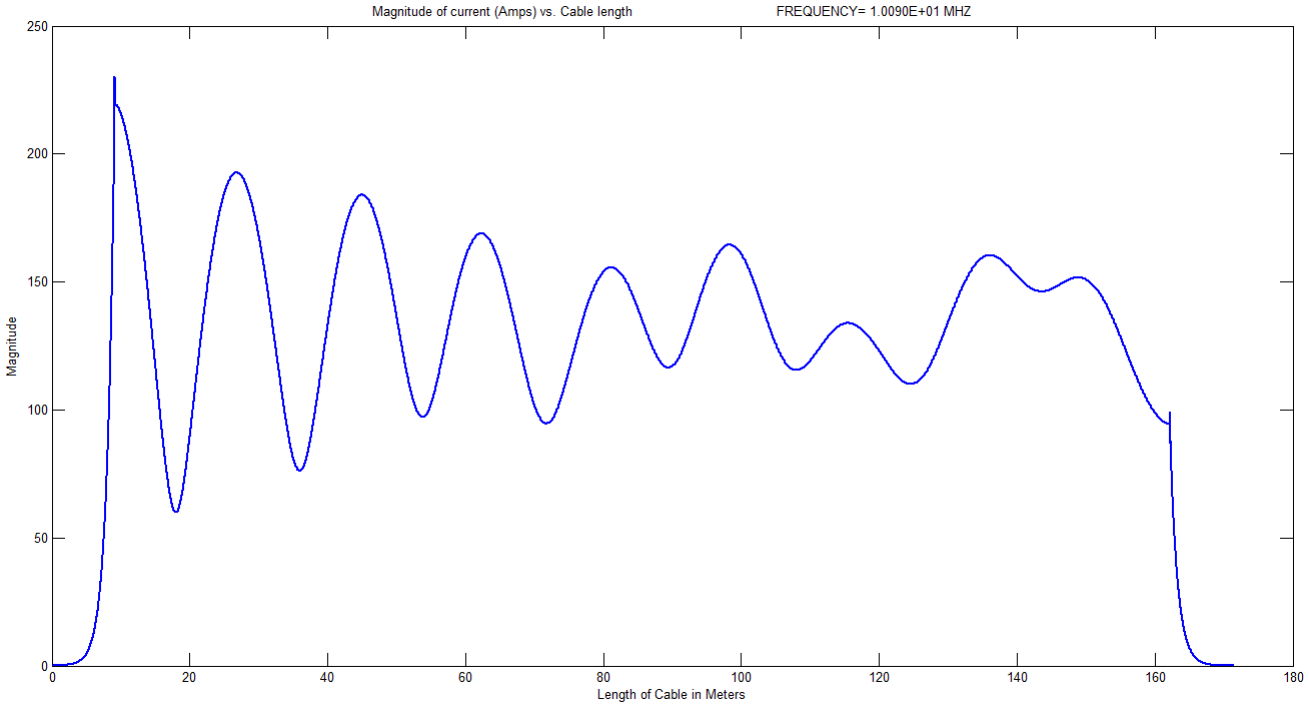

As we can see in the above, electromagnetic field couples to the cable and at a frequency of 10 MHz the wavelength of the incident wave is 30 meters. The length of the cable is 5 times the wavelength so there is going to be some phase offset. Towards the end of the cable when the reflected returns there is some distortion from the difference in phases from the incoming and reflected waves. At the terminals of the cable the current is shunted to ground by the grounding rods. There is another effect that must be taken into consideration, that is the reflection of the incidence field from the ground plane. This causes some cancelation of the horizontal current being produced along the cable length. As the frequency of the incident wave increases the signal along the cable becomes less distorted and reaches a point where there is equilibruim in the center of the cable with oscillations towards the ends.

Figure 25: Magnitude of Current for Frequency of 20 MHz. Model 4

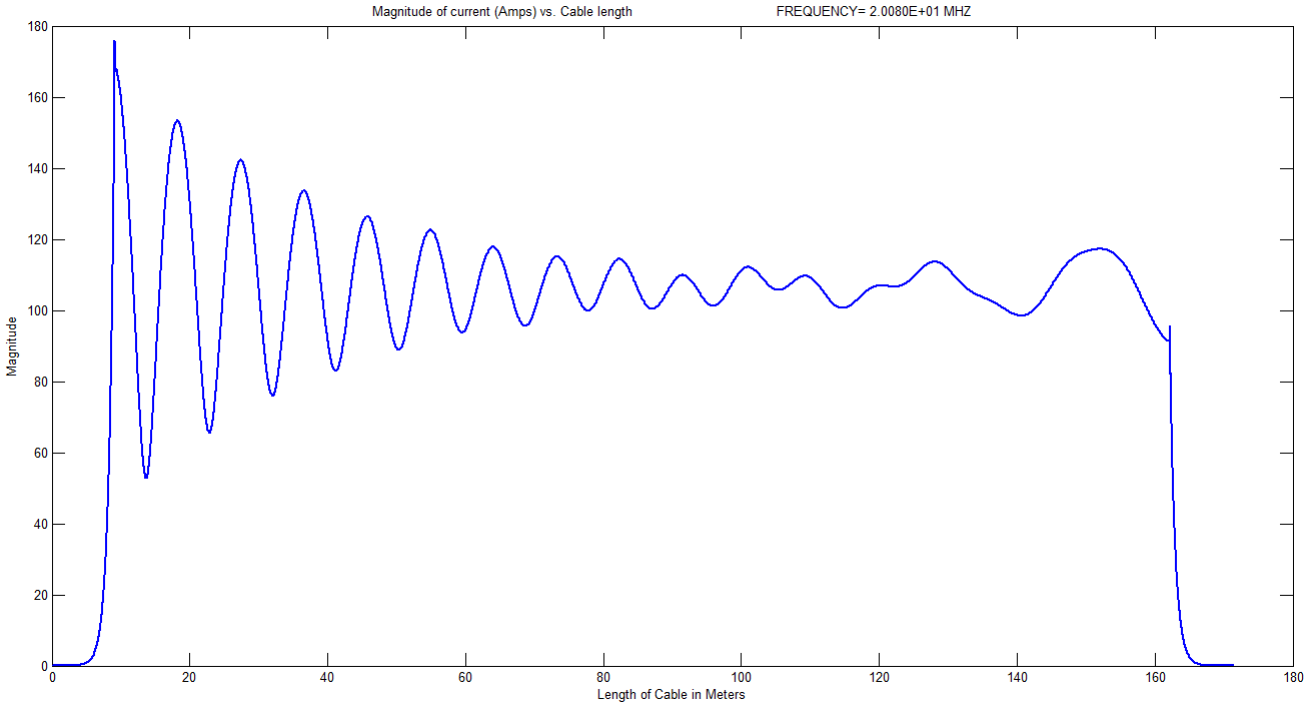

At a frequency of 20 MHz that is a total wavelength of 15 meters. This is half the wave length of the preceding model but as can be seen in Figure 25 there is still some distortion towards the end of the cable. This is due to the reflected waves being out of phase with the incoming signal. The influence of the grounding rod is also very apparent as the currents along the end of the cable quickly drop to zero. Increasing the frequency to 30 MHz The current signal along the end of the cable at approximately 150 meters are becoming more and more in phase with the signal coming down the wire. Towards the center of the cable at approximately 80 meters, the oscillations of the signal become less and less apparent as the incoming and reflected waves cancel.

Figure 26: Magnitude of Current for Frequency of 30 MHz. Model 4

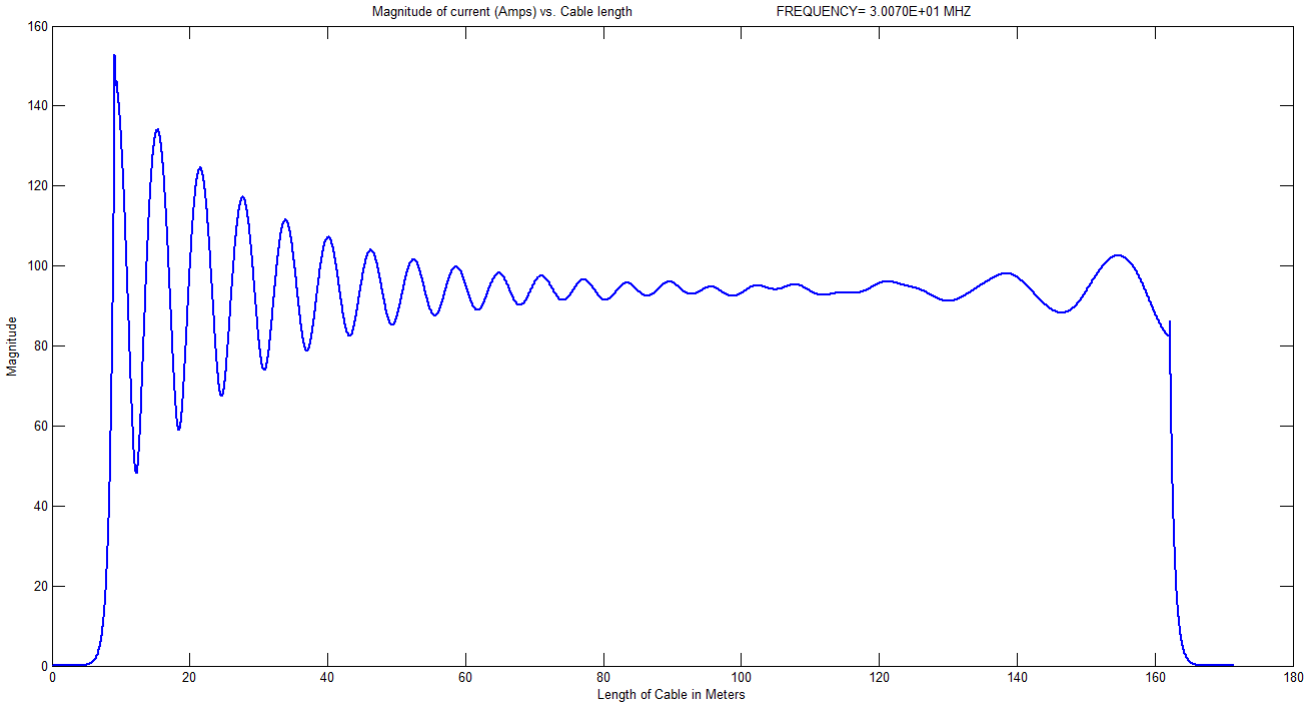

At 30 MHz the wavelength of the incoming electromagnetic wave is 10 meters. This means that the cable length is approximately 15 wavelengths of the electromagnetic field. At 15 times the wavelength the cable is acting essentially like a long wire antennna. As the frequency increases there is less and less oscillations at the center of cable due to phase effects.

Figure 27: Magnitude of Current for Frequency of 40 MHz. Model 4

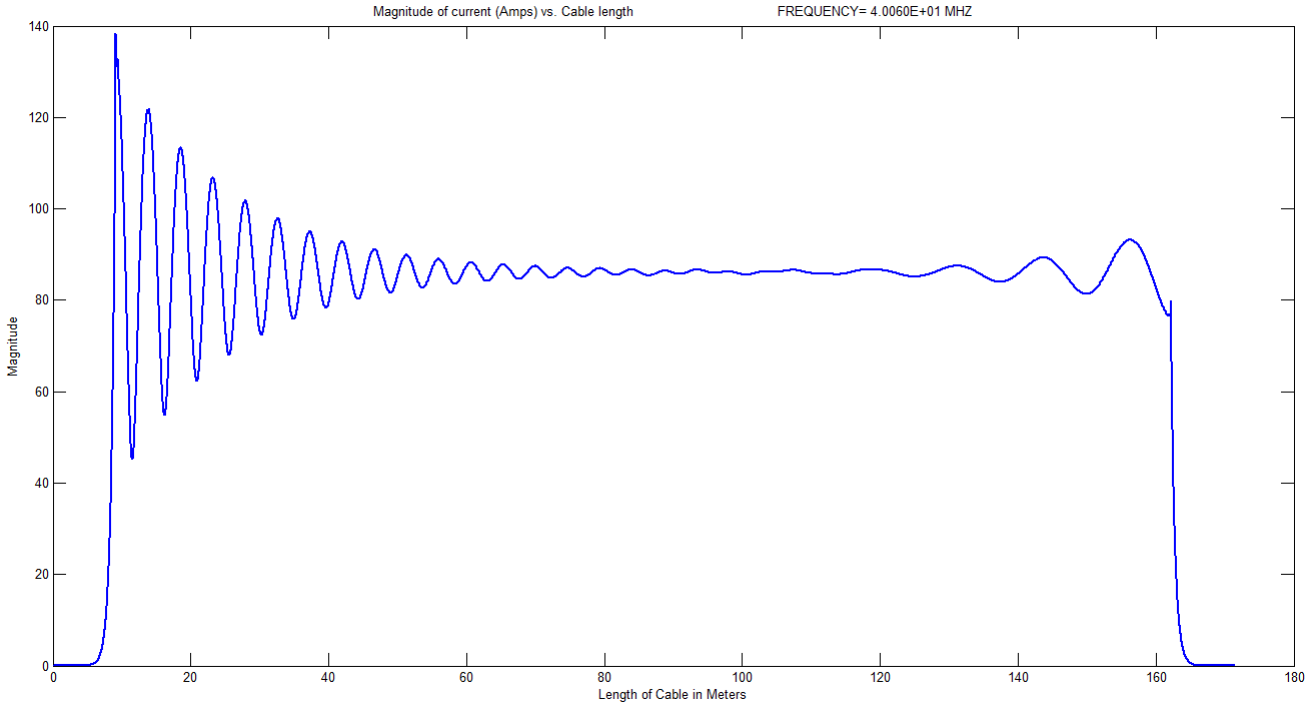

Figure 28: Magnitude of Current for Frequency of 50 MHz. Model 4

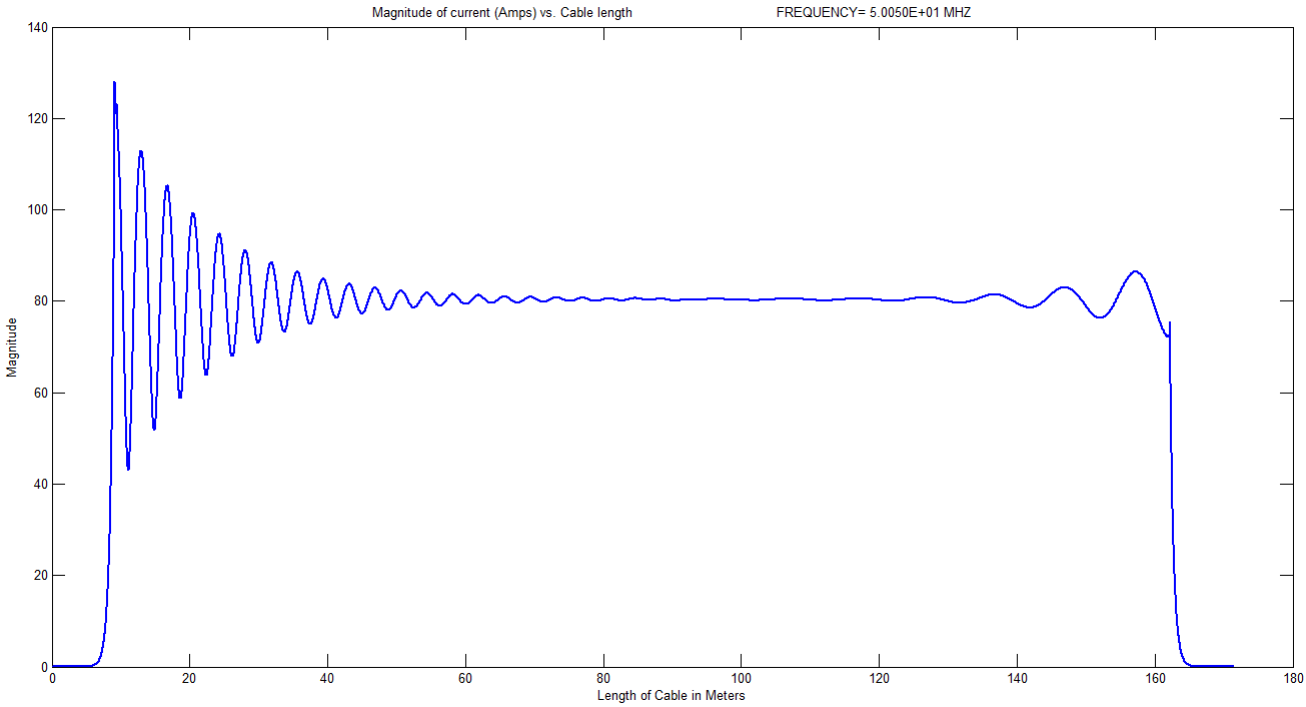

Figure 29: Magnitude of Current for Frequency of 60 MHz. Model 4

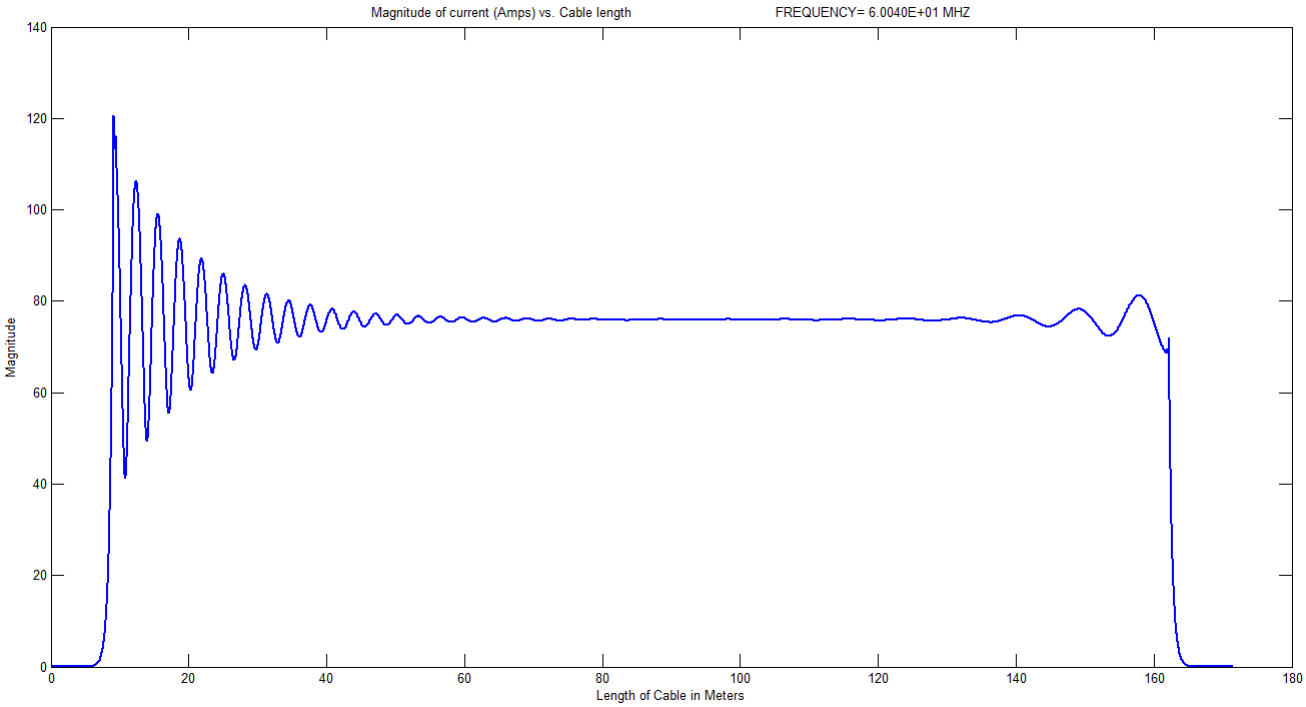

Figure 30: Magnitude of Current for Frequency of 70 MHz. Model 4

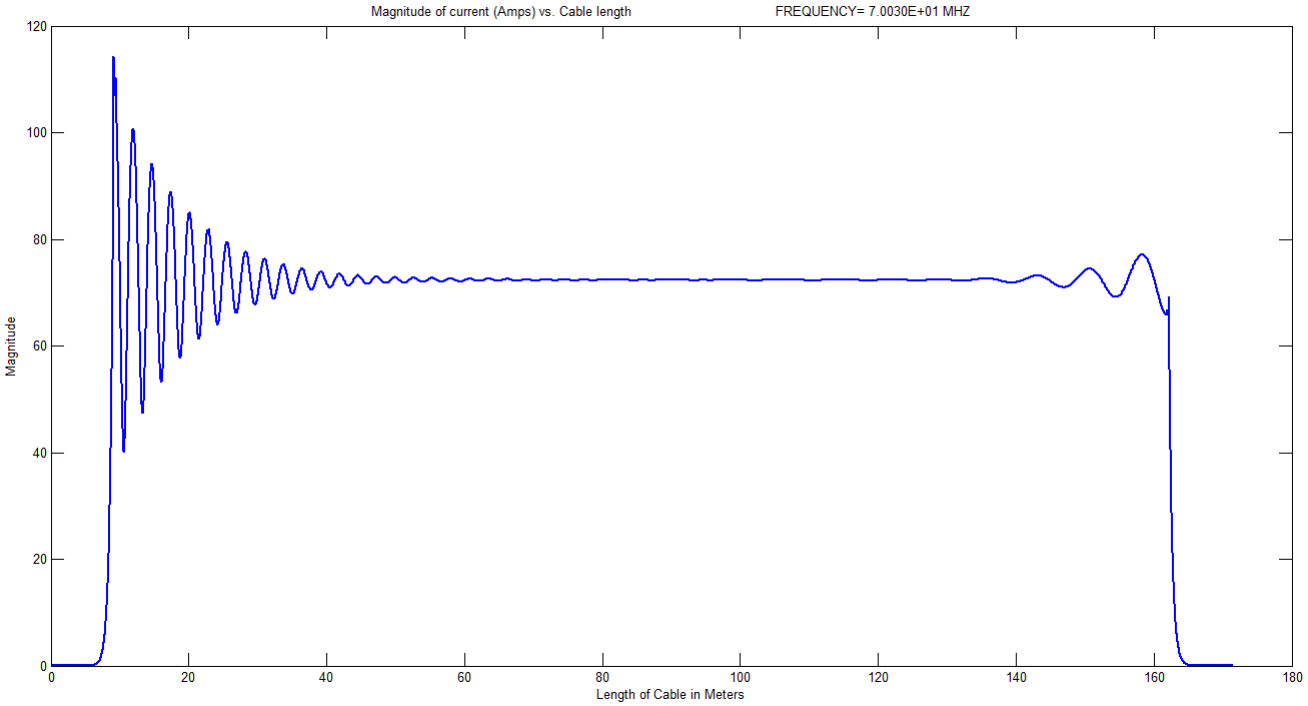

As can be seen that as the incoming wave form increases in frequency the oscillations along the cable decrease and the only things that are left are the reflections at the terminals. These NEC models run for single frequencies and the entirety of the pulse is the superposition of the effects of all the frequencies contained within the pulse. In order to proceed with the analysis these NEC models have to be verified versus some sort of theoretical proof.

7.3 The Transmission Line Model

The development of the transmission line model was taken from [13]. Within the text a model of the coupling of an incident plane wave to a horizontal cable above ground is developed using transmission line theory. The equations describing these incident fields are available in the background section of this report, and the matlab functions that were used to model these incident fields are available in Appendix A of this report. What is not readily observable in the analysis provided by NEC is how changes in key parameters (ground conductivity, dielectric constant, height, radius... etc) effect the incident electromagnetic field and the currents induced along the cable. Using the transmission line model, these parameters can be readily changed and quickly analyzed vs. NEC which would take several hours to do the same analysis.

The first part of this analysis consists of changing the ground parameters and understanding how these changes effect the horizontally polarized incident plane wave.

Horizontally Polarized Incident Plane Wave

Ground Dielectric Constant $\epsilon_r = 13$

Elevation Angle $\psi = \frac{pi}{6}$

Azimuth Angle $\phi = \frac{pi}{2}$

Height 0.1016 m or 4 inches.

Cable Radius: 0.00712704259 m
Ground Conductivity: 0.01

7.3.1 How Changes in the key Parameters effect the incident field

Figure 31: Horizontally Polarized Incident Wave with Sigma = 0.01

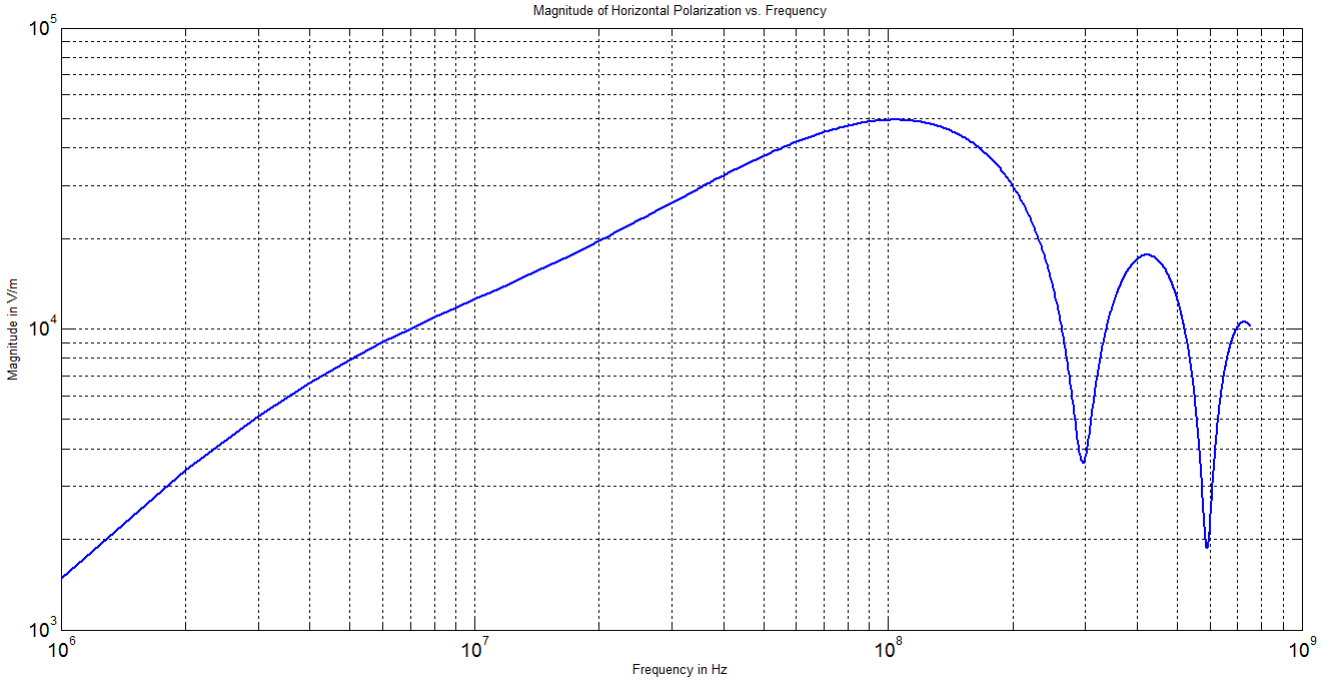

Ground Conductivity: 0.05

Figure 32: Horizontally Polarized Incident Wave with Sigma = 0.05

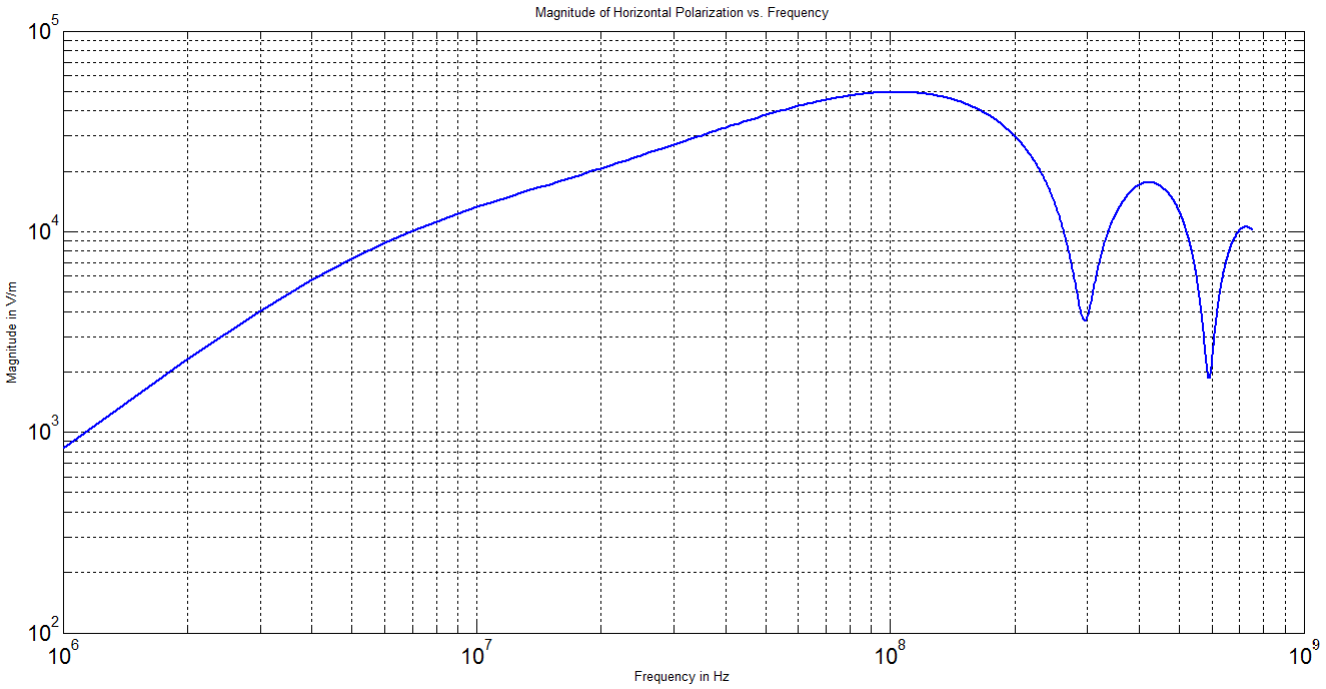

Ground Conductivity: 0.10

Figure 33: Horizontally Polarized Incident Wave with Sigma = 0.10

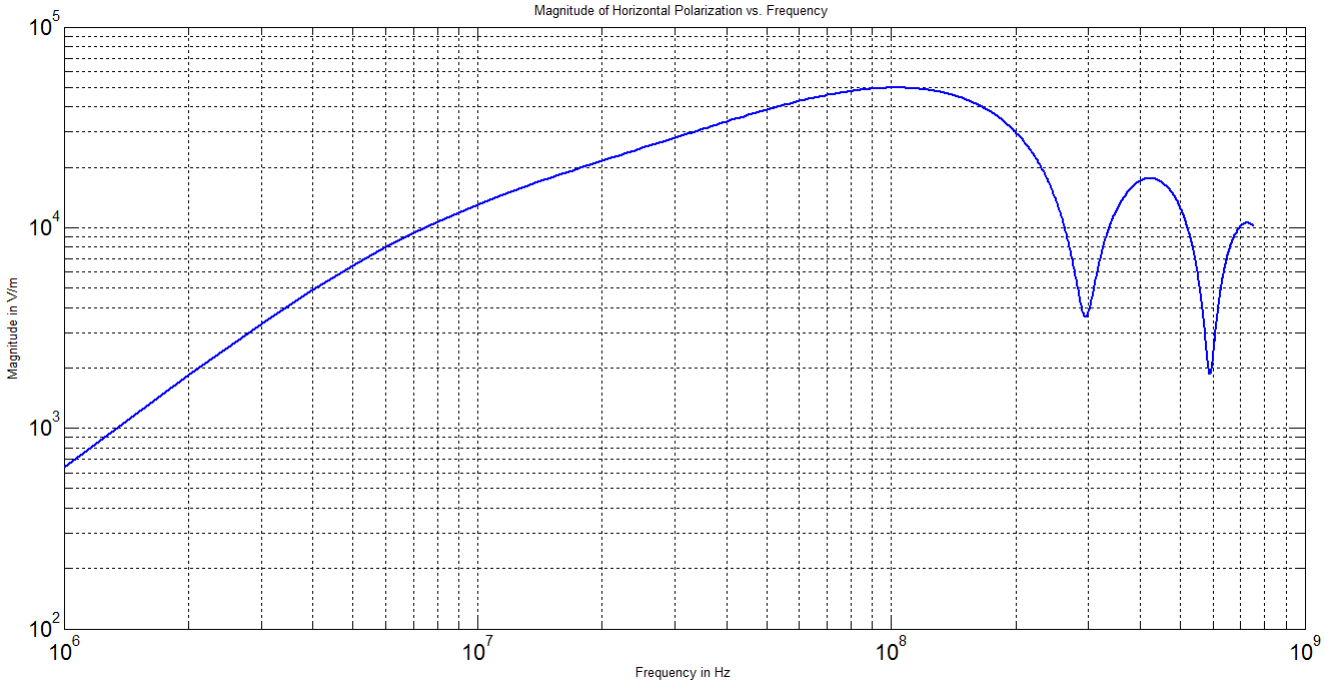

Ground Conductivity: 0.15

Figure 34: Horizontally Polarized Incident Wave with Sigma = 0.15

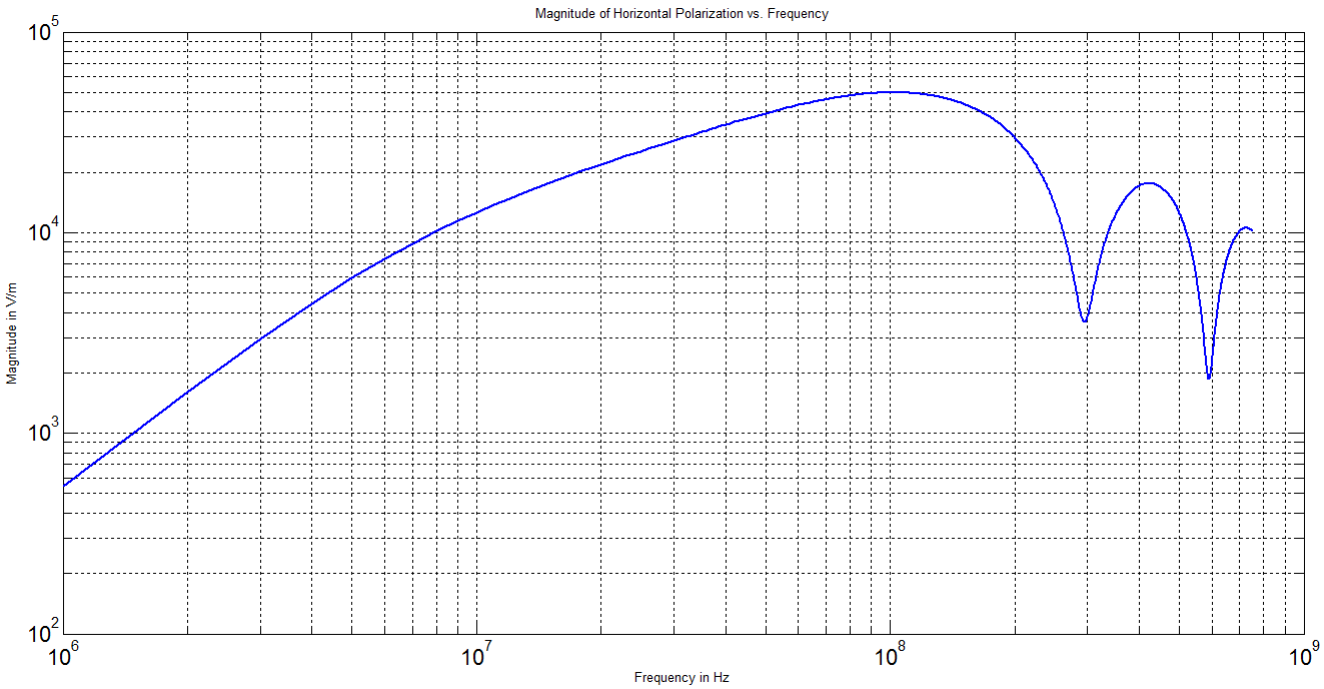

It seems that with increasing ground conductivity the only effect it has on the incident electromagnetic field is lower magnitudes at frequencies below 10MHz. The graphs indicate that other than this there is really no change in the horizontally polarized electromagnetic field. Now moving on to changes in the dielectric constant with everything else being equal and sigma set to 0.2 mhos/m. For a dielectric constant representing Dry, Sandy Coastal Land from [13] where $\epsilon_r = 10$.

Figure 35: Horizontally Polarized Incident Wave with Epsilon = 10

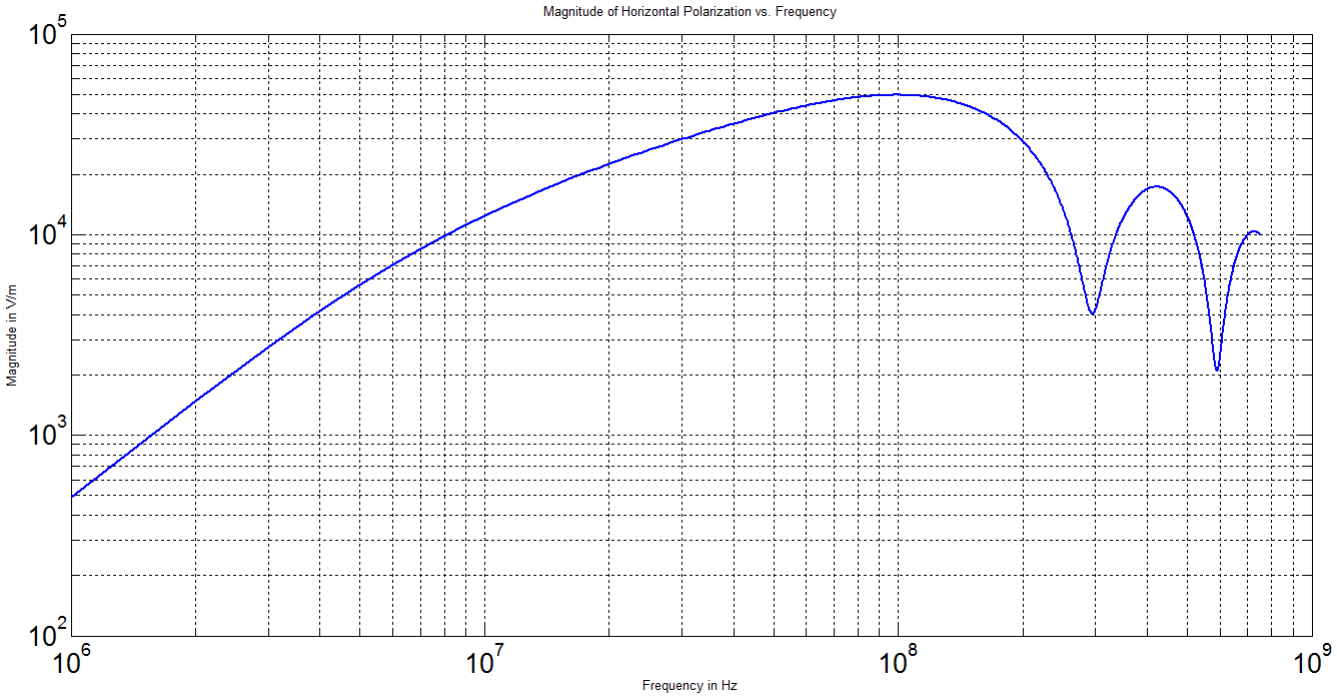

Dielectric constant, ϵ_r, representing Rich agricultural land

Figure 36: Horizontally Polarized Incident Wave with Epsilon = 15

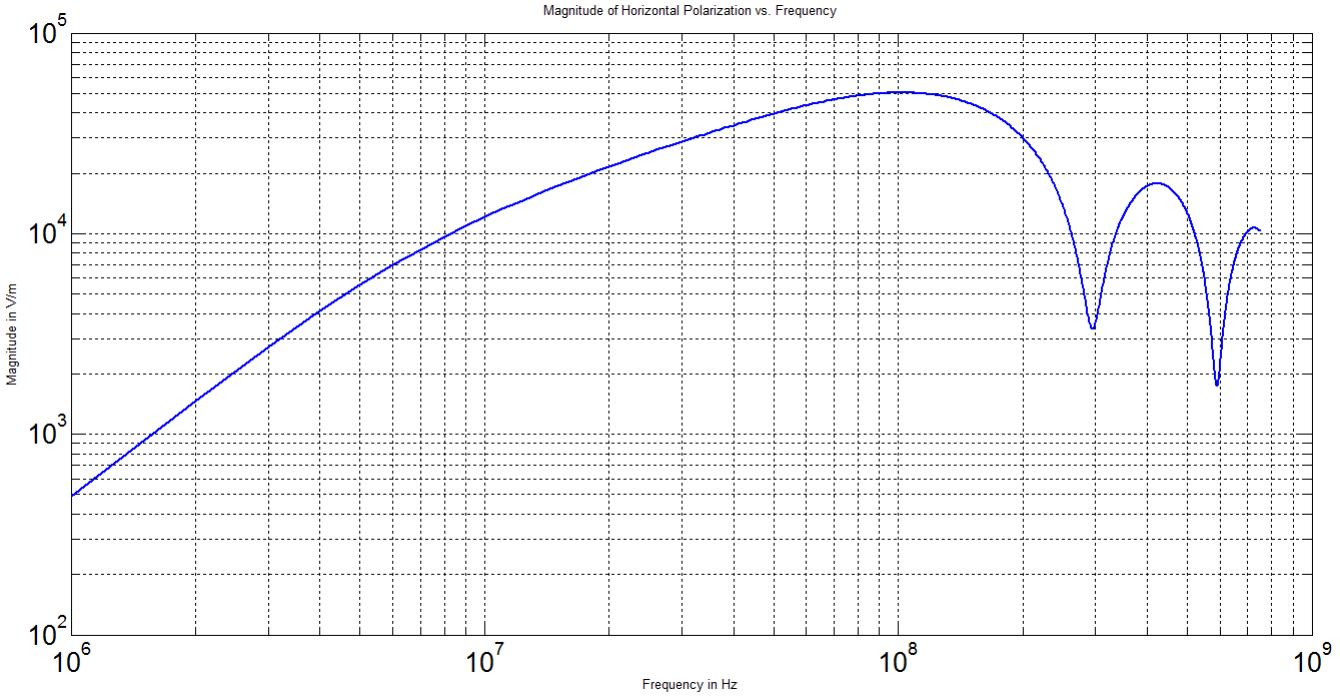

Dielectric constant, ϵ_r, representing Fresh Water

Figure 37: Horizontally Polarized Incident Wave with Epsilon = 80

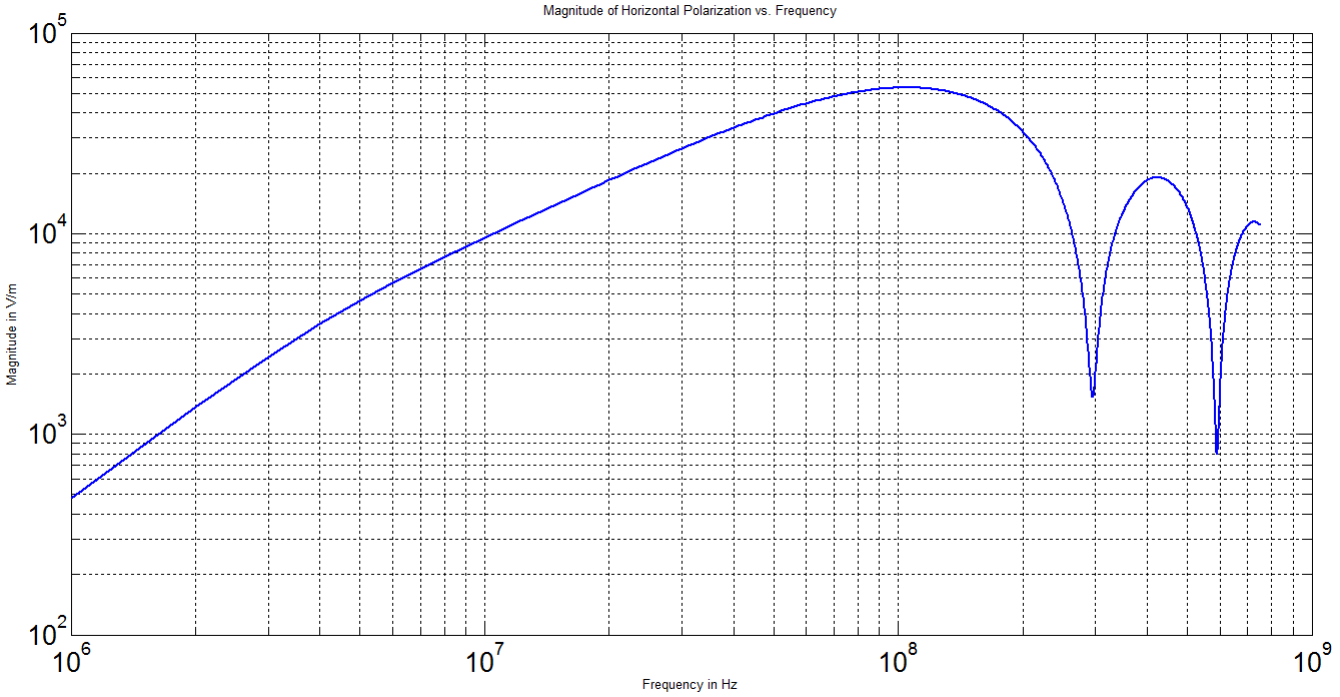

What these graphs indicate is that changes in the dielectric constant of the soil do not imply substantial changes in the incident electromagnetic field. As can be seen in the third figure the dielectric constant of the soil has to increae dramatically in order to cause a large change in the incident field. Something else to notice is that changes of the dielectric constant of the soil does not have much effect on the lower frequency amplitudes. It is only at frequencies above 100 MHz that these effects are noticeable. The ground parameters, the soil dielectric and conductivity, effect how much the electromagnetic wave penetrates into the ground and how much is reflected. The importance of the reflected wave comes when considering the height of the cable above ground. Changing the height of the cable above ground should demonstrate how this effects the magnitude of the horizontally polarized incident wave.
Assuming everything else constant, with a dielectric constant of 13 and soil conductivity of 0.2 mhos/m.
At a height of 4 inches the incident wave vs frequency looks like this:

Figure 38: Horizontally Polarized Incident Wave with Height = 4 inches

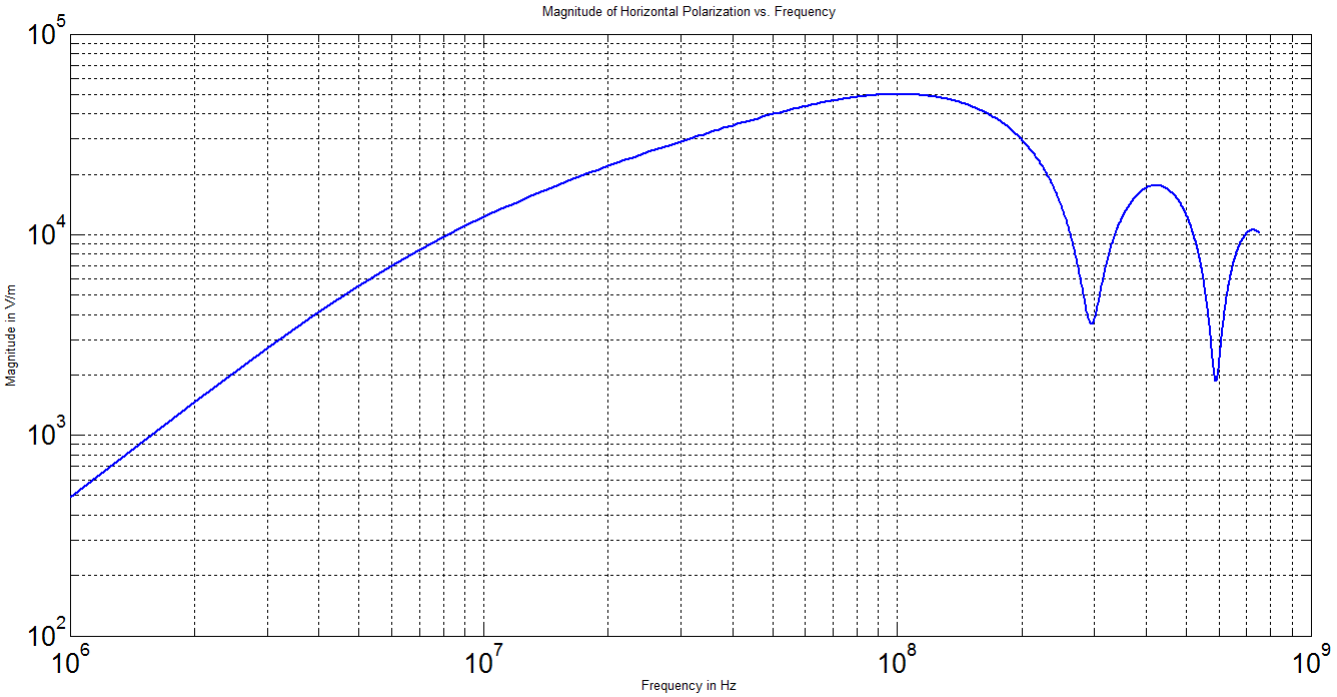

At a height of 1 ft

Figure 39: Horizontally Polarized Incident Wave with Height = 1 ft

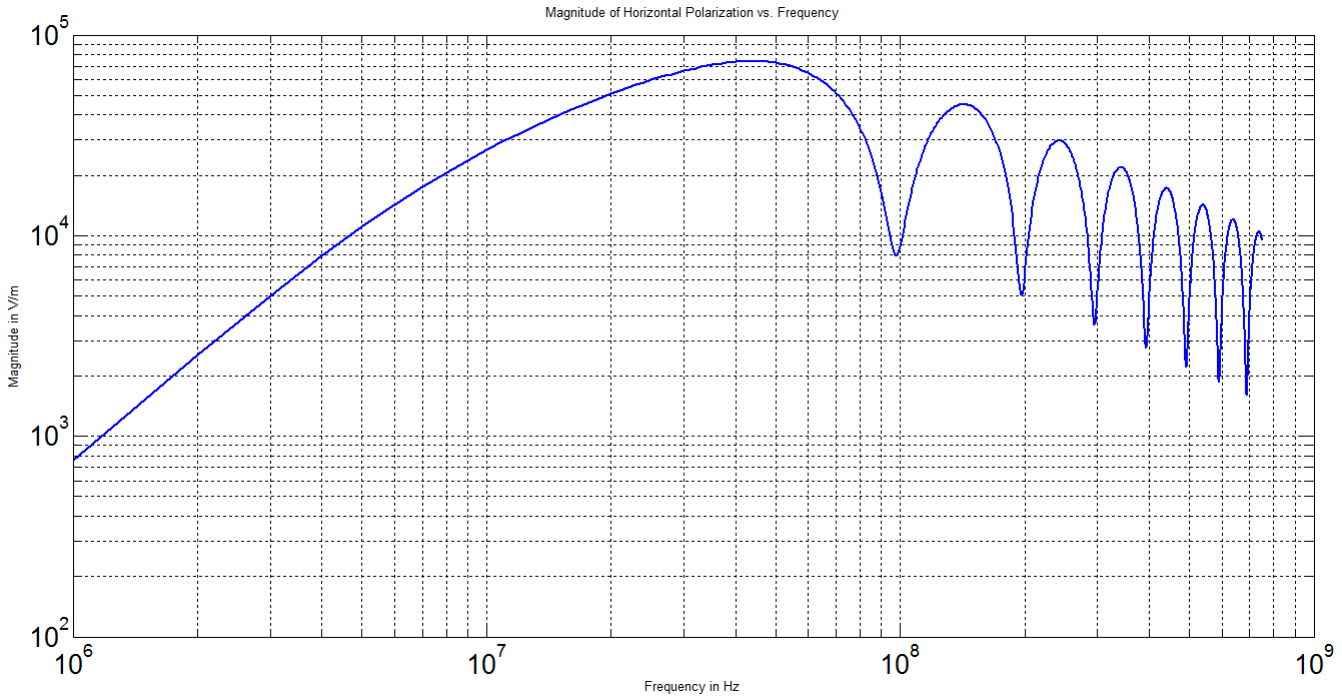

At a height of 5 ft

Figure 40: Horizontally Polarized Incident Wave with Height = 5 ft

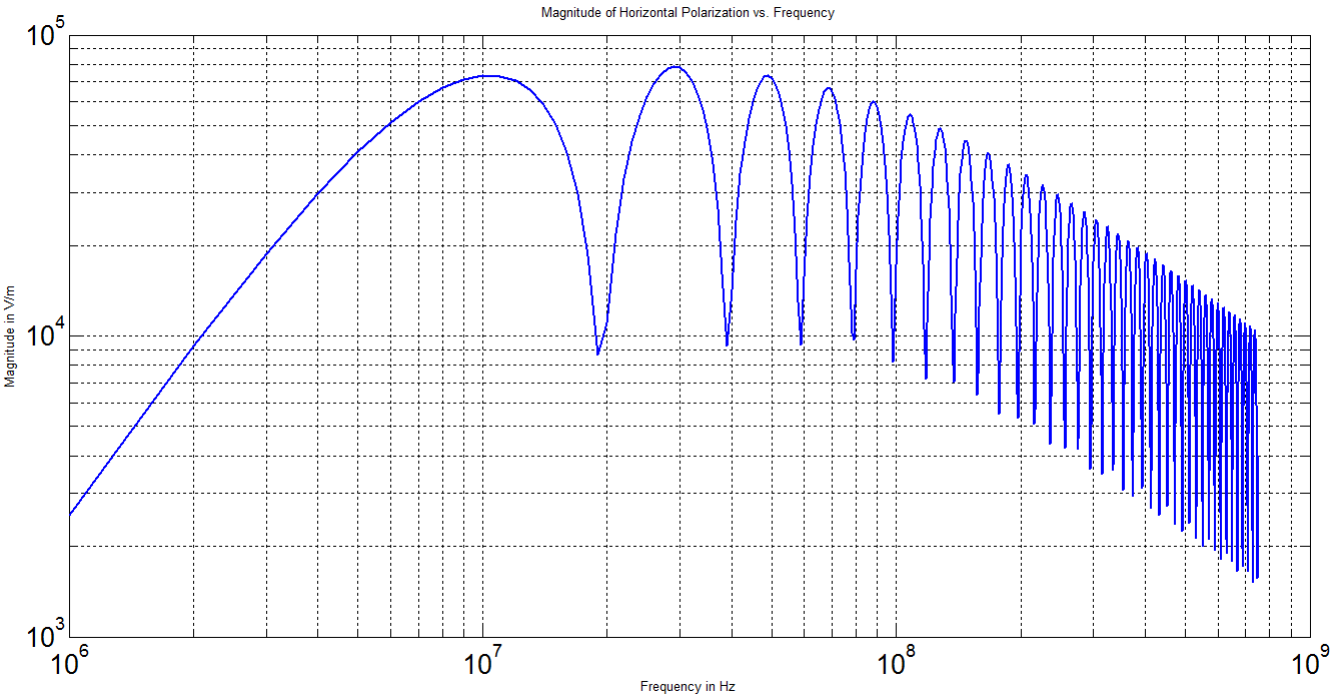

Changes in height cause dramatic variations in the incident electromagnetic field. If the cable is raised to a height of 5 ft or 1.524 meters, the peak incident field decreases and this peak is reached at a

much lower frequency, this is due to ground reflections canceling out some portion of the horizontally polarized incident field. These changes in height contribute greatly to the amount of the pulse that is incident on the cable. Given that the origin of the pulse is occurring at heights much greater than the height of the cable the direction that the pulse is traveling cannot be predicted. Thus analyzing changes in the illumination angle and azimuth angle should give a better idea of what happens when the pulse approaches at different degrees to the cable.
Everything else being equal and the height of the cable being returned to 4 inches, changes in the illumination angle will cause the following changes in the incident field. An illumination angle $\psi = \frac{\pi}{6}$

Figure 41: Horizontally Polarized Incident Wave with Illumination Angle $\frac{\pi}{6}$

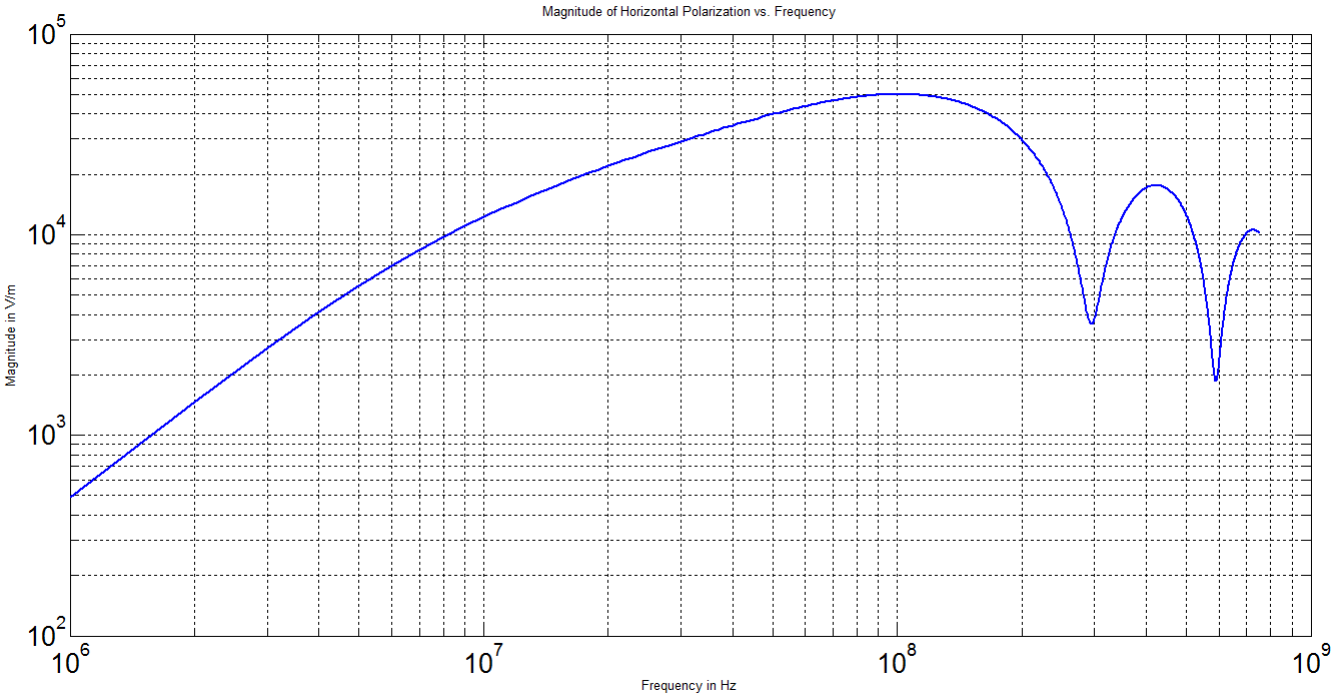

An illumination angle $\psi = \frac{\pi}{4}$

Figure 42: Horizontally Polarized Incident Wave with Illumination Angle $\frac{\pi}{4}$

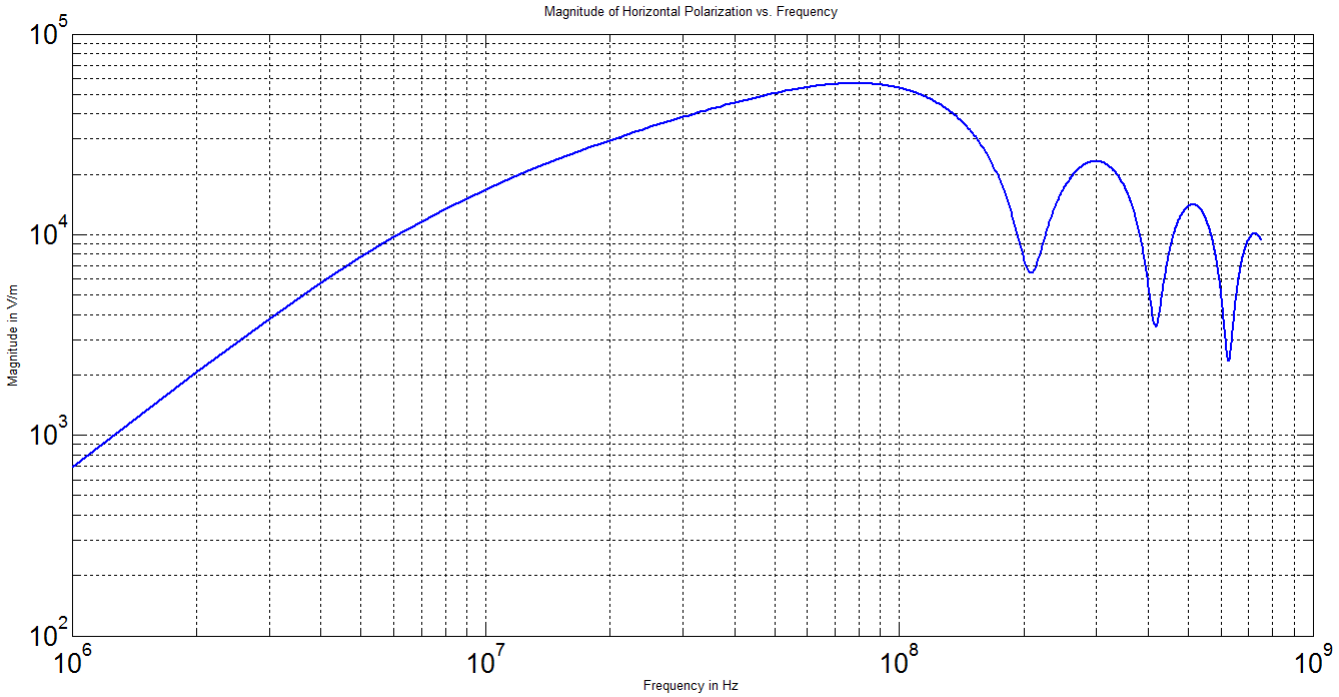

An illumination angle $\psi = \frac{\pi}{4}$

Figure 43: Horizontally Polarized Incident Wave with Illumination Angle $\frac{\pi}{2}$

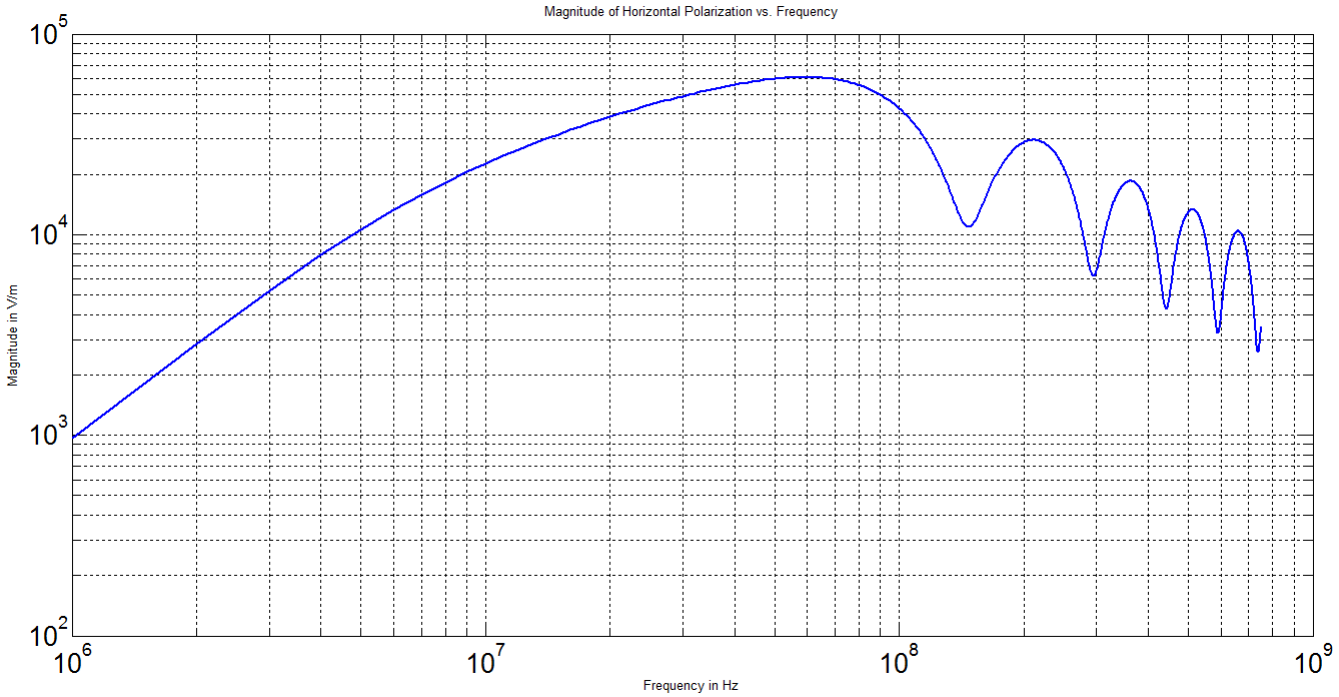

Changes in the illumination angle have a significant influence in the nature of the incident field at

frequencies greater than 10 MHz. As the illumination angle approaches 90 degrees, the peak of the incident field moves to lower frequencies and at the higher frequencies the incident field experiences more reflections from the ground. Now keeping the illumination angle constant and changing the value of the azimuth angle. The incident field changes in the following ways.

Azimuth Angle $\phi = \frac{\pi}{6}$

Figure 44: Horizontally Polarized Incident Wave with Azimuth Angle $\frac{\pi}{6}$

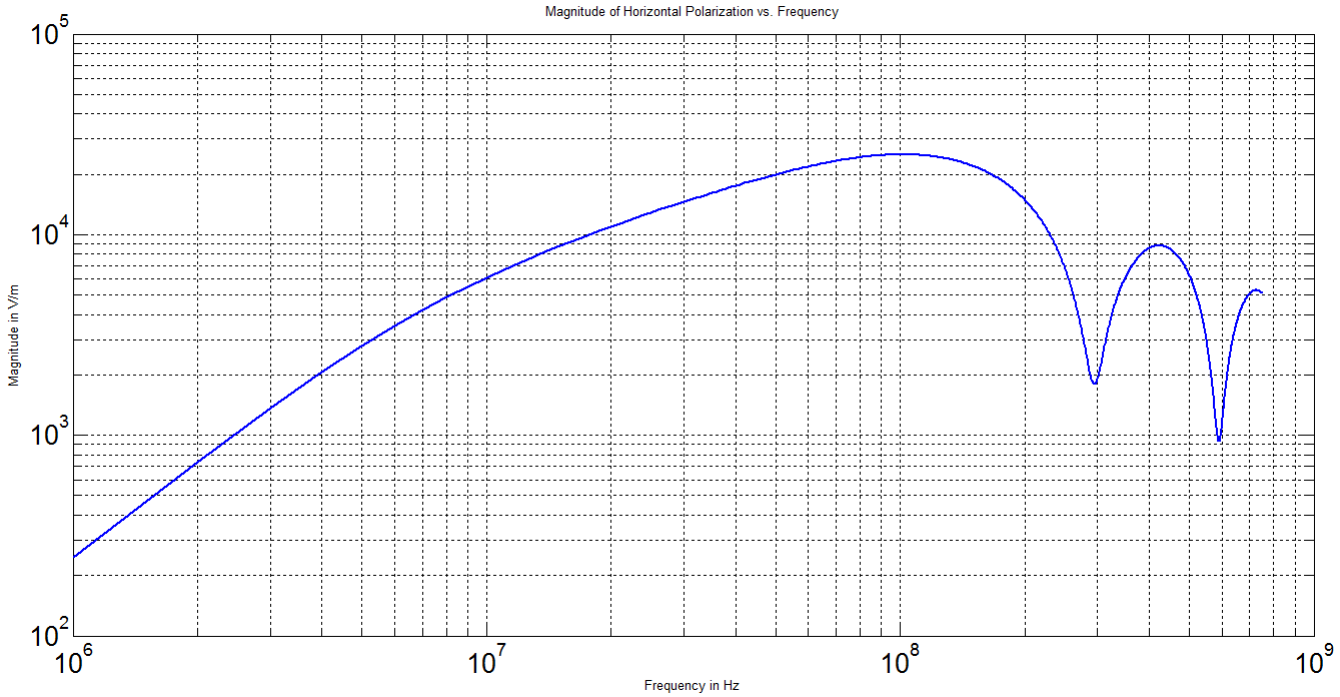

Azimuth Angle $\phi = \frac{\pi}{4}$

Figure 45: Horizontally Polarized Incident Wave with Azimuth Angle $\frac{\pi}{4}$

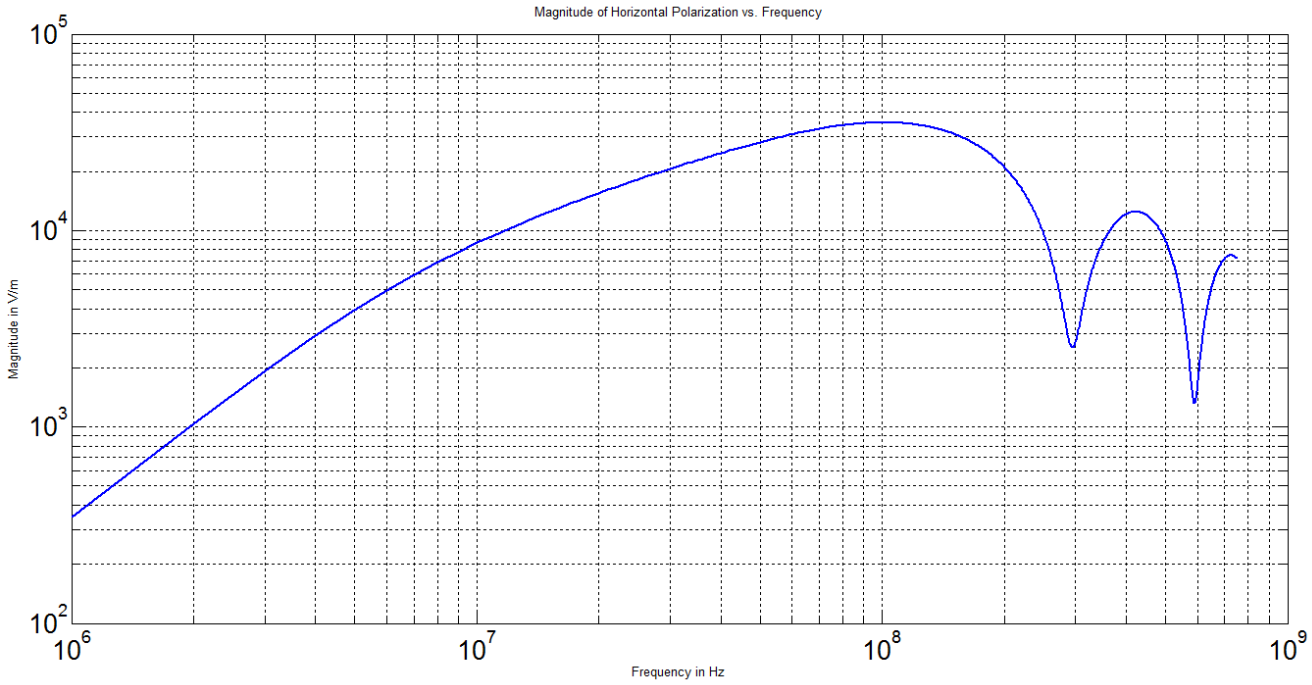

Azimuth Angle $\phi = \frac{\pi}{2}$

Figure 46: Horizontally Polarized Incident Wave with Azimuth Angle $\frac{\pi}{2}$

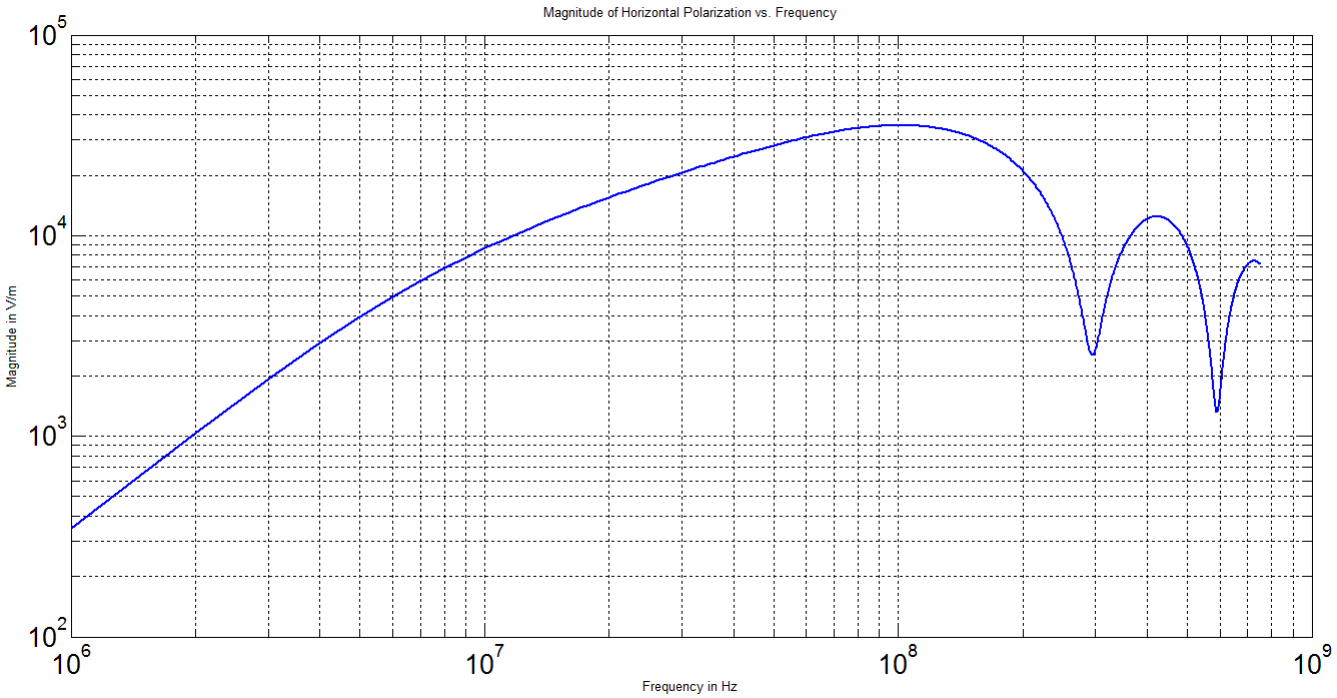

Changing the azimuth angle has a slight change on the maximum of the incident field, but other than this there is no visible effect on the incident field when there is variation in the azimuth angle. A similar analysis can be done for the vertical polarization angle, the Matlab code in Appendix A and the script of the transmission line model in Appendix B should provide enough information to do this analysis with whatever values are relevant to the user. The next step in the transmission line analysis was finding values for the characteristic impedance.

Characteristic Impedance of the Transmission Line

The equation that defines the characteristic impedance Z_o is defined in [13]. This equation was converted into a Matlab function and is being used for this analysis. The unique property of this particular Z_o is that it is the characteristic impedance of the cable with ground as the return path, which is analogous to the model being used for the antenna system.
The charcteristic impedance is complex valued in that it takes into account both the magnitude and phase. The phase refers to the instantaneous relationship between voltage and current. According to transmission line theory the characteristic impedance is independent of length. The concept of a characteristic impedance comes from imagining an infinitely long cable and then measuring the voltage and current accross that cable. From these two measurements the *characteristic* impedance can be found.

Figure 47: Characteristic Impedance as a function of frequency

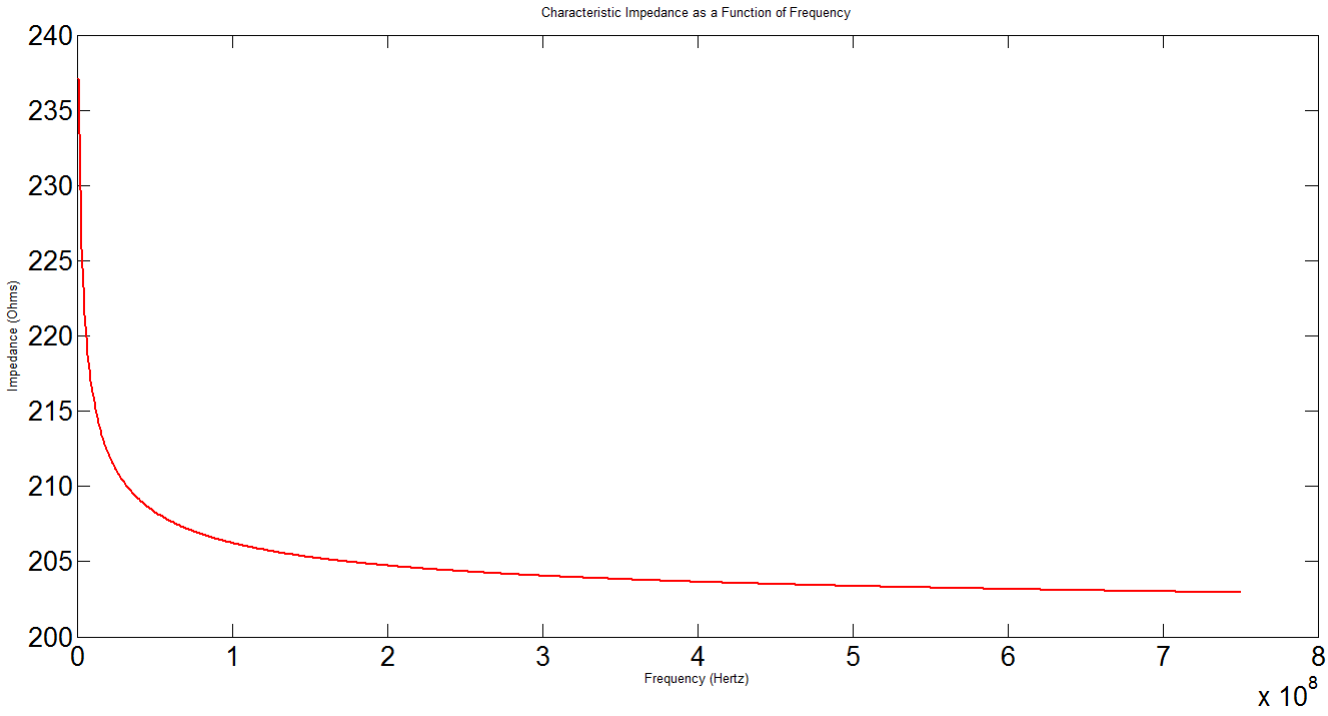

As is illustrated by the graph the characteristic impedance of the cable decreases with increasing frequency. In the lower frequencies the characteristic impedance is dependent on its capacitive and inductive reactances. Thus the magnitude of this impedance is larger for the lower frequencies. At higher frequenices the inductive and capacitive components of the characteristic impedance become independent of frequency. This is illustrated by the figure above in which the characteristic impedance starts to flat line to its pure resistance at the higher frequencies. Now because the characteristic impedance in this case is being determined with ground as the return path of the cable, both the ground conductivity and the dielectric constant will have an effect on the value of the characteristic impedance. Another important parameter of the characteristic impedance is the radius of the cable. The reason this is true is because the greater the radius the more current can flow through the cable. Other than the characteristic impedance another important facor to consider when dealing with the coupling of an electromagnetic wave with a cable is the propagation constant of the cable.

Effect of the propagation constant

The propagation constant of an electromagnetic wave is a measure of the change undergone by the amplitude of the wave as it propagates in a given direction. For this particular case the equation for the propagation constant was taken from [13] and it is the propagation constant for an above ground cable with ground as the return path.
The graph below illustrates the relationship for the attenuation factor, the real value of the propagation constant, and frequency.

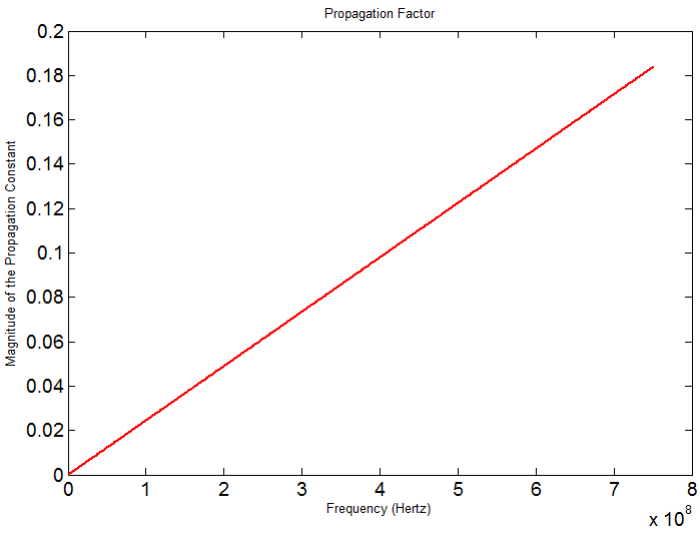

Figure 48: Attenuation factor vs. Frequency

As can be seen there is a direct relationship between the attenuation of the signal along the cable and the frequency that is coupling to the cable. At higher frequencies there will be greater attenuation of the signal. There are two main components to this loss of power between electromagnetic wave and the cable. The metal loss and the dielectric loss. The loss of most transmission lines are dominated by the metal loss, which causes a frequency dependence due to finite conductivity of metals, and the skin effect inside a conductor. The skin effect is the tendency of an alternating electric current to become distributed within a conductor such that the current density is largest near the surface of the conductor. The electric current flows mainly at the "skin" of the conductor, between the outer surface and a level called the skin depth. The skin effect causes the effective resistance of the conductor to increase at higher frequencies where the skin depth is smaller, thus reducing the effective cross-section of the conductor. The skin effect is due to opposing eddy currents induced by the changing magnetic field resulting from the alternating current. The skin effect causes the resistance of the conductor to be approximately dependent on frequency according to the relationship $R \propto \sqrt{\omega}$.
For the transmission line analysis the currents produced along the length of the cable for single frequencies do not exactly match in magnitude and behavior at the currents produced by the NEC model. This is primarilly because the NEC model uses a method of moments approximation and allows for ground cables to go into the ground. The transmission line model does not allow for grounding cables that shunt the current along the horizontal cable to zero.

Figure 49: Transmission Line Analysis with Frequency at 10 MHz

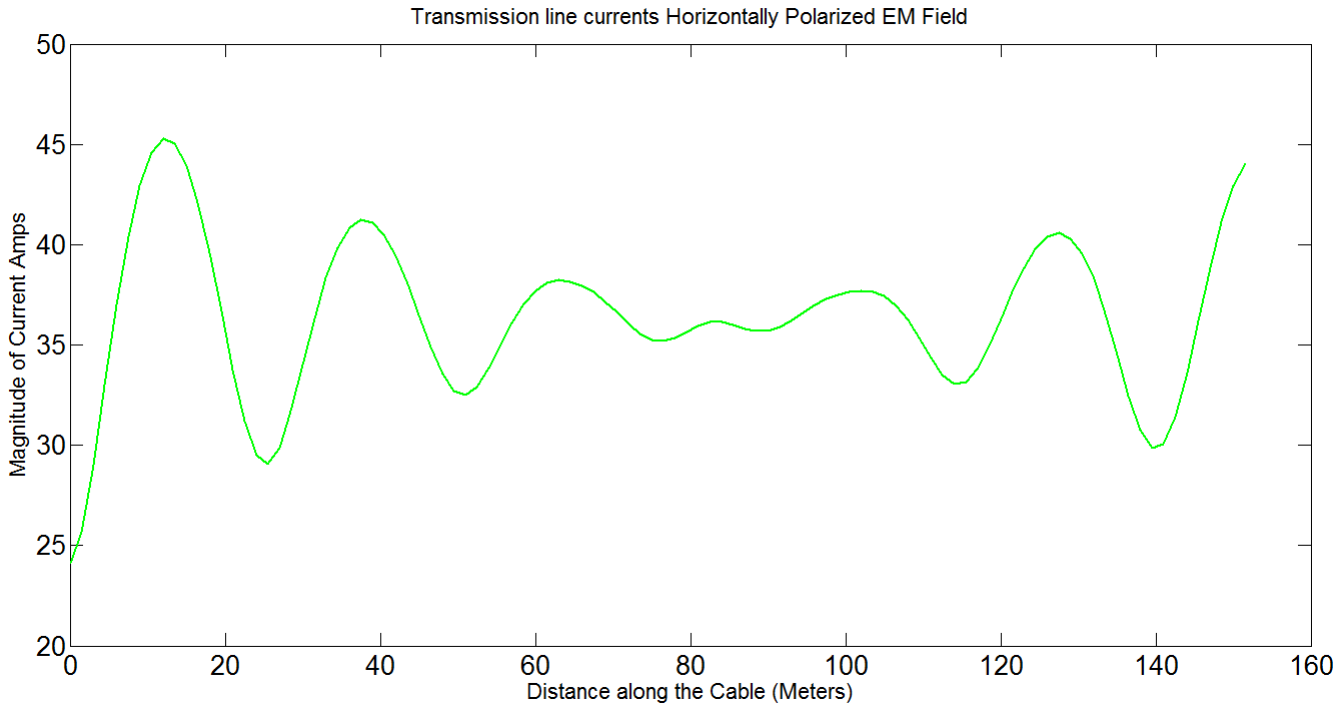

The induced currents in the transmission line model are significantly less at lower frequencies than the currents produced by the model used in NEC. For instance the maximum of the transmission line model at 10 MHz is approximately 45 Amps versus the maximum at in the NEC model of 225 Amps. This is approximately 5 times the current developed on the NEC model versus the transmission line model. The electromagnetic field used in the NEC model is the standard E_o, this does not necessarilly represent the magnitude of the electromagnetic field for each frequency. Thus the actual value of the electromagnetic field for a frequency of 10 MHz is a little bit less than half of E_o. This accounts to some extent for the disparity in the currents produced along the cables. Other reasons can include the way that the NEC model accounts for the ground reflections and how it calculates the currents per segment while the transmission line model does not do such a sophisticated analysis. The NEC model uses the sommerfeld/norton method for calculations of the reflected incident wave from the ground. Which is more accurate than the Fresnel coefficient approximation used in the transmission line analysis. As the frequency of the transmission line analysis increases the magnitudes of the NEC model and the transmission line model slowly approaches similar values for the total current induced along the line. Thus in order to perform the required calculations the NEC model was used, this guarantees accuracy in the results generated. Allowing for design of the filters being used to protect the electronics on the antenna to be designed to shunt or filter out any residual traces of the signal from the cable. The remaining graphs of the transmission line model are available in the Appendix section of this report.

7.4 Total Current Along the Transmission Line

After comparing the transmission line models and the models produced in NEC the total current along the line for different segments was calculated. This was done using a script that cycled through a folder containing 200 NEC outputs. The program would then go through each file and remove the

real and imaginary components for the current at different segments. Once this was completed the total current was calculated by summing up the real and imaginary components for each frequency for a given segment to find the total. The 200 was chosen as the number of samples in the frequency domain to use because it provided a level of accuracy greater than the original 80 samples that were used previously. With 200 samples the period of the pulse could be extended from 150 nano-seconds to 400 nano-seconds. Making it easier to see what happens to the currents along the cable as the energy of the pulse approaches zero. The points chosen along the cable were at z = 0,0.0305, 0.06094, 32.5435, 32.574, 32.6045, 76.25, 76.2805, 76.311, 119.926, 119.9565, 119.987, 152.339, 152.3695, and 152.4 meters.

Figure 50: Current at Z = 0, 0.0305, and 0.06094 meters

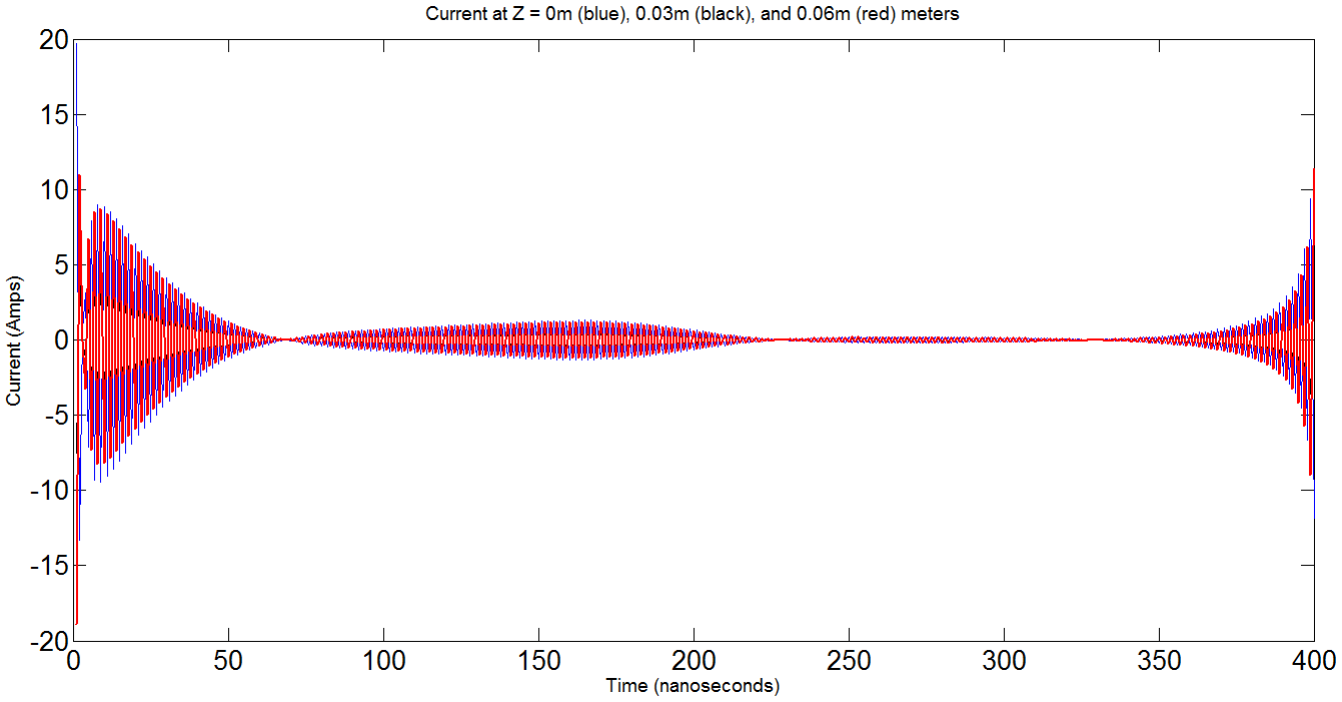

In Figure 50 we can see that the current along the segments is great during the first 50 to 100 nano seconds, representing the times where the majority of the pulse energy lies. After about 200 nano-seconds the current dies down to zero. At around 350 nano-seconds the current increases again. The reason for this increase in current is due to the way the Fourier Transform works. The Fourier transform assumes that the time domain form of the waveform is periodic, thus in this graph the current around 400 nano-seconds is increasing because it is acting like it is going to repeat itself during the next 400 nano-seconds. This increase in current at 400 nano-seconds does not necessarilly imply that there is a physical increase in the current, only that the mathematical construct of the Fourier transform requires a periodic waveform. At the next set of points it will be easier to see a clearer example of this behavior and the large magnitudes of current induced along the cable.

Figure 51: Current at Z = 32.5435, 32.574 and 32.6045 meters

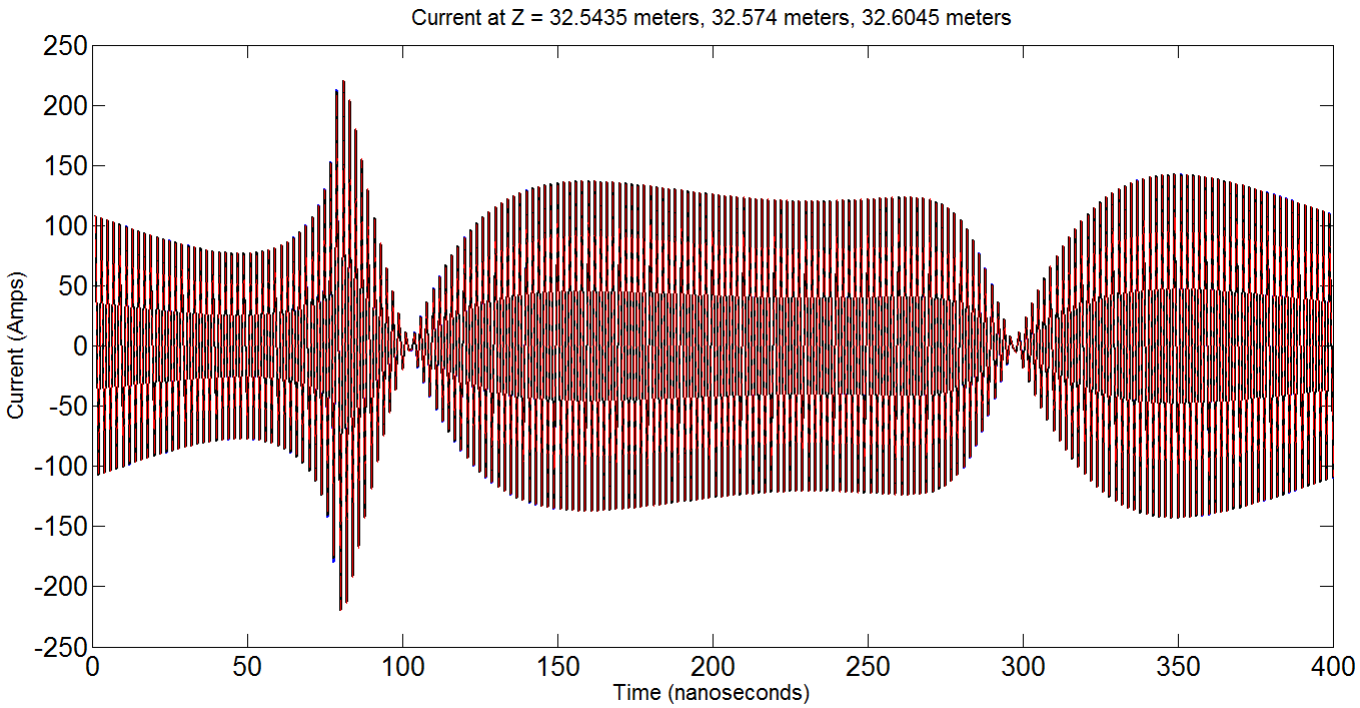

The signal in figure 51 is located approximately a quarter of the cable length away from Z = 0. It is evident that as the current progresses along the cable the greater the amplitude of the signal. This is due to the effectiveness of the grounding rods at the end of the cable. If there was no grounding rod there would be ringing along the end of the cables, this was apparent in the transmission line model. Similar to figure 50, the signal at 32.5435 is in blue, at 32.574 is in black, and at 32.6045 meters the signal is colored red. As the analysis continues farther down the cable it is easy to see that the maximum current far exceeds the capability of the cable to transmit.

Figure 52: Current at Z = 76.25, 76.2805 and 76.311 meters

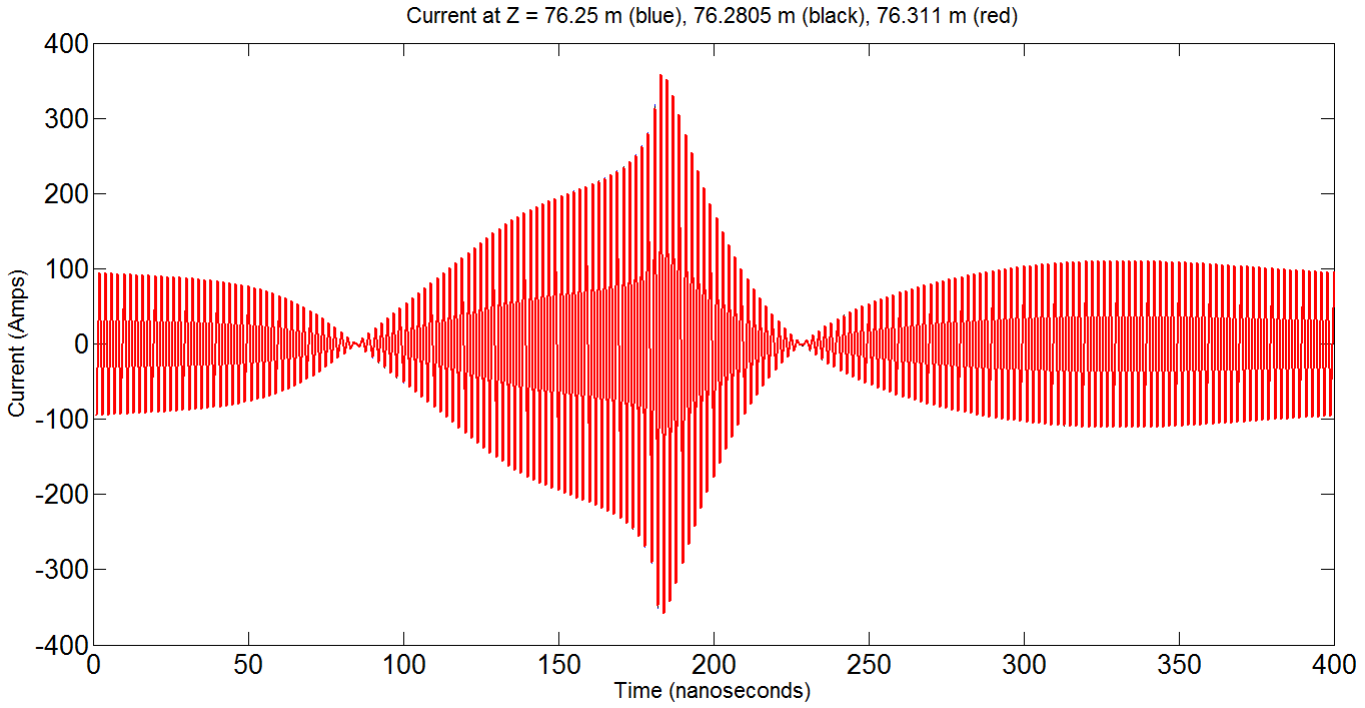

Figure 52 represents the currents at approximately the center of the cable. Here the current reaches a peak around 300 Amps. Although these curent spikes are rather large they occurr over very short lengths of time. Here the current reaches the peak of 300 Amps around 175 nano-seconds, this time is slightly higher than the pulse period that was chosen during a previous stage of the analysis, but what this represents at the center of the cable is that the pulse propagates slower through the cable than it does through air or free space. Thus the pulse will reach its peak at different points throughout the cable, due to this propagation delay. The currents along the cable are also getting reflected back by the two load impedances, thus there will be some addition and cancelation of reflected waves along the length of the cable. It just so happens that the sum of all currents along the cable from multiple frequencies of the incident pulse add up to a maximum at the center of the cable.
It is also easy to see the results of the Fourier transform on the shape of the waveform. From about 250 nano-seconds and onwards the Fourier transform assumes that the pulse is periodic repeating this period, the current carries over throughout the 400 nano-second duration and does not fade to zero as would be expected. Given that the current gets reflected along the length of the cable, there should be some residual current after the end of the pulse, it is unlikely that this current will be at amplitudes of 100 Amps.

Figure 53: Current at Z = 119.9565, 119.987 and 120.0175 meters

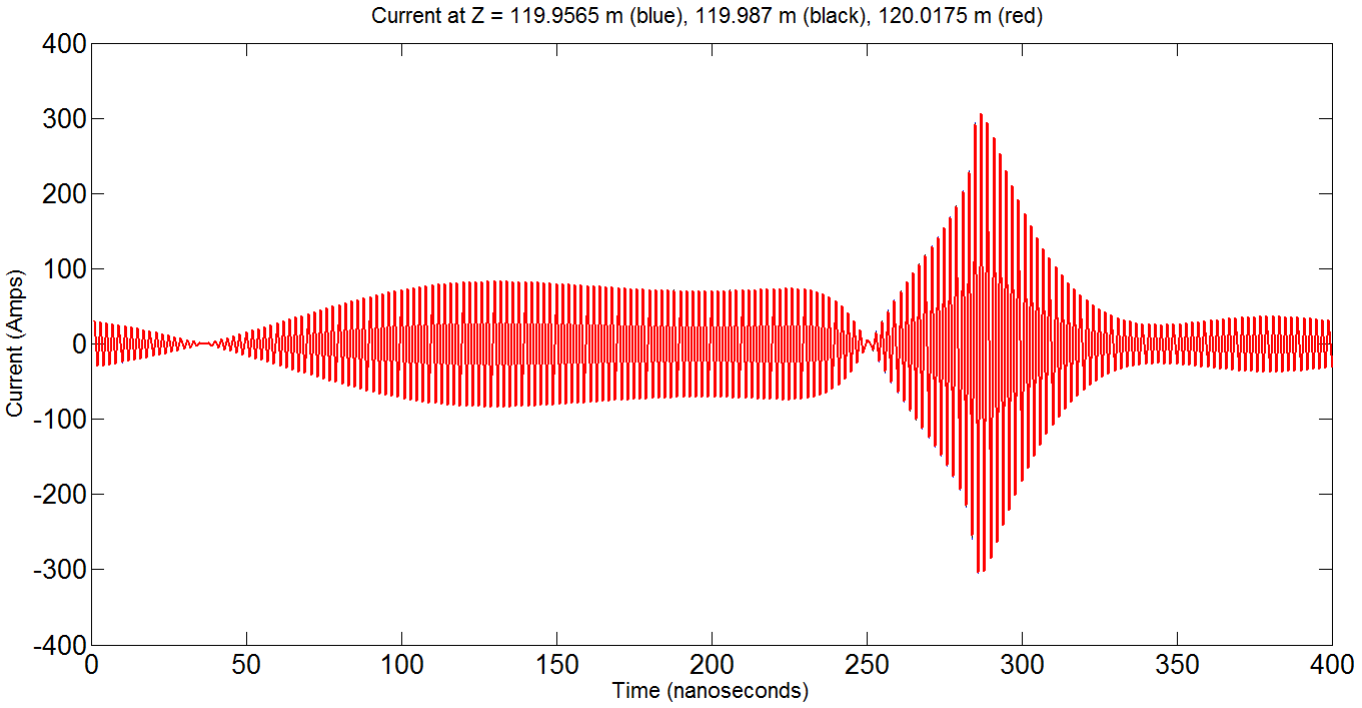

In Figure 53 the peak along this segment occurs approximately at 275 nano-seconds. As was explained earlier as there is a propagation delay between the signal in free space and the signal traveling through the cable. This delay causes the maximum energy of the pulse to couple to the length of the cable at different times. This with the effects of reflections of the signal accross the cable change the peak amplitude and its temporal location. Another interesting thing to note is that prior to the signal reaching its maximum the current decreases to zero and then suddenly increases. This could indicate that the signal is out of phase at a time of approximately 250 nano-seconds then between the 250 and 300 nano-seconds the signals are in phase allowing for the large increase in current. The indvidual phases of each of the frequencies coupling to the cable are available in the NEC output data. By simply taking the real and imaginary parts and following the elementary formula: $\theta = arctan(\frac{X}{R})$ where X is the imaginary component of the current and R is the real component, the resulting phase can be found. Or a simpler method can be used if MATLAB is accessible by inputting the imaginary and real coefficients into the angle function in MATLAB and the software will solve for the phase.

Figure 54: Current at Z = 152.339, 152.3695, and 152.4 meters.

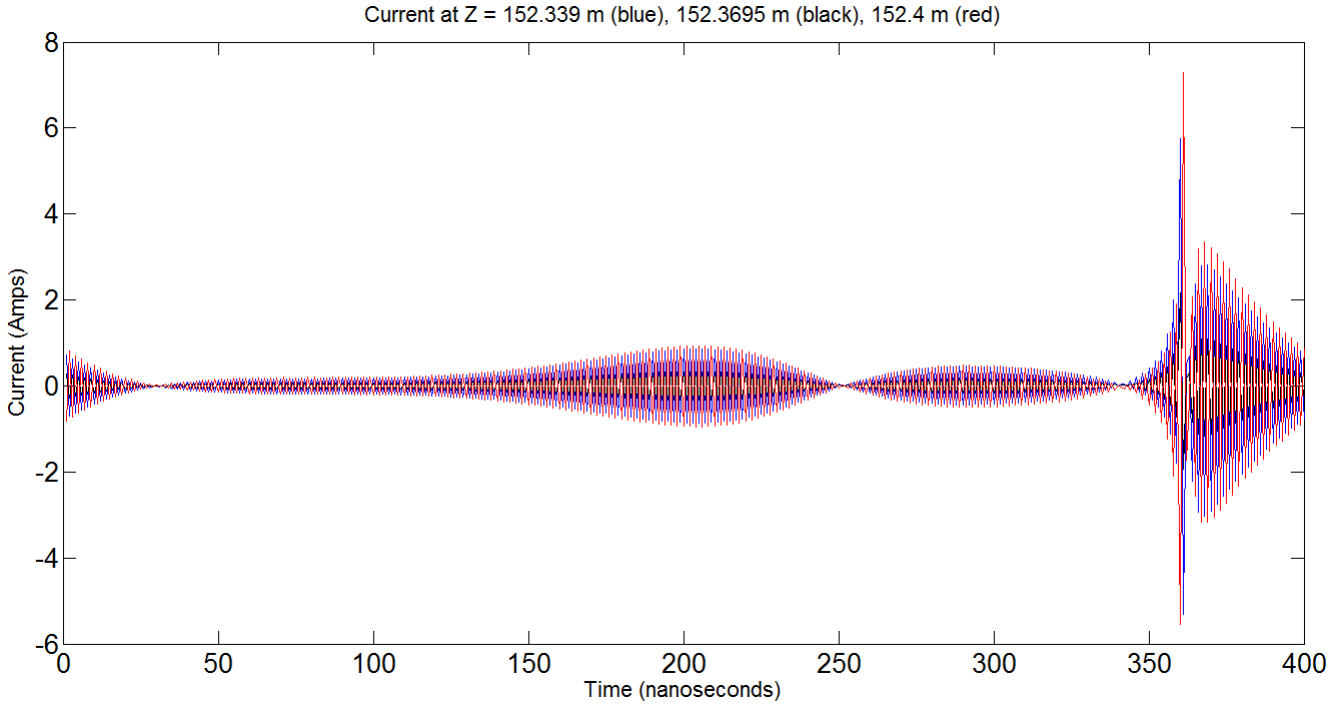

At the end of the cable the current reaches its peak at a time of approximately 360 nano-seconds. This time is significantly greater than when the majority of the pulse energy reaches the cable. This delay is due to the propagation delay of the signal between the air and the cable and the reflected currents from the terminal impedances. The amplitude of the current signal is also much less than the amplitudes at the other measured locations along the wire. This is due to the grounding rod delivering most of the built up currents along the cable to ground at the end. As can be seen thanks to the grounding rods significant portions of the induced current are grounded at the terminals. Thus any residual current that could flow to the electronics on the antenna would be somewhere in the vicinity of 2 to 3 amps. The current at the ends are small enough that they can be reduced by multiple filters if need be. To get a better idea of the maximum of the current distributed along the length of the cable the plot in Figure 55 illustrates this below.

Figure 55: Max Currents along the length of the cable

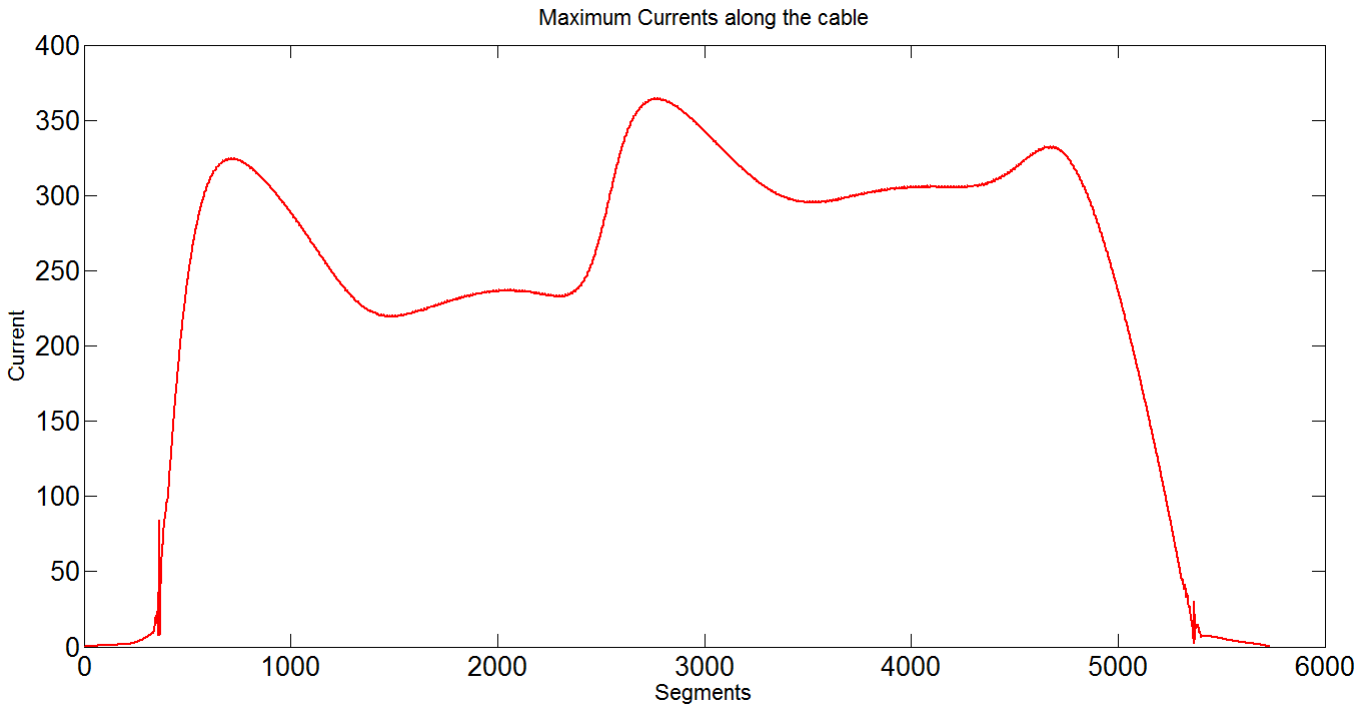

Figure 54 shows that the peak current amplitude is located approximately at the center of the cable. The maximum current is a total of 350 Amps. This is about twelve times greater than the maximum current that is supposed to be transported across the cables in order to deliver power to the antenna electronics. Taking the sum of at each segment and then dividing by the total number of segments gives an average current of 238.37429533 Amps. The cable is rated for 30 watts for power transmission, with an average current of 238.37429533 Amps dissipated across all the segments for a approximately 400 nano-seconds.

8 Observations and Conclusions

The greatest challenge was planning and meeting a specified deadline. For most projects it is the case that there will be enough randomness during the timeline of the project that will create delays in its overall completion. This project was no different. A historic example of a project that was effected by overly optimistic planners is the Sydney Opera House. The original cost and scheduling estimates in 1957 projected a cost of $ 7 million and a completion date of 26 January 1963. In actuality, the project was completed ten years late and more than fourteen times over budget. The Sydney Opera house, being a fairly extreme example of a project costing more and lasting longer than projected, is nonetheless, a good example of how optimisim can effect the scheduling and budgeting of a project. The next general observation that could be made in regards to this project is the problem of scale. When creating any model, the question must be asked as to how well it will scale and what are the effects of scaling the model. Scaling in this context is to be taken as the increase or decrease of the size of the model relative to some sort of metric. For instance within the models produced and studied in this report the number of segments along the cable and in the antenna design would be the metric that determines the scale of the model. At the beginning of this project the models that were being analyzed could be considered small given the number of segments that were under scrutiny. As the

project approached the deadline, the model size scaled exponentially. At the beginning of this project the model size was between 50,000 and 5 million segments. This included multiple observations made using different frequencies. When analyzing multiple illumination angles for each frequency the size of the model grew to beyong 100 million segments. This increased computation time exponentially. Thus for the case of this project the larger the model the greater the cost in time to compute, using the processor available on a Dell portable computer. Given that this is not the fastet computing tool out there, the size of the model nonetheless reduces the portability of making an analysis. The model previously described was only the model of the cable, not including the antenna. The cable itself is approximately 6000 segments. With the addition of the antenna model, this becomes a total of 26,000 elements. Taking the number of illumination angles under scrutiny which is 168 and the total number of frequencies used to sample the pulse, 200, and multiplying these together. The model which was once between 50000 and 5 million segments now becomes, 873,600,000 segments. This is a huge increase in the amount of information that the programs that were developed to originally handle at most 5 million segments need to parse through. Increasing the compuation time dramatically. Thus making this project not only one of analysis but of optimization.

The project itself is only a subset of the knowledge gained from the experience at MITRE. One of the many truths about working in a large company is that meetings will be ubiquitous and ever present. Communication is important and the flow of information must be exact. Disseminating knowledge to the wrong people is not only foolish but in some cases may be dangerous. Thus the flow of information must have one direction if it is to have any direction at all, and that direction is up. It is the job of management to know what is going on so keeping them informed is important.

As much of the project was learning about the problem but also dealing with people. When asked when a task will be completed, it is best to never allow anyone make that decision but the person to which the task is assigned. Knowing the limits of skill is also an important factor. The easiest way to lose respect amongst a team, management or other group of people is to over sell and under deliver. Therefore know what it is you don't know and make that apparent. A person cannot be reprimanded for having a lack of knowledge, as knowledge is a product of time, given enough time and motivation that person can easily gain the knowledge required.

9 Appendix

9.1 Appendix A: Matlab Functions

$function[Zo] = char\_impedance(sigma, h, a, w)$

This function calculates the characteristic impedance of a transmission line with the ground as a return path. This is an approximation of the characteristic impedance of a wire with the ground as a return path. The function is dependent on the height above the soil h, the radius of the wire a, the inductance and capacitance of the wire, and the frequency of the excitation field.

$mu\_o = 4 * pi * 10e - 7;$
$tau\_h = mu\_o * sigma * h^2;$
$Zo = 60*log((2*h)/a)*(1+(1/(2*log((2*h)/a))*(log((1+sqrt(1i*w*tau\_h))/sqrt(1i*w*tau\_h)))));$

end

$function[current] = distributed\_currents(z, K1, P, K2, Q, gamma)$

distributed_current is a function that finds the current along any point along a transmission line.

$current = (K1 + P). * exp(-gamma * z) + (K2 + Q). * exp(gamma * z);$

end

$function[E\_Field] = horizontal\_polarization\_field(h, E\_i, w, R\_h, psi, phi, z)$

This function takes in an argument called h, for height in meters, $E_i$for the incident field magnitude measured in V/m, w for frequency in rad/sec and sigma (soil conductivity measured in mhos/m ,and the dielectric constant *epsilon_r* which has no units. psi which stands for the elevation angle of incidence. phi which is the azimuth angle of incidence, and z which is distance in the horizontal (z) directon measured in meters. H_excite_field outputs the Electric Field at that Height.

$mu\_o = 4 * pi * 10e - 7;$ magnetic permeability of free space
$epsilon\_o = 8.85 * 10e - 12;$ electric permittivity of free space
$phase\_factor = w. * sqrt(mu\_o * epsilon\_o);$ phase factor for the air.

Horizontally Polarized Electric Field, with fresnel reflection coefficient embedded into the equation. E_i is either a single value or a vector. k is also either a single value or a vector. $R\_h(h, a)$ is also either a single value or a vector

$E\_Field = E\_i * sin(phi). * (1 + R\_h. * exp(-1i * 2. * phase\_factor. * h * sin(psi))). * exp(-1i * cos(psi) * cos(phi). * z. * phase\_factor);$

end

$function[reflect\_coeff] = horizontal\_reflection\_coefficient(sigma, epsilon\_r, w, psi)$

Fresnel Reflection coefficient that is used to predict the amount of reflection of an electromagnetic wave as it travels through different mediums R_h accepts two inputs and outputs either a single number or a matrix. The first input is the conductivity measured in mhos/m. The second input is the dielectric constant. The third input is the frequency, (single number or vector) and psi is the elevation angle of incidence. This reflection coefficient is for horizontal polarization in its most general form. Such that the azimuth and elevation angles can be anything. Psi is the elevation angle of incidence and is measured in radians.
$epsilon\_o = 8.85 * 10e - 12$; electric permittivity of free space
$epsilon = epsilon\_r * epsilon\_o$; electric permittivity of ground

fresnel reflection coefficient, for a perfectley conducting ground sigma will be equal to infinity, and the reflection coefficient for a horizontally polarized excitation is -1.
$reflect\_coeff = (sin(psi) - (epsilon\_r. * (1 + sigma./(1i * w * epsilon)) - cos(psi)^2).^{(1/2)})./(sin(psi) + (epsilon\_r * (1 + sigma./(1i * w * epsilon)) - cos(psi)^2).^{(1/2)})$;

end

$function[V] = horizontally\_polarized\_voltage(Zo, K1, P, gamma, z, K2, Q)$

horizontally_polarized_voltage is a function that calculates the voltage along a transmission line that is excited by a horizontally polarized electromagnetic field. The inputs to this function are Zo which is the characteristic impedance, K1 which is a constant defined in Coupling to Shielded Cables "Vance", P which is an integral defined in the same book, gamma which is the propagation factor, z the distance along the line in the horizontal direction, K2 another constant defined in Vance, and Q another integral defined in Vance. V is the output as a matrix and it give the total voltage along different points in the line, V is solved for in Vance on page 32.

$V = Zo * ((K1 + P). * exp(-gamma. * z) - (K2 + Q). * exp(gamma. * z))$;

end

$function[K1] = K1(z1, z2, Zo, gamma, E_zh, rho\_1, rho\_2, psi, phi, w, Rh, h)$

This is a function of the constant K1, which is used in the equation for the induced currents along a transmission line. This constant K accepts multiple inputs. Z1 is the terminating impedance at one end of the line. Z2 is the terminating impedance at the other end of the line. Zo is the characteristic impedance of the transmission line. gamma is propagation factor in soil. E_zh is the horizontally polarized excitation field. rho_1 is the reflection coefficient for the beginning of the line. rho_2 is the reflection coefficient for the other end of the line. The output of this function is K1 which is a constant that is used in determining the total induced currents anywhere along a line.

$K1 = rho\_1. * exp(gamma * z1). * ((rho\_2. * (P(Zo, E_zh, gamma, z2, z1, psi, phi, w, Rh, h)). * exp(-gamma. * z2) - (Q(Zo, E\_zh, gamma, z1, z2, psi, phi, w, Rh, h))$
$. * exp(gamma. * z2))./(exp(gamma. * (z2 - z1)) - rho_1 * rho_2. * exp(-gamma * (z2 - z1))))$;

end

$function[K\_2] = K2(z1, z2, Zo, gamma, E\_zh, rho\_1, rho\_2, psi, phi, w, Rh, h)$

This is a function of the constant K2, which is used in the equation for the induced currents along a transmission line. This constant K accepts multiple inputs. Z1 is the terminating impedance at one end of the line. Z2 is the terminating impedance at the other end of the line. Zo is the characteristic impedance of the transmission line. gamma is propagation factor in soil. E_zh is the horizontally polarized excitation field. rho_1 is the reflection coefficient for the beginning of the line. rho_2 is the reflection coefficient for the other end of the line. The output of this function is K1 which is a constant that is used in determining the total induced currents anywhere along a line.

$K_2 = rho\_2. * exp(gamma * -z2). * ((rho\_1. * (Q(Zo, E\_zh, gamma, z1, z2, psi, phi, w, Rh, h)). * exp(gamma * z1)$
$-(P(Zo, E_zh, gamma, z2, z1, psi, phi, w, Rh, h)). * exp(-gamma * z1))./(exp(gamma. * (z2 - z1)) - rho\_1 * rho\_2. * exp(-gamma. * (z2 - z1))));$
end

$function[P2] = P(Zo, E\_zh, gamma, z, z1, psi, phi, w, R\_h, h)$

The current from a point Z1 to Z along the transmission line. This function accepts five inputs. Zo the characteristic impedance, E_zh the horizontal excitation, gamma the propagation factor, z the distance along the transmission line, and z1 the location of the first terminal impedance. P outputs a value P which is the current from the first terminating impedance to a point along the transmission line.

$mu\_o = 4 * pi * 10e - 7;$
$epsilon\_o = 8.85 * 10e - 12;\ k = w * sqrt(mu\_o * epsilon\_o);$

$P2 = ((E\_zh. * sin(psi). * (1 + R\_h. * exp(-1i * 2 * k * h * sin(psi))))./(2 * Zo * (gamma - 1i * k * cos(psi) * cos(phi)))). * (exp(z. * (gamma - 1i * k * cos(psi) * cos(phi))) - exp(z1. * (gamma - 1i * k * cos(psi) * cos(phi))));$

end

$function[Q2] = Q(Zo, E\_zh, gamma, z, z2, psi, phi, w, R\_h, h)$

The current from a point Z1 to Z along the transmission line. This function accepts five inputs. Zo the characteristic impedance, E_zh the horizontal excitation, gamma the propagation factor, z the distance along the transmission line, and z1 the location of the first terminal impedance. P outputs a value P which is the current from the first terminating impedance to a point along the transmission line.

$mu\_o = 4 * pi * 10e - 7;$
$epsilon\_o = 8.85 * 10e - 12;$

$k = w * sqrt(mu\_o * epsilon\_o);$

$Q2 = ((E\_zh. * sin(psi). * (1 + R\_h. * exp(-1i * 2 * k * h * sin(psi)))./(2 * Zo * (-gamma - 1i. * k * cos(psi) * cos(phi)))). * (-exp(-z. * (gamma + 1i * k * cos(psi) * cos(phi))) + exp(-z2 * (gamma + 1i * k * cos(psi) * cos(phi))));$

end

$function[temp] = read\_nec\_ouput()$

read_nec_ouput does not take anything as input, instead it is a function that opens up NEC file within a certain folder and then goes through that file pulling out data from the NEC output. This function is the base function that was modified to make *read_nec_output* the function used to analyze the total induced currents along the cable. setting up a directory, point it to a place on the machine

$direc =' C : \backslash Users \backslash abennett \backslash MyDocuments';$

This goes through the directory and extracts the file in quotations " which in this case is $'Model\_2out'$. $(Note : Model2outhastoexistalreadywithinthedirectoryinordertoactuallybeusedbythisfunction.)$

$files = fullfile(direc,' Model\_2out');$

this line of code opens the file and allows matlab to read from it, that is what the $r+$ is for.

$fid = fopen(files,' r+');$

the following while loop is for cycling through the data in order to find specific information. In this case the while loop will flow down the NEC output until it finds the string '— CURRENTS AND LOCATION —' when it does find this string it will proceed.

$while\ 1\ tline = fgetl(fid);$
$if\tilde{i}sempty(strfind(tline,'---CURRENTSANDLOCATION---')), break, end$
end

tline jumps between the lines, the way the NEC output is setup the tline will skip over unnecessary strings until it gets to the actual output of the data.
$tline = fgetl(fid);$
$tline = fgetl(fid);$
$tline = fgetl(fid);$
$tline = fgetl(fid);$
$tline = fgetl(fid);$

current1 scans through the text and allows the user to take the floating point data from the NEC output. There are exactly 11 columns of data within the NEC output each representing something different. f allows the user to choose this column which turns out to be the number of segments. The $*$ in $\%*f$ tells textscan to skip over this column of data, thus it will not be saved in the matrix current1.

$current1 = textscan(fid,'\%f\%*f\%*f\%*f\%*f\%*f\%f\%f\%f\%f');$
$segment = [current11];$

real and imaginary are the real and imaginary components of the current in the frequency domain. Thus the magnitude and phase of the induced currents in the frequency domain.

$real = [current12];$
$imaginary = [current13];$

with these values you can do whatever you like with them, plot them etc etc.

end

$function[current\_per\_segment] = read\_nec\_output2()$
$read\_nec\_ouput$ does not take anything as input, instead it is a function that opens up NEC file within a certain folder and then goes through that file pulling out data from the NEC output. This function outputs an n x m matrix where n is the number of rows and it represents each frequency that was used in NEC and m is the number of segments used in the analysis.

$direc =' C : \backslash Users\backslash abennett\backslash MyDocuments'$; setting up a directory, point it to a place on the machine
$files = fullfile(direc,' Model_4out')$; take the directory and merge it with test.out

$fid = fopen(files,' r+');$
$test = fullfile(direc,' test.pl');$
$current_per_segment = [];$
$nfreqs = str2double(perl(test, files));$
$i = 1;$
$adder = 2;$
$count = 2;$
$real_total = [];$
$imaginary_total = [];$
$final_mag = 0;$
$final_phase = 0;$

this while loop cycles through the NEC data to the different frequency outputs and takes the data from these output to analyze it.

$whilenfreqs > i - 1$

$fid = fopen(files,' r+');$
$while\ 1$
$tline = fgetl(fid);$
$count = count - \tilde{i}sempty(strfind(tline,' FREQUENCY ='));$
$ifcount == 1,$

$strfind(tline,'FREQUENCY =');$
$frequency = tline;$
$break,$
end
end
$fid = fopen(files,'r+');$
$while\ 1$
$tline = fgetl(fid);$
$adder = adder - \tilde{i}sempty(strfind(tline,'---CURRENTSANDLOCATION---'));$
$if adder == 1,\ break,\ end$
end
$strfind(tline,'---CURRENTSANDLOCATION---');$
$tline = fgetl(fid);$
$tline = fgetl(fid);$
$tline = fgetl(fid);$
$tline = fgetl(fid);$
$tline = fgetl(fid);$
$current1 = textscan(fid,'\%f\%*f\%*f\%*f\%*f\%*f\%f\%f\%f\%f');$

$segment = [current11];$
$real\_total = [real_total; current12'];$
$imaginary\_total = [imaginary\_total; current13'];$
$current\_per\_segment = [current\_per\_segment; real\_total(i,:) + 1j.*imaginary\_total(i,:)];$

$i = i + 1;$
$adder = adder + i;$
$count = count + i;$
end

end

9.2 Appendix B: Matlab Scripts

Transmission Line Analysis Script

The script below is the MATLAB code that runs the transmssion line analysis.
clc
clear all

The following script is used to define HEMP E1 and the horizontally
polarized excitation field and the induced currents along a transmission
line due to this field .

LIST OF KEY PARAMETERS

$Eo = 50000;$ peak amplitude

$alpha = 4e7$; Constant
$beta = 6e8$; constant
$k = 1.3$; Constant
$f = 100000$; frequency range for HEMP E1
$w = 2 * pi * f$; Angular Frequency for HEMP E1
$psi = pi/2$; Elevation angle of incidence
$phi = pi/2$; Asimuth angle of incidence
$h = 0.1016$; Height above the surface
$sigma = .2$; Conductivity of the ground
$epsilon_r = 13$; Dielectric constant of the ground
$c = 3.0e8$; Speed of light in free space
$mu\_o = 4 * pi * 10e - 7$; Magnetic Permeability
$tau\_h = mu\_o * sigma * h^2$; time constant
$theta = pi/2$; theta is the polarization angle

$Z1 = 10$; measured in Ohms
$Z2 = 10$; measured in Ohms
$z1 = 0$; distance along the transmission line measured in meters

$z2 = 152.4$; distance at the end of the transmission line measured in meters
$z = z1 : .001 : z2$; distance along the line broken up into lambda/60 segments

$a = 0.00712704259$; radius of the cable. Wire gauge 6, three wire cable, add the areas, then solve for new radius.

The HEMP Pulse is defined as a double exponential. Taking the Fourier transform of this double exponential gives the frequency spectrum of the pulse.

HEMP E1 Frequency Spectrum $(V/(m - Hz))$

$frequency_spectrum = Eo * (1./(1i * w + alpha) - 1./(1i * w + beta))$;

Taking the Frequency spectrum and multiplying by the frequency content, should give a vector containing the Electric Field Amplitudes at specific frequencies.

Electric Field Amplitude at Different Frequencies

$electric\_content = abs(frequency\_spectrum. * w)$;

Fresnel reflection coefficients determine the propagation of electromagnetic waves through medias with different conductivities and electric permitivities.

---

electric field magnitude for horizontal or vertical polarization

---

$E\_iv = electric_content * cos(theta);$
$E\_ih = electric_content * sin(theta);$

Fresnel Reflection coefficients

$Rv = vertical\_reflection\_coefficient(epsilon\_r, sigma, w, psi);$
$Rh = horizontal\_reflection\_coefficient(sigma, epsilon\_r, w, psi);$

---

electromagnetic waves at the interface between media with different dielectric and conductive properties. I multiply by omega because the frequency spectrum uses angular frequency. Taking these magnitudes and inputting them into the function H_excite_field should give me the total horizontally polarized excitation due to the HEMP E1. The parameters for H_excite_field are as follows. First there is h, which is the height above the ground. According to MIL-STD 188-2-125 the maximum height a cable can be above the ground is 4 inches. In meters this would be 0.1016m. The parameter E_i is the magnitude of the incident field which is defined in the vector *electric_content*. f is the frequency vector or the range of frequencies that this function will cover.Sigma and *epsilon_r* are ground constants, sigma is the conductivity of the ground and *epsilon_r* is the dielectric constant of the ground.

E_zh is equal to the values of the horizontal excitation field

---

$E\_zh = horizontal\_polarization\_field(h, E\_ih, w, Rh, psi, phi, z);$
$E\_zv = vertical\_polarization\_field(E\_iv, z, pi/6, 0, Rv, h, w);$

Once the horizontal excitation field was calculated now the currents induced along the wire can also be calculated using transmission line analysis. The first thing to do is to calculate the characteristic impedance of the line. This is done using the function *char_impedance*. *char_impedance* calculates the characteristic impedance of a cable with ground as the return path. The parameters to this equation are h the height the cable is above ground, soil conductivity, radius of the cable, and frequency of the excitation field. *char_impedance* outputs a vector with the characteristic impedance of the line for different frequencies.(Assuming for now that both sigma and *epsilon_r* stay constant.

---

char_impedance calculates the characteristic impedance for multiple frequencies along the wire

---

$Zo = char\_impedance(sigma, h, a, w);$ ---

the next function to consider is gamma which is the propagation factor. the propagation factor helps describe the propagation of waves through the soil. in the case of a transmission line with ground as the return path gamma is equivalent to.

Gamma (propagation factor)

$gamma = 1i * w/c * (1 + 1/(2 * log(2 * h/a)) * (log((1 + sqrt(1i * w * tau\_h))/(sqrt(1i * w * tau\_h)))));$

Other factors that must be considered are the reflection coefficients caused by the terminating impedances. The parameters that define these coefficients are described below.

---

rho_1,rho_2: Reflection coefficients from the end of the line

---

$rho\_1 = (Z1 - Zo)/(Z1 + Zo)$; unitless
$rho\_2 = (Z2 - Zo)/(Z2 + Zo)$; unitless

K1 and K2 are the constants that go into the equation for the induced currents along the line.

Constants K1 and K2

$K\_1 = K1(z1, z2, Zo, gamma, E\_zh, rho\_1, rho\_2, psi, phi, w, Rh, h)$; $K\_2 = K2(z1, z2, Zo, gamma, E\_zh, rho\_1$
$K\_1v = K1v(z1, z2, Zo, gamma, E\_zv, rho\_1, rho\_2, psi, phi, Rv, h, w)$; $K\_2v = K2v(z1, z2, Zo, gamma, E\_zv, r$

Now that the constants K1 and K2 have been found the next step is to find the currents induced on the wire. The last equations that must be solved for are the integrals P(z) and Q(z).

Solution to the Intergrals P(z) and Q(z)

$Ph = P(Zo, E\_zh, gamma, z, z1, psi, phi, w, Rh, h)$;
$Qh = Q(Zo, E\_zh, gamma, z, z2, psi, phi, w, Rh, h)$;
$Pv = P\_v(E\_iv, Rv, h, psi, phi, Zo, z, z1, gamma, w)$;
$Qv = Q\_v(E\_iv, Rv, h, psi, phi, Zo, z, z2, gamma, w)$;

---

to solve for the induced currents along the line plug in the equation for the distributed currents.
$current = distributed\_currents(z, K\_1, Ph, K\_2, Qh, gamma)$;
$total\_voltage = horizontally\_polarized\_voltage(Zo, K\_1, Ph, gamma, z, K\_2, Qh)$;

```
    a = figure;
plot(z, abs(current));
title('Transmission line currents Horizontally Polarized EM Field');
xlabel('Distance along the Cable (Meters)');
ylabel('Magnitude of Current Amps');
b = figure;
plot(z, abs(total_voltage));
title('Transmission line voltage Horizontally Polarized EM Field');
xlabel('Distance along the Cable (Meters)');
ylabel('Magnitude of Voltage V');
```

Table 9: Parameters of the GE card [21]

gpflag	I1	Geometry ground plain flag.
gpflag	I1 = 0	no ground plane is present
gpflag	I1 = 1	Indicates a ground plane is present. Structure symmetery is modified as required, and the current expansion is modified so that the currents an segments touching the grounnd (X, Y plane) are interpolated to their images below the ground (charge at base is zero).
gpflag	I1 = -1	indicates a ground is present. Structure symmetry is modified as required. Current expansion, however, is not modified, thus, currents on segments touching the ground will go to zero at the ground.

Table 10: Parameters of the EN card [21]

End of Run	EN	To indicate to the program the end of all execution
No parameters	NA	NA

Table 11: Parameters of the EX card (Incident Plane Wave Excitation) [21]

Excitation	EX	Specifies the excitation for the structure. The excitation can be voltage sources on the structure, an elementary current source or a plane wave incident on the structure.
I1		determines the excitation that is used
	0	voltage source (appliex-E-field source)
	1	incident plane wave, linear polarization.
	2	incident plane wave, right-hand (thumb along the incident k-vector) elliptic polarization.
	3	incident plane wave, left-hand elliptic polarization.
	4	elementray current source.
	5	voltage source (current - slope- discontinuity).
I2		Number of theta angles desired for the incident plane wave.
I3		Number of phi angles desired for the incident plane wave.
I4		Only column 19 is used. Options are:
	1	maximum relative admittance matrix asymmetry for network connections will be calculated and printed
	0	No action
F1		Theta θ in degrees. Theta is a standard spherical coordinate, measured from the Z-axis.
F2		Phi ϕ in degrees. Phi is the standard spherical angle defined in the XY plane, measured around the Z-axis.
F3		Eta η in degrees. Eta is a polarization angle, defined as the angle between the theta-directed unit vector and the electric-field (E) vector for linear polarization, or the major ellipse axis for elliptical polarization.
F4		Theta angle stepping increment in degrees
F5		Phi angle stepping increment in degrees.
F6		Ration of minor axis to major axis for elliptic polarization.

Table 12: Parameters of the FR card [21]

Frequency	FR	To specify the frequency (frequencies) in MegaHertz.
IFRQ	I1	determines type of frequency stepping
	0	linear stepping
	1	multiplicative stepping.
NFRQ	I2	Number of frequency steps. If this field is blank one is assumed.
	I3, I4	Blank.
FMHZ	F1	Frequency in MegaHertz.
DELFRQ	F2	frequency stepping increment. If the frequency stepping is linear, this quantity is added to the frequency each time. If the stepping is multiplicative this is the multiplication factor.
	F3...F6	Blank

Table 13: Parameters of the GN card [21]

Ground Parameters	GN	To specify the relative dielectric constant and conductivity of ground in the vicinity of the antenna. In addition, a second set of ground parameters for a second medium can be specified, or a radial wire ground screen can be modeled using a reflection coefficient approx.
IPERF	I1 -1 0 1 2	ground- type flag. The option are: nullifies ground parameters previously used and sets free-space condition. The remainder of the card is left blank in this case. finite ground, reflection-coefficient approximation. perfectley conducting ground finite ground, Sommerfeld/Norton method.
NRADL	I2	Number of radial wires in the ground screen approximation blank or 0 implies no ground screen.
	I3, I4	Blank.
EPSE	F1	Relative dielectric constant for ground in the vicinity of the antenna. Leave blank in case of a perfect ground
SIG	F2	conductivity in mhos/meter of the ground in the vicinity of the antenna. Leave blank in the case of a perfect dielectric constant $Ec = Er - j * sigma/(omega * epsilon_o)$ is set to EPSR
	F3...F6	Blank (for an infiinite ground plane)

9.3 NEC Models

CE Model 1: 500 ft Power Wire in Dry, Sandy Coastal Land, with HEMP pulse at 750 MHz
GW, 1, 457, 0, 0, -3.048, 0, 0, 0, 0.00636
GW, 2, 16, 0, 0, 0, 0, 0, 0.1016, 0.00636
GW, 3, 7620, 0, 0, 0.1016, 152.4, 0, 0.1016, 0.00636
GW, 4, 16, 152.4, 0, 0.1016, 152.4, 0, 0, 0.00636
GW, 5, 457, 152.4, 0, 0, 152.4, 0, -3.048, 0.00636
GE -1 1
FR, 0, 12, 0, 0, 62.5, 62.5
GN, 2, 0, 0, 0, 13, .2
EX, 1, 1, 1, 0, 45., 0., 0., .25, 1., 0., 50000
LD, 4, 0, 473, 474, 10
LD, 4, 0, 8093, 8094, 10
XQ

CE, Model 2 Horizontal Polarization
GW, 1, 457, 0, 0, -3.048, 0, 0, 0, 0.00636
GW, 2, 16, 0, 0, 0, 0, 0, 0.1016, 0.00636
GW, 3, 7620, 0, 0, 0.1016, 152.4, 0, 0.1016, 0.00636
GW, 4, 16, 152.4, 0, 0.1016, 152.4, 0, 0, 0.00636

```
GW, 5, 457, 152.4, 0, 0, 152.4, 0, -3.048, 0.00636
GE -1 1
FR, 0, 12, 0, 0, 62.5, 62.5
GN, 2, 0, 0, 0, 13, .2
EX, 1, 1, 1, 0, 90., 90., 90., .25, 1., 0., 50000
LD, 4, 0, 473, 474, 10
LD, 4, 0, 8093, 8094, 10
XQ
```

CE, Model 3: Vertical Polarization, specific case of vertical polarization of the incident field

```
GW, 1, 457, 0, 0, -3.048, 0, 0, 0, 0.007127
GW, 2, 16, 0, 0, 0, 0, 0, 0.1016, 0.007127
GW, 3, 7620, 0, 0, 0.1016, 152.4, 0, 0.1016, 0.007127
GW, 4, 16, 152.4, 0, 0.1016, 152.4, 0, 0, 0.007127
GW, 5, 457, 152.4, 0, 0, 152.4, 0, -3.048, 0.007127
GE -1 1
FR, 0, 12, 0, 0, 62.5, 62.5
GN, 2, 0, 0, 0, 13, .2
EX, 1, 1, 1, 0, 0., 90., 0., .25, 1., 0., 50000
LD, 4, 0, 473, 474, 10
LD, 4, 0, 8093, 8094, 10
XQ
```

CE, Model 4 Vertical Polarization

```
GW, 1, 457, 0, 0, -3.048, 0, 0, 0, 0.019
GW, 2, 16, 0, 0, 0, 0, 0, 0.1016, 0.019
GW, 3, 7620, 0, 0, 0.1016, 152.4, 0, 0.1016, 0.007127
GW, 4, 16, 152.4, 0, 0.1016, 152.4, 0, 0, 0.019
GW, 5, 457, 152.4, 0, 0, 152.4, 0, -3.048, 0.019
GE -1 1
FR, 0, 20, 0, 0, 0.1, 4.995
GN, 2, 0, 0, 0, 13, .2
EX, 1, 1, 1, 0, 30., 0., 0., .25, 1., 0., 50000
LD, 4, 0, 473, 474, 10
LD, 4, 0, 8093, 8094, 10
XQ
```

CE, Model 5 Horizontal Polarization

```
GW, 1, 457, 0, 0, -3.048, 0, 0, 0, 0.019
GW, 2, 16, 0, 0, 0, 0, 0, 0.1016, 0.019
GW, 3, 7620, 0, 0, 0.1016, 152.4, 0, 0.1016, 0.007127
GW, 4, 16, 152.4, 0, 0.1016, 152.4, 0, 0, 0.019
GW, 5, 457, 152.4, 0, 0, 152.4, 0, -3.048, 0.019
GE -1 1
FR, 0, 20, 0, 0, 0.1, 4.995
GN, 2, 0, 0, 0, 13, .2
```

EX, 1, 1, 1, 0, 30., 90., 90., .25, 1., 0., 50000
LD, 4, 0, 473, 474, 10
LD, 4, 0, 8093, 8094, 10
XQ

CE Model 6: 500 ft Power Wire in Dry, Sandy Coastal Land, with HEMP pulse at 750 MHz
GW, 1, 457, 0, 0, -3.048, 0, 0, 0, 0.019
GW, 2, 16, 0, 0, 0, 0, 0, 0.1016, 0.019
GW, 3, 7620, 0, 0, 0.1016, 152.4, 0, 0.1016, 0.007127
GW, 4, 16, 152.4, 0, 0.1016, 152.4, 0, 0, 0.019
GW, 5, 457, 152.4, 0, 0, 152.4, 0, -3.048, 0.019
GE -1 1
FR, 0, 20, 0, 0, 0.1, 4.995
GN, 2, 0, 0, 0, 13, .2
EX, 1, 1, 1, 0, 45., 0., 0., .25, 1., 0., 50000
LD, 4, 0, 473, 474, 10
LD, 4, 0, 8093, 8094, 10
XQ

9.4 Transmission Line Model Graphs

Figure 56: Transmission Line Analysis with Frequency at 20 MHz

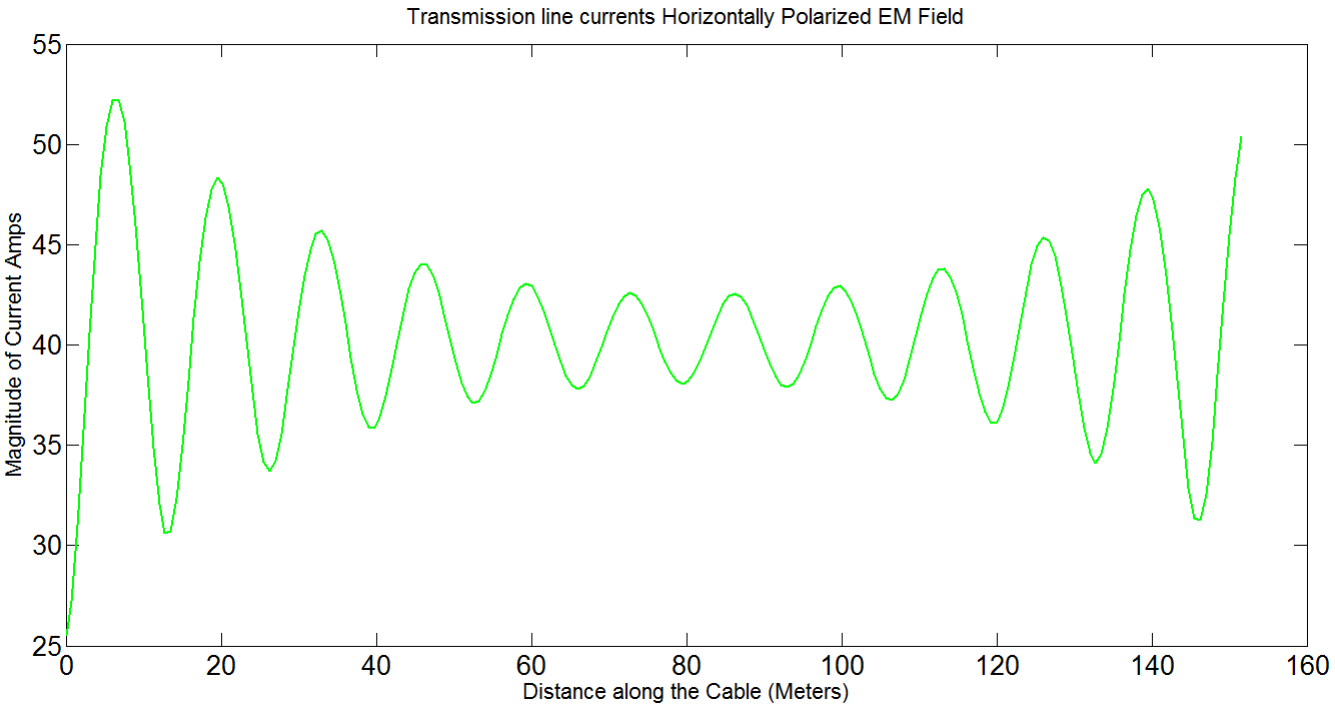

Figure 57: Transmission Line Analysis with Frequency at 30 MHz

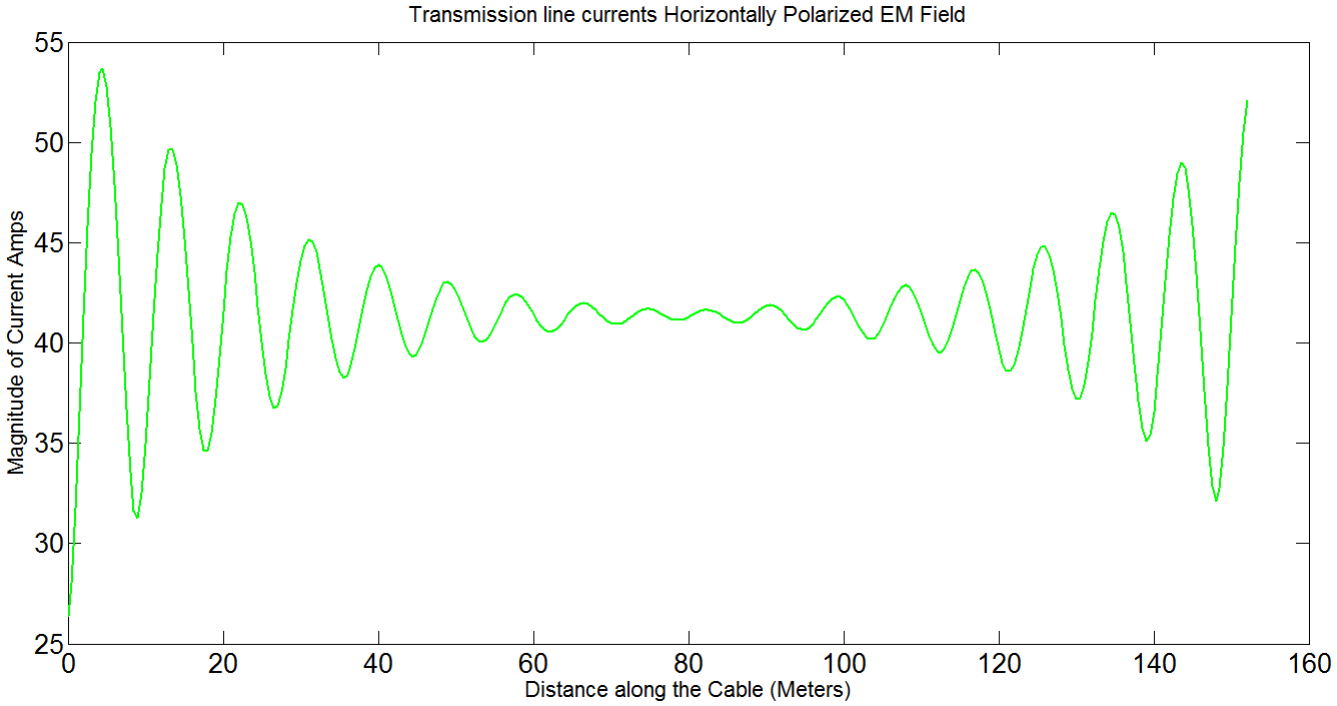

Figure 58: Transmission Line Analysis with Frequency at 40 MHz

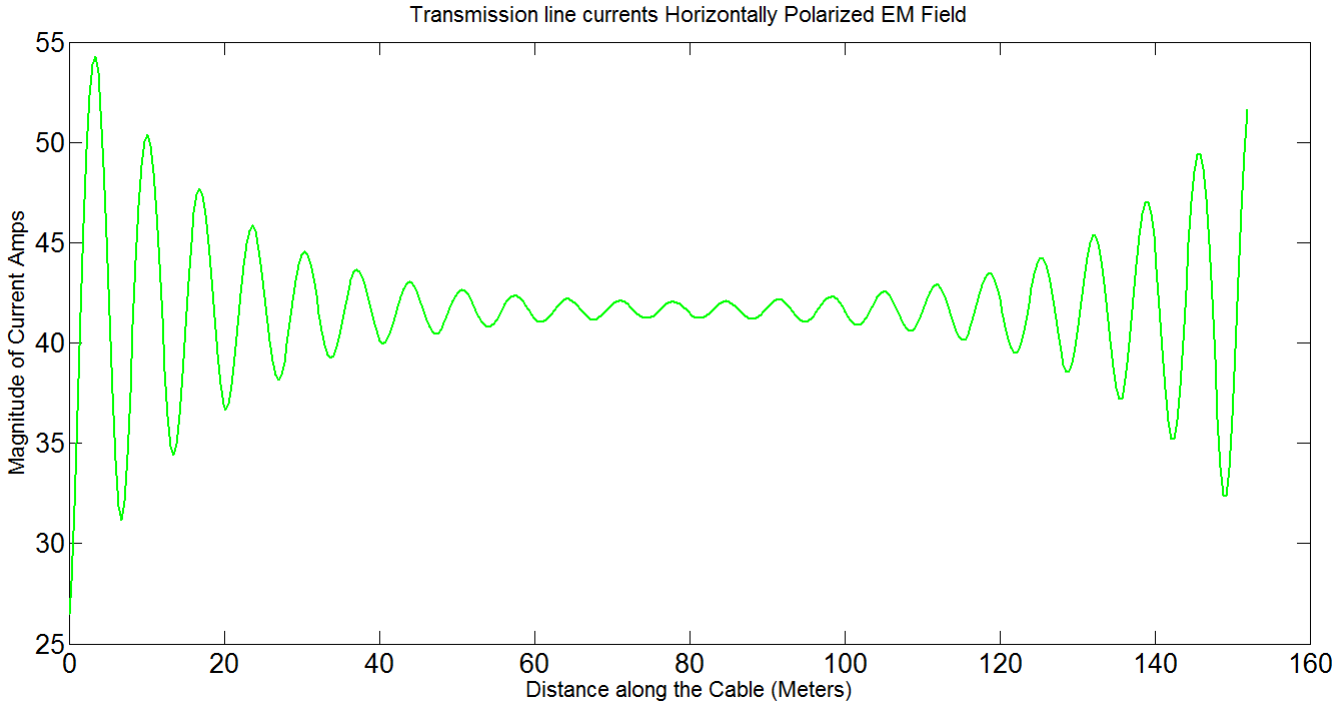

Figure 59: Transmission Line Analysis with Frequency at 50 MHz

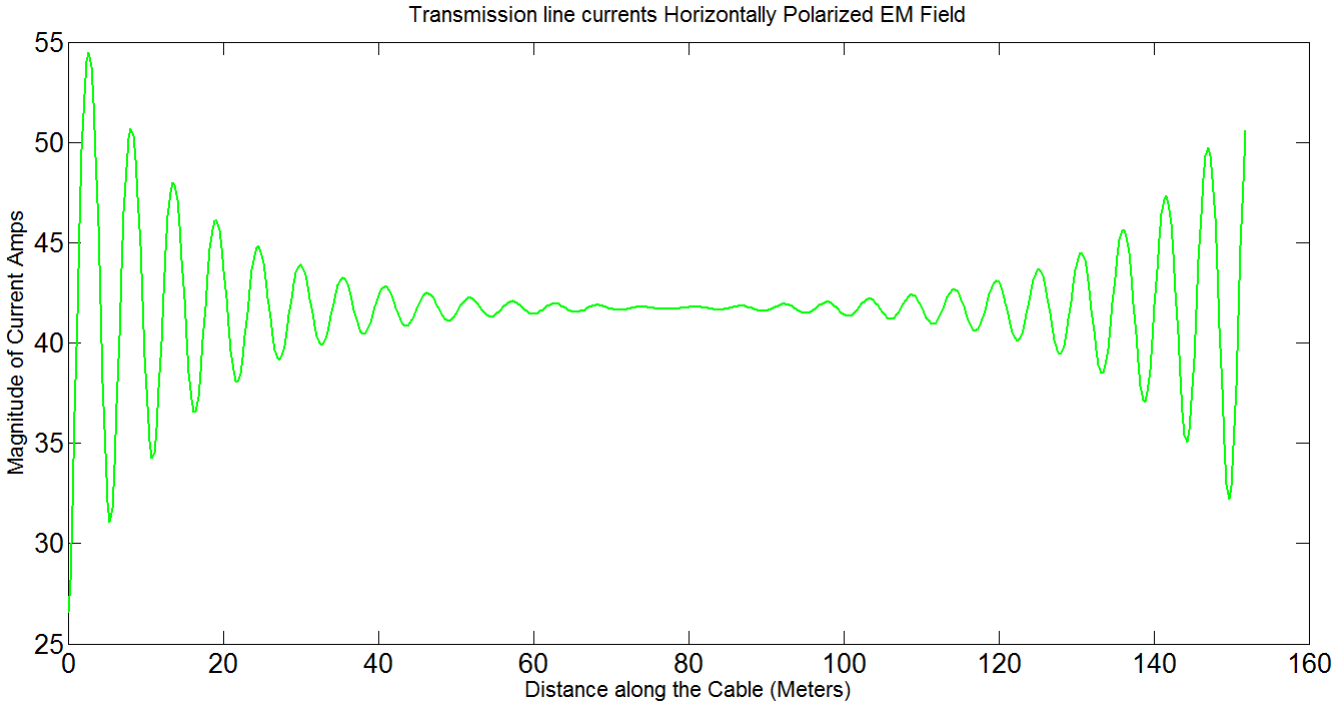

Figure 60: Transmission Line Analysis with Frequency at 60 MHz

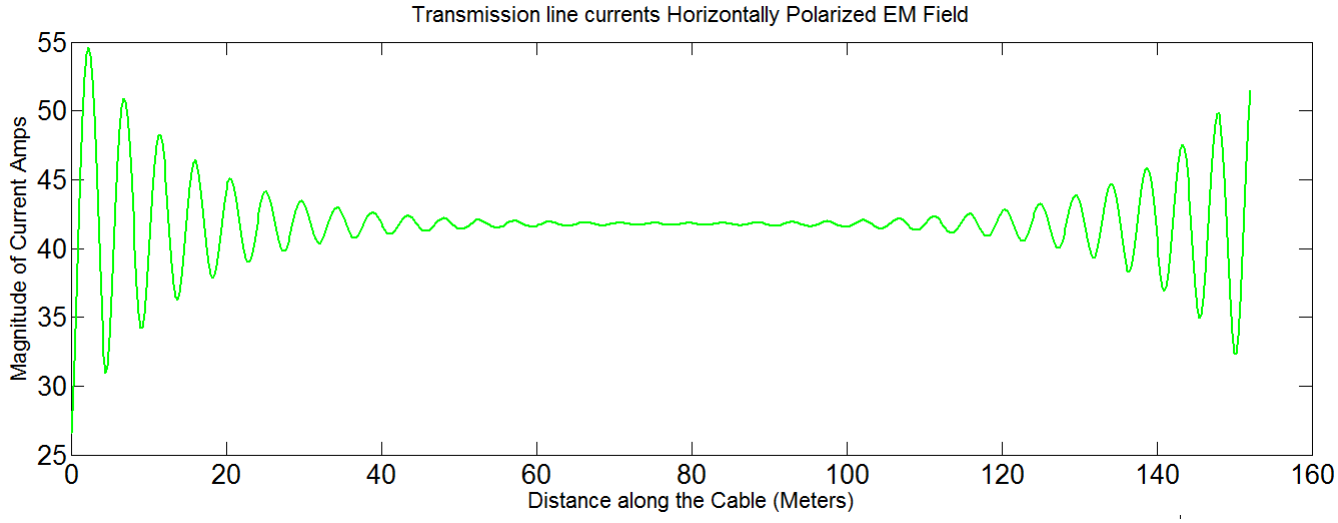

Figure 61: Transmission Line Analysis with Frequency at 70 MHz

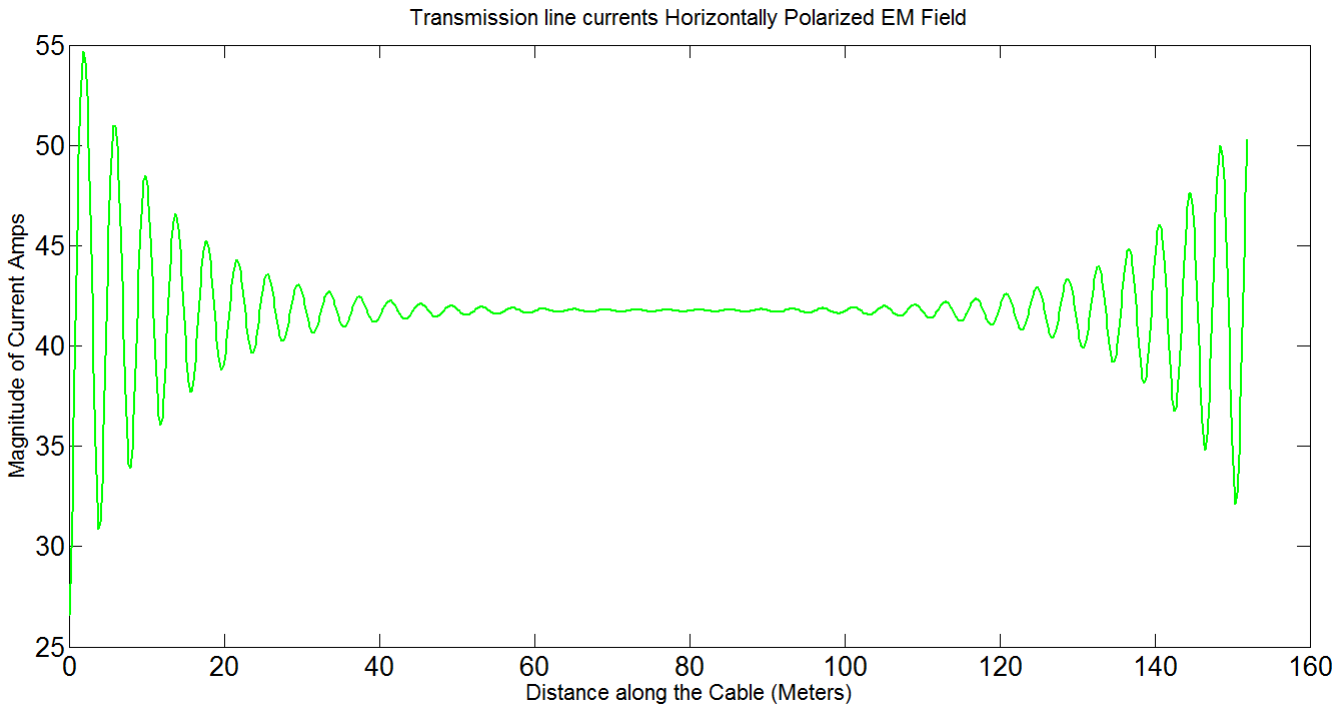

Figure 62: Transmission Line Analysis with Frequency at 80 MHz

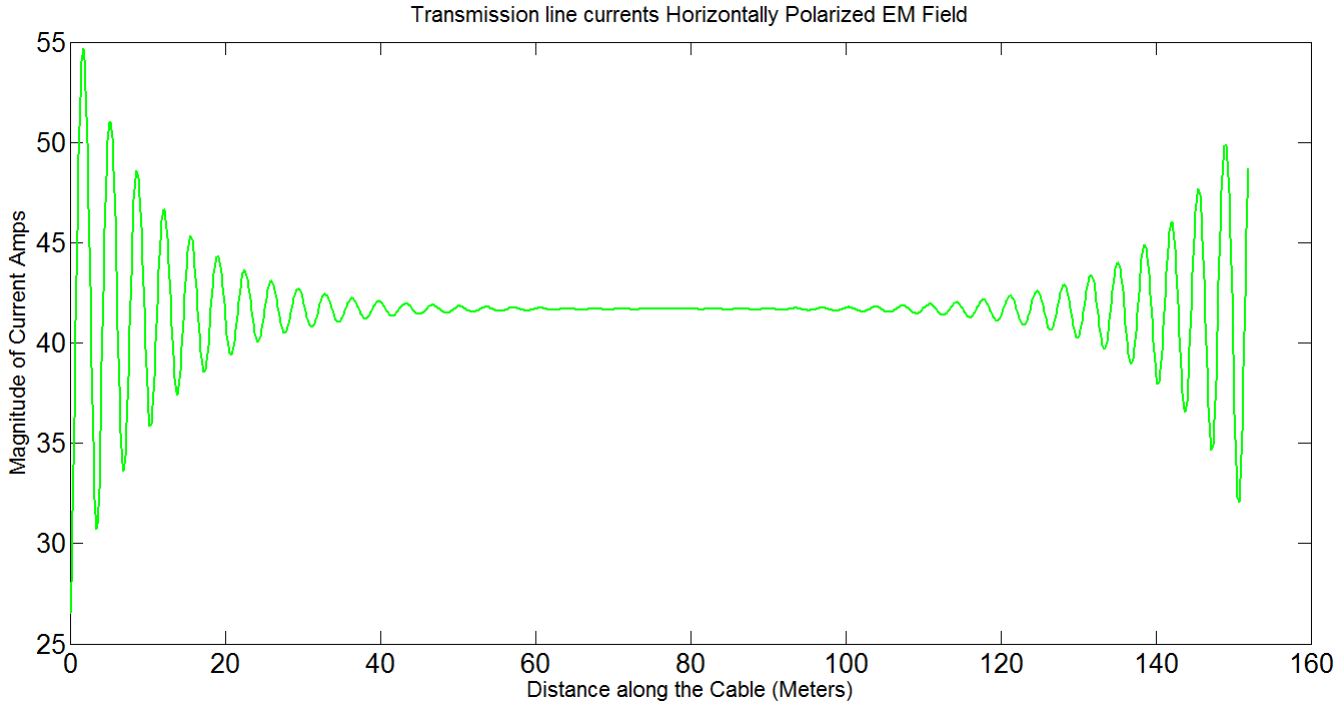

Figure 63: Transmission Line Analysis with Frequency at 90 MHz

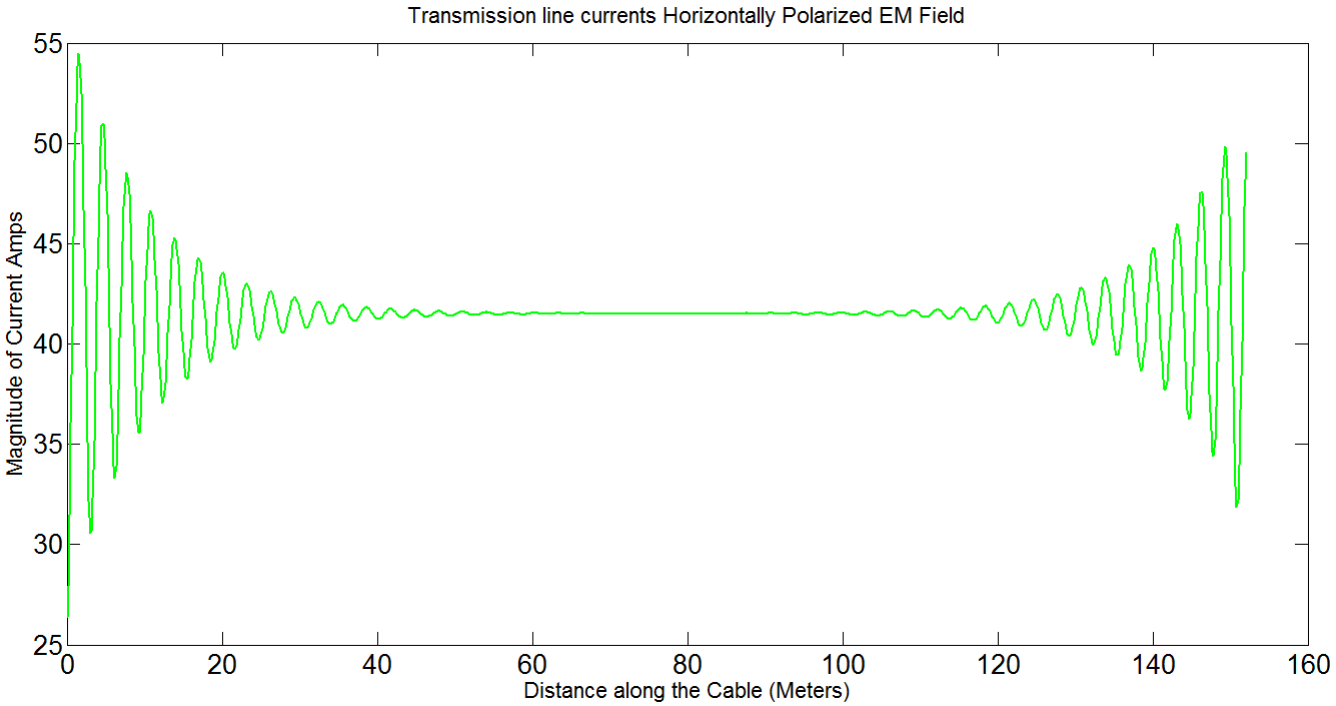

Figure 64: Transmission Line Analysis with Frequency at 100 MHz

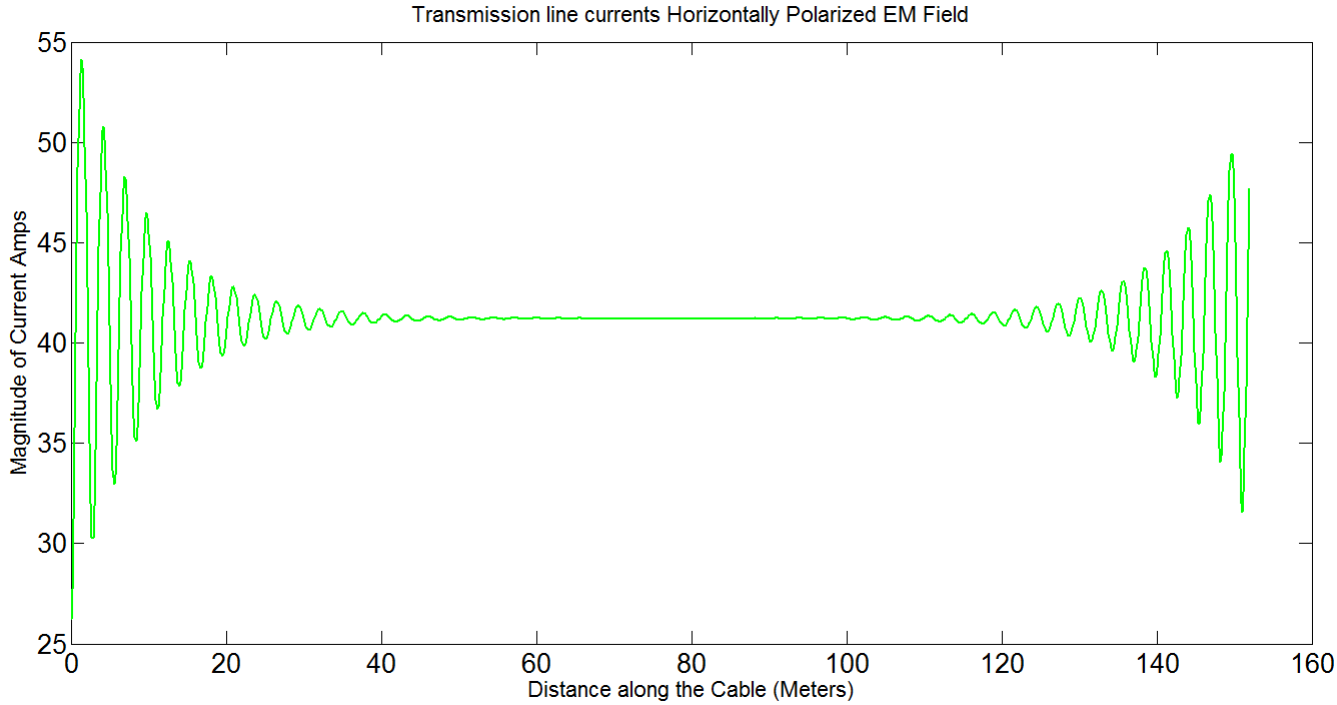

References

[1] E. Savage *et al*, "The Early-Time (E1) High-Altitude Electromagnetic Pulse (HEMP) and Its Impact on the U.S. Power Grid," Metatech Corp., Goleta, CA, Rep. Meta-R-320, January 2010.

[2] E. Savage *et al*, "The Late-Time (E3) High-Altitude Electromagnetic Pulse (HEMP) and Its Impact on the U.S. Power Grid", Metatech Corp., Goleta, CA, Rep. Meta-R-320, January 2010

[3] C. Wilson 'Specialist in Technology and National Security Foreign Affairs, Defense, and Trade Division' "High Altitude Electromagnetic Pulse (HEMP) and High Power Microwave (HPM) Devices: Threat Assessments" EMP Commission, March 26, 2008.

[4] F. M. Tesche, "Comparison of the Transmission Line and Scattering Models for Computing the HEMP Response of Overhead Cables," *IEEE Trans. Electromagn. Compat.*, vol. 34, pp. 93-99, May 1992.

[5] C. Meng, "Numerical Simulation of the HEMP Environment," *IEEE Trans. Electromagn. Compat.*, vol.55, pp. 440-445, June 2013.

[6] Bell Laboratories, *EMP Engineering and Design Principles.* Whippany, NJ: Electrical Protection Dept., Bell Telephone Laboratories, 1975.

[7] M.Wik, "International electrotechnical commission IEC-77C," presented at the EUROREM 94, Bordeaux, France, Jul. 1994.

[8] K.-D. Leuthauser, "A complete EMP environment generated by high-altitude nuclear bursts: Data and standardization," Theoretical Note 364, Air Force Phillips Laboratory, Feb. 1994.

[9] VG95371-10 from Bundesamtfur Wehrtechnik und Beschaffung, Germany (replaces Edition 1993-2008)

[10] *High-Altitude Electromagnetic Pulse (HEMP) Protection For Ground-Based C^4I Facilities Performing Critical, Time-Urgent Missions: Part 2 Transportable Systems*, Department of Defence Interface Standard, 3 March 1999.

[11] *Grounding, Bonding, and Shielding for Electronic Equipments and Facilities*, Volume 1 of 2, Military Handbook, Washington DC, 21 January 1982.

[12] IEC 61000 2-9, "Electromagnetic compatibility (EMC) Part 2: Environment - Section 9: Description of HEMP environment - Radiated disturbance. Basic EMC publication," (1996). [Online] Available: http://webstore.iec.ch

[13] E. F. Vance, *Coupling to Shielded Cables*, New York, NY: Wiley, 1978

[14] E.D. Sunde, *Earth Conduction Effects in Transmission Systems.* New York: Van Norstrad, 1949.

[15] D. V. Giri and W. D. Prather, "High-Altitude Electromagnetic Pulse (HEMP) Risetime Evolution of Technology and Standards Exclusively for E1 Environment", *IEEE Trans. Electromagn. Compat.*, vol.55, pp. 484-491, June 2013

[16] W. Radsky "The Application of IEC 61000-2-10 to Establish E1 HEMP External Conductor Protection Specifications", *Metatech Corporation*, Goleta CA

[17] F. Sabath "Tolerance Values and the Confidence Level for High-Altitude Electromagnetic Pulse (HEMP) Field Tests", *IEEE Trans. Electromagn. Compat.*, vol. 55, pp. 518-525, June 2013

[18] V. Dorle *et al*, "Electromagnetic Field Coupling to Multiple Finite Length Transmission Lines Above an Imperfect Ground", *Department of Electronics* University of Split, Rudera Boskovica, pp. 595-598. 2003

[19] V. Greetsai *et al*, "Response of Long Lines to Nuclear High-Altitude Electromagnetic Pulse (HEMP)", *IEEE Trans. Electromagn. Compat.*, vol. 40, pp. 348-354, November 1998

[20] M. Ianoz, *et al*, " Modeling of an EMP Conducted Environment", *IEEE Trans. Electromagn. Compat.*, vol. 38, pp. 400-413, August 1996

[21] "NEC-2 Manual, Part III: User's Guide", WBDN version 0.92, pp. 1-131, September 24 1996